# UNIVERSITÀ DEGLI STUDI DI MILANO

Facoltà di Medicina e Chirurgia

Scuola di Dottorato in Scienze Biomediche Cliniche e Sperimentali

Dipartimento di Biotecnologie Mediche e Medicina Traslazionale

(BIOMETRA)

Dottorato di Ricerca in

**PATOLOGIA E NEUROPATOLOGIA SPERIMENTALI**

(XXVI CICLO)

TESI DI DOTTORATO DI RICERCA

# "Regulation of the hematopoietic self-renewal and lineage choice: role of Pbx1 and micro-RNAs"

(MED 03/04/05)

**Laura Crisafulli**

Matr. R09319

Relatore :

**Dr. Anna Villa**

Coordinatore del dottorato:

**Prof. Massimo Locati**

Anno accademico 2012/2013

# INDEX

# 1. INTRODUCTION

## 1.1 HEMATOPOIESIS

Haematopoiesis (from Ancient Greek: αἷμα, "blood"; ποιεῖν "to make") literally means the formation of blood. Hematopoiesis is the process by which all the different cellular populations that constitute blood and immune system are generated starting from common multipotent hematopoietic stem cells (HSCs), through a succession of progressive differentiation pathways. Approximately $10^{11}$–$10^{12}$ new blood cells are produced every day in a human healthy adult in order to maintain proper hematopoietic homeostasis (Tristram G. Parslow, 2001). However the hematopoietic system is also able to immediately respond to higher cellular demands in response to stress signals like infection or bleeding, thus specifically producing more cells according to the peripheral needs. The capability to replenish all the different cell lineages is due to the presence of HSCs, rare cells with the unique capacity to self-renew and differentiate to all of the different mature blood cell types throughout all lifespan (Spangrude et al., 1988). The remarkable regenerative properties of HSCs are best illustrated by the success of marrow transplantation in human patients, a well-established therapy for a variety of genetic and acquired bone marrow (BM) diseases, and cancers.

In the adult hematopoiesis occurs in the BM, were multipotent self-renewing HSCs generate a hierarchy of progenitors that ultimately produce the hematopoietic cell lineages. Some of them are directly released in the blood circulation as mature cells while others, like lymphocytes, reach their full maturation in secondary lymphoid organs.

### 1.1.1 Hematopoiesis sites

During the life of an individual, there are two hematopoietic waves, the first one named “primitive” and the second one named “definitive”. Both arise during embryonic development but only the second one persists in the adult. Primitive hematopoiesis has the primary function to provide red blood cells for oxygen transport to the rapid growing embryo, when the definitive specialized hematopoietic structures have not yet developed. It occurs (starting from E7.5 in the mouse) in the mammalian yolk sac in

aggregates of blood cells called blood islands, mainly composed of nucleated erythroid cells. An additional embryonic population of macrophages was detected in the yolk sac as early as the first erythrocytes, both in Zebrafish and in mouse (Bertrand et al., 2005; Herbomel et al., 1999; Palis et al., 1999). These cells bypass the conventional developmental pathway that lead to macrophage differentiation in the hematopoietic organs (Ginhoux et al.). The primitive hematopoietic system is transient and rapidly replaced by definitive hematopoiesis which starts within the embryo itself in the Aorta-Gonad-Mesonephro (AGM) region, through a specific developmental specification pathway that finally leads to the formation of permanent hematopoietic stem cells (Figure 1.1.1).

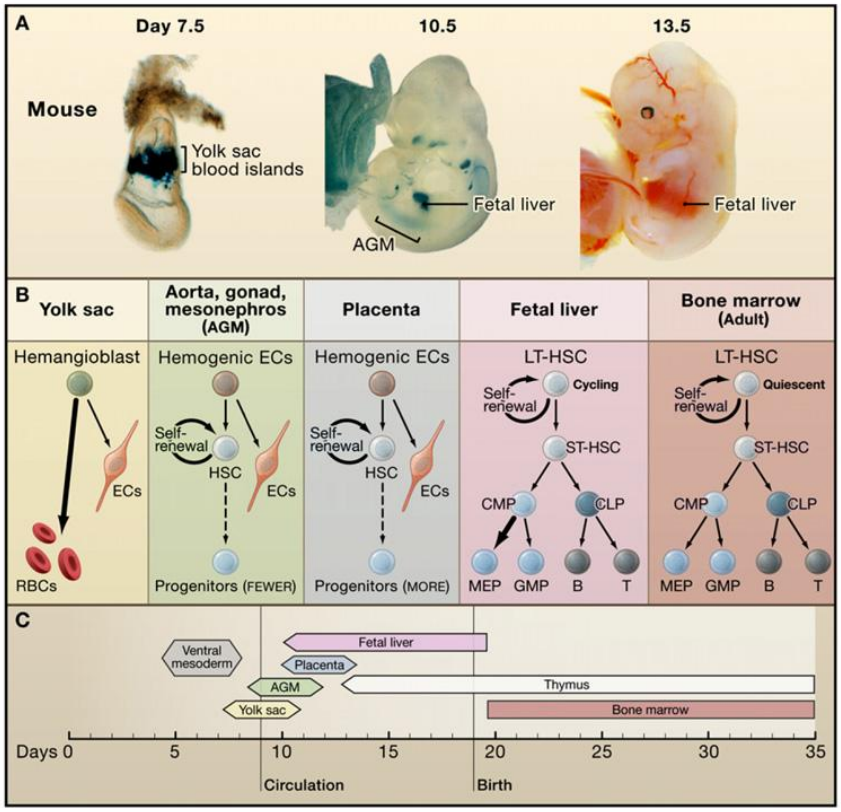


**Figure 1.1.1 Developmental Regulation of Hematopoiesis in the Mouse.** (A) Hematopoiesis occurs first in the yolk sac (YS) blood islands and later at the aorta-gonad mesonephros (AGM) region, placenta, and fetal liver (FL). YS blood islands are visualized by LacZ staining of transgenic embryo expression GATA-1- driven LacZ. AGM and FL are stained by LacZ in Runx1-LacZ knockin mice. (B) Hematopoiesis in each location favors the production of specific blood lineages. Abbreviations: ECs, endothelial cells; RBCs, red blood cells; LT-HSC, long-term hematopoietic stem cell; ST-HSC, short-term hematopoietic stem cell; CMP, common myeloid progenitor; CLP, common lymphoid progenitor; MEP, megakaryocyte/erythroid progenitor; GMP, granulocyte/macrophage progenitor. (C) Developmental time windows for shifting sites of hematopoiesis (from (Orkin and Zon, 2008)).

Definitive HSCs emerge from the Tie2-expressing haemogenic endothelium in the ventral wall of the dorsal aorta at embryonic day 10.5, although with little HSC activity,

whereas by day 11 engrafting activity is present. After this time, definitive HSCs isolated from the AGM are able to long-term reconstitute the entire blood system upon transplantation to irradiated mice (de Bruijn et al., 2000; Muller et al., 1994), whereas mouse yolk sac tissue does not (Cumano et al., 1996; Medvinsky and Dzierzak, 1996; Orkin and Zon, 2008). This is important since the presence of HSCs is defined by their reconstitution capacity.

There are other sites in which additional hematopoietic activity is subsequently detected in the mouse embryo, like the umbilical arteries and the allantois in which hematopoietic and endothelial cells are colocalized (Inman and Downs, 2007). Umbilical veins lack hematopoietic potential, suggesting a specific correlation between HSCs and artery specification. In addition, significant numbers of HSCs are found in the mouse placenta (Gekas et al., 2005; Orkin and Zon, 2008; Ottersbach and Dzierzak, 2005). The relative contribution of each of the above mentioned sites to the final pool of adult HSCs remains largely unknown. During embryo development the definitive hematopoiesis site moves from AGM first to the fetal liver, the main hematopoietic embryonic organ, then to thymus, spleen, and ultimately the bone marrow before birth, where it continues throughout adult life (Figure 1.1.1). In children, hematopoiesis occurs in the bone marrow of the long bones such as the femur and tibia, while in adults mainly in the pelvis, cranium, vertebrae, and sternum. In some cases liver, thymus, and spleen may resume their hematopoietic function, if necessary, leading to extramedullary haematopoiesis, which can support some medullary failure.

## 1.1.2 The hematopoietic hierarchy

Hematopoiesis proceeds through a hierarchical system with progressive levels of differentiation, at the apex of which there are rare HSCs that guarantee the presence of all terminally differentiated cells. While undergoing various cell divisions, HSCs generate progenitors with different degrees of maturation and increased restricted differentiation capacity, in a stepwise manner (Orkin, 2000).

In this tree, HSCs (also called long-term hematopoietic stem cells, LT-HSCs) are the only ones bearing the two characteristics of self-renewal ability and multipotent differentiation capacity, which are hallmarks of all tissue stem cells. Self-renewal and multi-potency is progressively restricted along maturation (Figure 1.1.2), as early as in the first step of multi potent progenitors, often called “short-term” HSCs (ST-HSCs, see later) which have only limited self-renewal capacity even if able to extensively

proliferate. On the contrary, differentiation level increases and the so-called "cell fate decision" becomes more and more restricted until reaching only unipotent ability (Kawamoto and Katsura, 2009). Each step of the hematopoietic hierarchy has been dissected during the past two decades by utilizing cell surface marker analysis by flow-cytometry in combination with functional analysis. However, there are continuous modifications in the branching scheme, according to newly identified intermediate populations, and these constant efforts to refine these heterogeneous populations often lead to changes in the nomenclature of the cell population itself.

In the classical model, LT-HSCs initially give rise to ST-HSCs, that are basically multi-potent progenitors that possess only limited self-renewal and reconstituting ability yet keeping full-lineage differentiation potential (Christensen and Weissman, 2001; Morrison and Weissman, 1994), and then to MPPs, multi-potent progenitors without self-renewal and reconstituting capacity. Further downstream, MPPs branch towards two oligopotent lineage restricted progenitors: the common lymphoid progenitor (CLP) that have the potential to become lymphoid cells (Karsunky et al., 2008; Serwold et al., 2009) and the common myeloid progenitor (CMP), which is responsible for the megakaryocyte/erythorid/myeloid cell fate (Akashi et al., 2000; Kondo et al., 1997; Luc et al., 2008) (Figure 1.1.2). The CMPs subsequently segregate into either myelo-monocytic precursors, also called granulocyte/macrophage progenitors (GMPs), or to megakaryocyte/erythrocyte progenitors (MEPs) (Nakorn et al., 2003), which in turn differentiate into red blood cells and megakaryocyes which produce platelets. This hierarchical classification was subsequently refined with additional populations. For example it was demonstrated that the MPP population is not uniform (Adolfsson et al., 2005; Arinobu et al., 2007; Christensen and Weissman, 2001; Forsberg et al., 2006; Kiel et al., 2005; Osawa et al., 1996) and it can be further divided in different groups according to the expression of specific surface markers and their degree of maturation and progressive loss of self-renewal ability (see later). In another study Pronk et al. have utilized new markers, like CD150, Endoglin, and CD41, to isolate additional myeloid progenitors, thus further modifying the existing hematopoietic tree with novel sets of intermediate progenitors (Pronk et al., 2007). Finally, according to more recent reports, a subgroup of multipotent progenitors can directly generate megakaryocyte/erythrocyte progenitors bypassing the common myeloid progenitor stage (Seita and Weissman, 2010), although the issue is still debated (Figure 1.1.2).

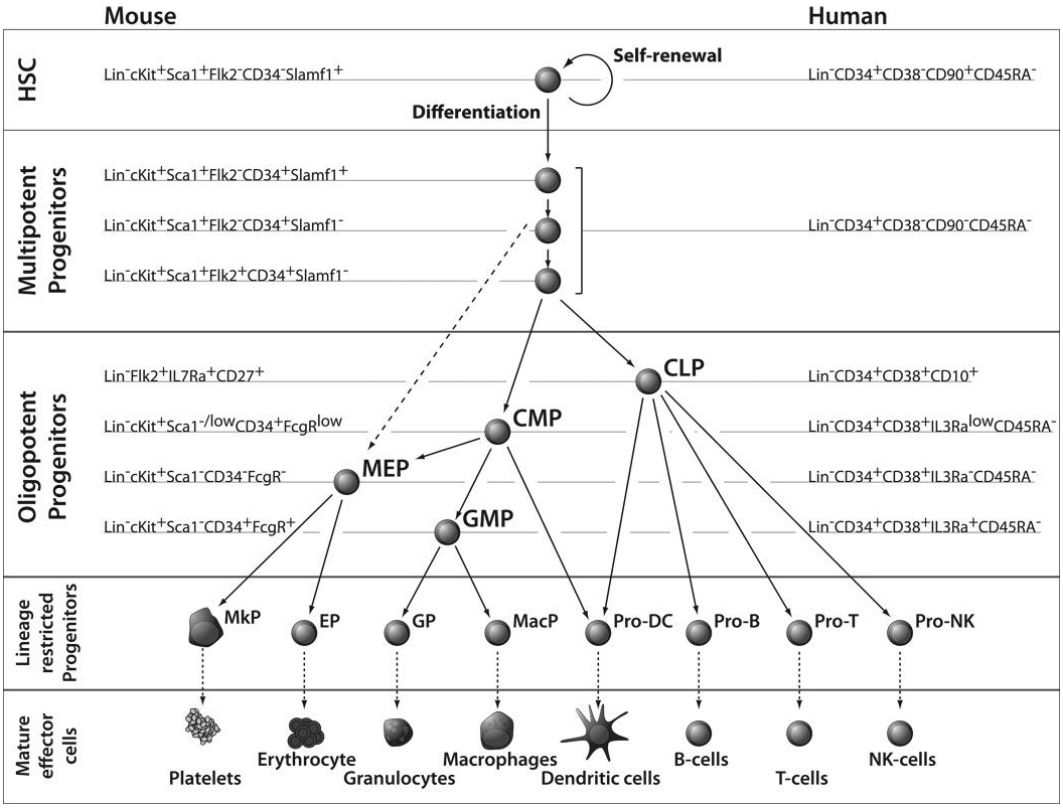


**Figure 1.1.2 Model of the hematopoietic hierarchy.** The HSC resides at the top of the hierarchy, and is defined as the cell that has both the self-renewal capacity and the potential to give rise to all hematopoietic cell types (multipotency). Throughout differentiation, a HSC first loses self-renewal capacity, then loses lineage potential step-by-step as it commits to become a mature functional cell of a certain lineage. The cell surface phenotype of each population is shown for the mouse and human systems. Intermediate precursors between the first lineage committed progenitors and final mature cell, and different subsets of mature B- and T-cells are omitted. In the mouse system, heterogeneity of MPPs has been revealed by differences in cell surface marker phenotypes and functional differences of their subsets discussed. For example, evidence suggests that some of MPPs directly give rise to MEP without passing through a CMP stage (dashed arrow) (From Seita and Weissman 2010 (Seita and Weissman, 2010)).

Importantly, true HSCs are functionally defined: they are endowed with the ability to reconstitute a lethally irradiated host throughout life, thus showing *in vivo* their multipotency and self-renewal ability (Coulombel, 2004). Cells with these feautures have been prospectively isolated based on cell surface characteristics, however the haematopoietic stem cell definition in terms of unique cell surface markers profile is still a debated issue, since different laboratories often use slightly different combination of markers.

Like HSCs all the cell populations constituting the hematopoietic system can be identified and prospectively isolated through combinations of surface markers that finely distinguish them. In general, stem cells (as well as MPPs) are all negative for markers used for detection of lineage commitment and are, thus, called Lin$^-$. They also

express Sca1 and cKit leading to a phenotype which is commonly abbreviated as LKS, which include less than 10% of HSCs (see § 1.1.3.3).

## 1.1.3 Hematopoietic stem cells (HSCs)

### *1.1.3.1 The stem cells concept*

One of the earliest evidence of long-lived blood cell progenitors came from the observation that infusion of hematopoietic cells induced tolerance in fetal and neonatal mice, a discovery that was awarded the Nobel Prize in Medicine in 1960 (Billingham et al., 1953). Subsequently, the modern "stem cell" concept was first proposed by Till and McCulloch in a series of pioneering experiments on the *in vivo* blood system regeneration capacity, during the 1960s (Till and Mc, 1961). Briefly, they observed the formation of cellular colonies in the spleen of recipient mice ten days after transplanting a limited number of syngenic BM cells. Functional analysis of these colonies revealed that a very small sub-population of the donor BM cells possessed two remarkable properties: the ability to generate multiple types of myeloerythroid cells, and the ability to self-replicate (Becker et al., 1963; Siminovitch et al., 1963; Till and Mc, 1961; Wu et al., 1968).With these findings they defined the two hallmarks of stem cells i.e. multi-potency and self-renewal. Bona fide HSCs are the only cells within the hematopoietic system that possess both capacities. Specifically, multi-potency is the ability to differentiate into all functional blood cells, while self-renewal is the ability to give rise to identical daughter HSCs without differentiation (Orkin and Zon, 2008; Weissman and Shizuru, 2008). Like other adult stem cells, HSCs are able to perform self-renewal and differentiation simultaneously since they are endowed with the capacity of asymmetric cell division, according to which when a stem cell divides one daughter cell retains the stem-cell fate (self-renewal) while the other differentiates (Betschinger and Knoblich, 2004; Doe and Bowerman, 2001; Yamashita and Fuller, 2005). Asymmetric division is a particularly attractive strategy because it manages both tasks with a single division. However it leaves stem cells unable to expand in number, thereby making symmetric cell division processes necessary (Morrison and Kimble, 2006).

### *1.1.3.2 HSC quiescence*

It has long been recognized that, although mature blood cells are produced at a rate of more than one million cells per second in the adult human (Ogawa, 1993), most of the HSCs from which they derive are slowly cycling (quiescent) and primarily in the $G_0$ phase of the cell cycle under homeostatic conditions (Rossi et al., 2007). However, HSCs are still heterogeneous. Studies on the cycling behavior of HSCs *in vivo* suggested the presence of two HSC fractions: a deeply dormant HSC (d-HSC) fraction and an active HSC (a-HSC) fraction (van der Wath et al., 2009; Wilson et al., 2008). These two HSC states have been identified through long-term label-retaining assays that are based on an initial labeling of stem cells followed by the label dilution over time. Since the label is halved with each division and is no longer detectable after about five divisions (Waghmare et al., 2008; Wilson et al., 2008), it is possible to calculate the division history of different stem cell populations from the label decay kinetics. With these assays, the LSK $CD34^-CD48^-CD150^+$ HSC population (see §1.1.3.3) was shown to be composed by two subsets: a "dormant" HSC population (d-HSC), which represents about 15% and divide only about every 5 months, and an "active" HSC population (a-HSC) which divide about once every month and represent the 85%. Transplantation assays of these two isolated populations showed that the majority of long-term repopulation activity reside in dHSCs while the active fraction of HSCs, even with the same surface phenotype, shows significantly less self-renewal and fails to serially reconstitute lethally irradiated mice (Foudi et al., 2009; Wilson et al., 2008; Wilson et al., 2009). Due to their slow cycling, d-HSCs are unlikely to significantly contribute to the daily production of blood cells during homeostasis but they serve to maintain an HSC reservoir. The daily production of mature cells, as well as the rapid activation in response to injuries, resides in the active fraction of HSC and even more in the multi potent progenitors. The quiescent state is reversible since d-HSCs could be induced toward an active status (for example by administration of chemotherapeutic compound 5-Fluoro-Uracil) and go back to a dormant state after homeostasis has been re-achieved (Wilson et al., 2008). There is a strong correlation between quiescence and self-renewal since the number of HSC self-renewing divisions may be limited, and functional HSC exhaustion is reached by serially transplanting BM five to six times (Orford and Scadden, 2008). These features have been recently demonstrated also in a significant number of mouse mutants were HSCs show increased cycling activity. Although this initially causes an increase in HSC number, it mostly leads to the final

loss of stem cells likely due to their exhaustion, thus demonstrating the inverse correlation between stem cell proliferation and self-renewal capacity (Wilson et al., 2009). Why is quiescence an advantage for HSCs? During homeostasis a low number of cell divisions minimize the number of DNA mutations that may result in oncogenic transformation. In addition, quiescent HSCs would have sufficient time to repair any DNA damage, if it occurs, prior to fix it to the next cell generation. Moreover in an injury condition, quiescence protects HSCs from external toxic drugs like antiproliferative chemotherapeutic agents (Essers et al., 2009; Randall and Weissman, 1997; Venezia et al., 2004), allowing to a complete reconstitution of the hematopoietic system in which the more mature cells have been destroyed.

### *1.1.3.3 Identification of HSCs*

Regarding morphology, HSC resemble lymphocytes and are small non-adherent round cells, with a rounded nucleus and low cytoplasm-to-nucleus ratio.

There are different assays for identification of HSCs, mostly based on cell surface marker analysis by flow-cytometry, and evaluation of their function (Purton and Scadden, 2007). Nevertheless because no *ex vivo* assays can replace *in vivo* transplantation assay for measuring biological activity of HSCs, characterizing cell populations through their immunophenotype or by other *in vitro* assays cannot be synonymous of determining their function, especially in case of mutant mice.

#### *Immunophenotypical Analysis of HSC/Progenitors*

In the last 20 years, a number of different methods whereby HSCs (and progenitor cells) can be identified have emerged (Goldschneider et al., 1978; Spangrude et al., 1988; Visser and Bol, 1982; Visser et al., 1981), all of them relying on a combination of several positive or negative markers coupled with fluorescence-activated cell sorting (FACS) analysis (Weissman and Shizuru, 2008). Since the HSC population is rare (less than one out of $10^5$ BM cells), a common problem with these methods is to achieve a reasonable level of purity. Indeed, in all of them the obtained HSCs are still enrichment rather than pure populations. Nevertheless, with the different immunophenotyping methods the purity of HSC populations has progressively increased, reaching approximately 50%–96% of single cells able to long-term reconstitution after transplantation (Matsuzaki et al., 2004; Yilmaz et al., 2006a).

The first immunophenotypic characterization was performed in 1988 by Weissman laboratory, which isolated short-term repopulating HSCs based on the expression of

stem cell antigen- 1 (Sca-1), low expression of Thy1.1, and lack of expression of lineage markers (Spangrude et al., 1988). The same population was shown to contain long-term repopulating HSCs in a subsequent study (Uchida and Weissman, 1992) and was further purified by the expression of the stem cell factor receptor, c-Kit, in 1992 (Ikuta and Weissman, 1992). However, this combination of markers is not widely used since Thy1.1 is expressed only by a specific mouse strain but not by C57BL/6, worldwide used mice in HSC transplantation studies. Even if the Thy1.1 counterpart in C57BL/6 mice exist (Thy1.2) it does not have the same pattern of expression on HSCs (Spangrude and Brooks, 1992). Due to this important limitation, other immunophenotypical characterizations have been developed mostly based on the expression of c-Kit. After its first description as a marker of hematopoietic progenitor cells in 1991 (Ogawa et al., 1991), Suda and collaborators reported the isolation of HSCs from C57BL/6 mice in the $Lin^{-}Kit^{+}$, $Sca\text{-}1^{+}$ ($LKS^{+}$) population in 1992, following a similar protocol to that described by Weissman's lab (Okada et al., 1992). However, as mentioned earlier LKS population is only partially enriched in HSCs. To further purify HSC population, more recently the expression of CD34 (Osawa et al., 1996) and Flk2 (CD135) (Adolfsson et al., 2001; Yang et al., 2005) has been used. With the combination of these two markers it has been possible to separate long-term repopulating HSCs, which are $LKS^{+}CD34^{-}Flk2^{-}$, from short-term repopulating HSCs ($LKS^{+}CD34^{+}Flk2^{-}$) and multi potent progenitors ($LKS^{+}$ $CD34^{+}Flk2^{+}$) (Yang et al., 2005). However this method shows some limitations like differential expression of CD34 according to the age of mice, as in mice younger than 8 weeks it is expressed also by HSCs (Matsuoka et al., 2001).

Another strategy used to define HSC phenotype is based on fluorescent dyes efflux properties of HSCs, which identify HSCs as the so-called Side Population (SP). For this purpose two different vital dyes, the mitochondrial-binding dye rhodamine 123 and DNA-binding dye Hoescht 33342, have been used, either alone or in combination, to isolate HSCs (Goodell et al., 1996; Li and Johnson, 1992; McAlister et al., 1990; Phillips et al., 1992; Wolf et al., 1993). Both dyes are retained at very low intensity in HSCs due to high efflux capacity of these cells. The efflux is mediated by a membrane pump belonging to the ATP-binding cassette (ABC) transporter family. ABCs are highly expressed in HSCs and drive the efflux of drugs and other toxic molecules, including dyes, resulting in their low-retaining. HSCs labeled with these dyes are visualized by FACS analysis as SP cells by low emitting the dye. There are strong

technical limitations in the use of this method since it has been reported a poor reproducibility among different laboratories and even among different experiments, due to a high dependency on modifications in the staining techniques (Lin and Goodell, 2006) and to different performance of different batches of dyes (Matsuzaki et al., 2004). Furthermore the SP population is not as pure as HSCs enriched by other methods such as $LKS^{+}CD34^{-}Flk2^{-}$cells, although it can be used in combination with those markers to further purify HSCs with extreme efficiency (reviewed in (Purton and Scadden, 2007).
Additional improvement in HSC purity has been reached with the use of the signaling lymphocyte activation molecule (Arboleda et al.) code. Single cell reconstitution assay has shown that, using this code, is it possible to purify a population in which approximately 50% of the immunoidentified HSCs is able to long-term reconstitute lethally irradiated animals (Kiel et al., 2005; Wilson et al., 2009; Wilson and Trumpp, 2006). SLAM proteins are a family of cell surface glycoproteins belonging to the immunoglobulin superfamily, originally known to be involved in T-cell stimulation. This family is a group of more than 10 molecules whose genes are located mostly in tandem in a single locus on chromosome 1 (in the mouse). CD150 being the founding member is thus also called slamF1 (SLAM family member 1). According to the SLAM code HSCs were first defined as $CD150^{+}CD48^{-}CD244^{-}$. Subsequently it has been reported that $CD150^{+}CD48^{-}$ signature is sufficient. The use of SLAM signature overcomes most of the limitation of the previous methods for HSC identification, giving comparable stem cell purity in mice. Indeed, unlike Thy1.1 expression, the SLAM receptors appear to be expressed by many mouse strains (Kiel et al., 2005), and more faithfully detect HSCs in older, mobilized, or transplanted mice (Yilmaz et al., 2006a). However, recent work has shown that this method excludes a large number of HSCs and includes an equally large number of non-stem cells than the other methods do (Weksberg et al., 2008). In summary, we can conclude that the different HSC populations identified by SLAM code or CD34/CD135 are quite similar and the use of one combination rather than the other does not impair significantly HSC purity (see Figure 1.1.3, for schematic immunophenotypical analysis of HSC and progenitor cells, and Table 1.1.1, for summary of cell population immunophenotypes used in this study).

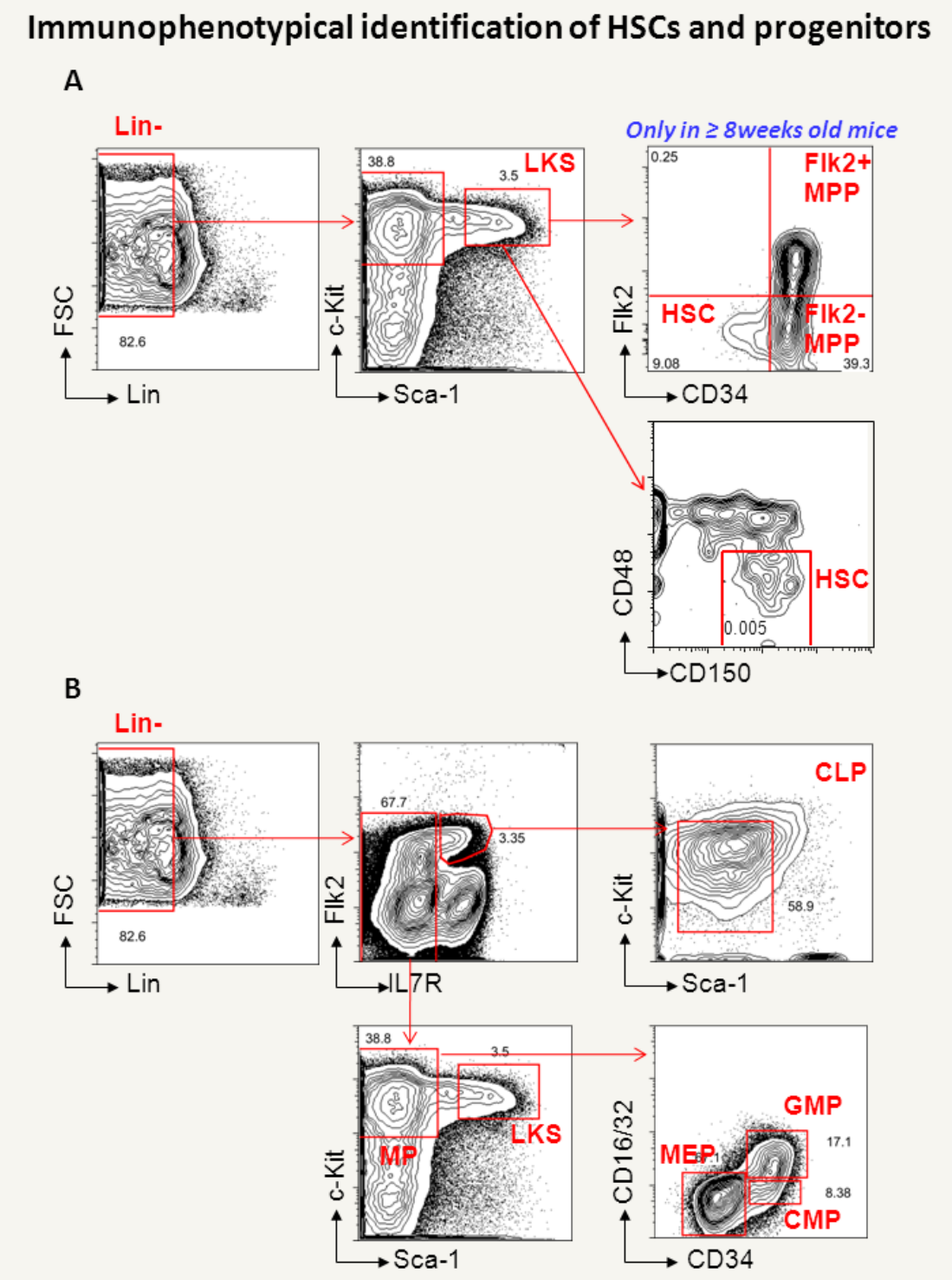


**Figure 1.1.3 Immunophenotypical analysis of HSC and progenitor cells.** Representative FACS plots show the gating strategy for identification of HSC and multipotent progenitors (A) and lineage restricted progenitors (common myeloid and common lymphoid progenitors) (B) that was used in our study. Both gating strategies refer to Lin$^-$ enriched BM cells. See text for details.

| Cell population | Acronym | Immunophenotype | Notes |
|---|---|---|---|
| Hematopoietic stem cell | HSC | $Lin^-/cKit^{hi}/Sca^{hi}$ (LKS)/$CD34^-Flt2^-$ *Not in mice younger than 8wks* | Also called LT-HSC |
| | | $LKS/CD150^+/CD48^-$ | SLAM code |
| Multipotent progenitor | MPP | $LKS/CD34^+/Flk2^{-/low}$ | Also called ST-HSC |
| Lymphoid-primed MPP | LMPP | $LKS/CD34^+/Flk2^{high}$ | |
| Common lymphoid progenitor | CLP | $Lin^-/IL7R^+/cKit^{low}/Sca^{low}$ | |
| Common myeloid progenitor | CMP | $Lin^-/cKit^+/CD34^{int}/CD16/32^{int}$ | |
| Granulocyte/macrophage progenitor | GMP | $Lin^-/cKit^+/CD34^+/CD16/32^+$ | |
| Megakaryocyte/erythrocyte progenitor | MEP | $Lin^-/cKit^+/CD34^-/CD16/32^-$ | |

**Table 1.1.1** Hematopoietic stem and progenitor cell populations with the markers used in our study. Table show name, acronym and commonly used immunophenotype to identify and purify them.

Irrespective of the combination of markers used, it has to be noted that reliability of all these markers is questionable in mutant mouse models, as the surface marker profile of HSCs and their progenitors may be distorted leading to phenotypically defined HSCs which not always correlate with their real number or quality (Purton and Scadden, 2007).

***Functional Assays***

The functional potential of HSCs and progenitors cannot be measured only on the basis of immunophenotypical analysis; hence, functional assays have been developed. HSCs are operationally defined by their ability to reconstitute the entire blood system of a recipient and therefore the gold standard for measuring HSCs is the long-term repopulating assay. Nevertheless, during the past other functional assays have been used, although most of them are indirect or surrogate assays and reflect more the progenitors rather than the HSC function. The most used functional HSC assays, which can be divided into *in vitro* and *in vivo* assays, are listed below.

One of the test most used worldwide is the colony-forming cell (CFC) assay, which evaluates progenitor cells in a given population using a well-defined methylcellulose-based culture media supplemented or not with different cytokines. After a specific time of culture, cells develop visible colonies of differentiated cells that allow to determine the cell they originated from. The majority of colonies derive from lineage-restricted cells: erythroid colonies, further divided into the more immature burst-forming units-erythroid (BFU-E) or colony-forming units erythroid (CFU-E); megakaryocyte-restricted colonies (CFU-Mk); colony-forming units-granulocytes (CFU-G), colony-

forming units-monocytes/macrophages (CFU-M) and colony forming units-granulocytes/macrophages (CFU-GM). More immature colonies may also be detected like CFU-GEMM, which originate from earlier multi potent progenitors and contains granulocytes, erythrocytes, macrophages, and sometimes megakaryocytes. HSCs can give rise to CFU-GEMM too, although in a longer time-frame due to their initial quiescent state. The CFC assay allow myelo-erythroid differentiation, while to detect B and T lymphocyte progenitors specialized co-culture systems are necessary (Schmitt and Zuniga-Pflucker, 2002; Whitlock and Witte, 1982). As mentioned above CFC assay is informative about the progenitor cell content of a population but do not measure HSC activity.

Another *in vitro* assay is the long-term culture-initiating cell (LTC-IC) assay, which detects the presence of very primitive hematopoietic progenitors. Hematopoietic cells are co cultured on a supportive feeder stromal layer, and after $\geq 4$ weeks their sustained capacity to produce myeloid colonies is detected by CFC assay. Although *in vitro*, the LTC-IC is the best surrogate functional assay for long term HSC capacity (Verfaillie, 1994; Woehrer et al., 2010).

The gold standard assay to measure both HSC numbers and functional potential are long term *in vivo* assays. Different types of long-term repopulating assays exist, the most common of which is the competitive repopulation assay (Harrison, 1980), which measures the functional potential of the unknown source of HSCs against a known number of HSCs. Through a mathematical formula the number of repopulating units (RU) present in the donor cell population can be determined (Harrison et al., 1993; Yuan et al., 2005). This assay provides functional information about HSC capability to repopulate host compared to the competing bone marrow but do not give information about their frequency. Frequency of HSCs (from which the number of HSCs can be estimated) is commonly measured using a more complex variation of the former competitive repopulation assay which is the limiting dilution assay. In this assay, series of dilutions of the unknown donor cells compete against a defined number of competing bone marrow cells. From the number of mice showing no reconstitution in each cell dose (negative fraction) the frequency of HSCs is calculated using Poisson statistics (Szilvassy et al., 1989; Taswell, 1981). However, the limitation of this assay is the elevated number of mice required to achieve statistical significance (at least eight recipient mice per cell dose, with a minimum of three cell doses) (Szilvassy et al., 1990). The most stringent test to measure HSC potential is the serial transplantation

assay in which the testing cells are transplanted into sequential serial recipients. Only the true (most immature) HSC is capable of sustaining hematopoiesis throughout serial transplantation (Lemischka et al., 1986; Purton et al., 2006; Rosendaal et al., 1979).
Limitations to all these *in vivo* assays are their dependence upon correct homing and engraftment processes, which may be perturbed in mutant mice due to defects in the stem cell niche or to other defects without altering stem cell function *per se*. Therefore this kind of assay is informative only when homing and engraftment are not affected.

### *1.1.3.4 HSC niche*

HSCs reside in the medulla of the bone (bone marrow) within a functionally tridimensional organized structure, termed niche, which is composed by different type of cells, all together contributing to maintain the proper HSC environment and functions. The concept of the "stem cell niche" was first proposed for the human hematopoietic system in the 1970s (Schofield, 1978), and a similar concept has been further proposed for stem cells in other tissues like the epidermis, intestinal crypts, nervous system and gonads (Fuchs et al., 2004; Suda et al., 2005). The hematopoietic niche is conceptually divided into two parts: an osteoblastic niche, located near the endosteum lined by osteoblasts (OBs) (Calvi et al., 2003), and a vascular niche, in association with sinusoidal endothelium (Kiel et al., 2005).
The osteoblastic niche is mainly formed by osteoblasts (OBs), bone forming cells derived from mesenchymal stem cells, which represent a crucial component of the HSC niche in adult BM by maintaining HSC quiescence (Calvi et al., 2003; Zhang et al., 2003). Moreover not only the quiescent status of HSC but also their number is regulated by the number and/or type of osteoblasts. For example an increasing number of osteoblasts expressing N-cadherin is positively correlated with an increase in HSC number (Zhang et al., 2003).
Regarding the vascular niche a strong functional interaction between endothelial cells and HSCs has been demonstrated during development, since HSC emerge from the hemogenic endothelium. However a similar link between endothelial cells and adult BM HSCs was not evident until few years after the osteoblastic niche definition, when sinusoidal endothelial cells within the bone marrow were found strongly associated with HSCs. The association is not simply functional to provide metabolic sustenance but also provides inductive signals, thus suggesting the existence of another HSC niche (Avecilla et al., 2004; Heissig et al., 2002; Kiel et al., 2005), the so called vascular

niche, which is associated with HSC mobilization or proliferation and differentiation rather than quiescence and self-renewal. Indeed, it has been postulated that HSCs in these two niches are functionally different: in the endosteal niche HSCs appear quiescent whereas the perivascular niche seems to house actively self-renewing HSCs (Wilson et al., 2008). Thus vascular niche does not exclude osteoblastic niche since the two niches are two functional sites rather than two physical separated sites.

Besides these two conventional niches, a third niche has been further proposed, composed by hematopoietic progenitor cells surrounding quiescent HSCs. Since it is well demonstrated that progenitor cells suppress proliferation of stem cells (by unknown factors) in other tissues (Gerber et al., 2002), a similar mechanism has been hypothesized also for the hematopoietic system. When the numbers of the surrounding progenitor cells decrease within the stem cell niche, for example after a myelo-ablative therapy, quiescent HSCs might be released from inhibition and start to divide, although this has not been formally demonstrated in the hematopoietic field yet (Suda et al., 2005).

Besides the cellular composition, there is an increasing interest regarding the signaling pathways that control HSC niche function. Indeed, together with the intrinsic cellular and molecular mechanisms, which have been extensively characterized and will be later discussed, the niche is thought to participate in regulating balance between self-renewal and commitment of stem cells. Thus regulatory molecules and signaling pathways have been further studied at the molecular level. Regarding functional interaction between HSCs and OBs important regulatory molecules include cell-adhesion molecules, such as N-cadherin and β1-integrin, and chemokines or chemoattractive proteins. N-cadherin is expressed both by quiescent HSCs and osteoblasts (Arai et al., 2004), while integrins α4β1 and α5β1 are expressed only by HSCs and promote HSC adhesion to BM stromal cells (Whetton and Graham, 1999), Chemokines or chemoattractive proteins are also involved in the mobilization and interactions of stromal cells with HSCs (reviewed in (Suda et al., 2005). Among chemokines, one of the most intensively investigated is the CXC chemokine ligand 12 (CXCL12), also known as stromal cell-derived factor-1 (SDF-1) from the cells in which it is highly expressed. CXCL12, together with its receptor CXCR4, is involved in HSC homing toward the BM and in maintaining HSC quiescence (Dar et al., 2006). Deletion of genes encoding either SDF-1 or CXCR4 results in normal fetal liver hematopoiesis but failure in marrow engraftment (Nagasawa et al., 1996; Tokoyoda et al., 2004). In addition, overexpression of CXCR4 by human

hematopoietic progenitor cells, and other blood cells, enhances marrow engraftment in nude mice, whereas anti-CXCR4 antibodies inhibit it (Peled et al., 1999). However, because there are no experimental evidences of CXCR4 expression in quiescent HSCs, it is likely that factors involved in HSC engraftment are different from adhesion molecules in the osteoblastic niche. Other adhesion molecules, such as activated leukocyte cell adhesion molecule (ALCAM) (Arai et al., 2002) and osteopontin (Chen et al., 1993), are also expressed by osteoblasts and might be involved in HSC–osteoblast interactions. Also extrinsic factors, such as bone morphogenetic protein (BMP), the Notch ligand Delta and angiopoietins (Angs), are thought to participate in the functional HSC–osteoblast interactions (Suda et al., 2005). Regarding the vascular niche, angiogenic factors are thought to regulate functional interaction of HSCs with endothelial cells. Indeed, due to their common developmental origin, endothelial cells and HSCs co-express CD31, CD133 (prominin-A), Flk1 (vascular endothelial growth factor (VEGF) receptor), CD34 (the latter not in mouse long-term HSCs) and Tie2 (Rafii et al., 2002). Thus, it is suggested that ligand–receptor signaling occurs between HSCs and endothelial cells. Indeed, HSCs themselves secrete Ang-1, which induces angiogenesis (Takakura et al., 1998).

In addition to the classic osteoblast and vascular signals, other factors such as Dkk1, an inhibitor of the canonical Wnt signaling pathway (Fleming et al., 2008), thrombopoietin (Yoshihara et al., 2007) and membrane-bound SCF (Driessen et al., 2003) (see § 1.1.3.5) have been implicated in the regulation of HSC self-renewal and quiescence in stem cell niches. Of note, emerging evidences support the involvement of miRNAs. Due to the established role of miRNAs in the regulation of HSC self-renewal and differentiation, as well as their involvement in maturation of the other niche cells, it is likely that miRNAs regulate HSC niche function. Furthermore, many of the miRNA-regulated signaling pathways associated with stem cell differentiation also play an important role in HSC niches (Laine et al., 2012). The role of miRNAs in regulating HSC niche will be discussed in the specific miRNA section (§1.3.6).

### *1.1.3.5 Regulation of HSC self-renewal*

The regulation of the balance between self-renewal and commitment of stem cells is a highly regulated network controlled by a combination of cell-intrinsic and external regulatory mechanisms, in part also coming from their protective microenvironments (niche).

Maintenance of HSC self-renewal mostly involves preservation of HSC dormancy, inhibition of differentiation, and protection from detrimental outside signals (Wilson et al., 2009). Regarding the external stimuli, there are numerous signaling pathways and adhesion molecules, coming from the niche environment, that maintain HSCs in an inactive quiescent stage preserving their self-renewal potential. One of these is represented by the interaction between the membrane bound Stem Cell Factor (mbSCF) on osteoblasts with the c-Kit receptor on HSCs (Czechowicz et al., 2007). This interaction is crucial for the binding of HSCs to OBs niche, and for the maintenance of HSC dormancy and function (Thoren et al., 2008). In addition to SCF two other signaling molecules are secreted by osteoblastic niche cells: Angiopoietin1 (Ang1) and Thrombopoietin (TPO). Both act through their receptors, Tie1/2 (see below) and c-Mpl respectively, to induce HSC dormancy. Mutants lacking either of the two result in increased HSC cycling followed by ultimate loss of HSCs due to exhaustion (Arai et al., 2004; Yoshihara et al., 2007).

In detail HSCs which express the receptor tyrosine kinase Tie2 are slow-cycling stem cells and Ang-1, which is a ligand for Tie2 (Davis et al., 1996), in the adult BM is expressed primarily by OBs. Tie2–Ang-1 signaling promotes tight adhesion of HSCs to OBs and maintains HSC self-renewal by blocking cell division and promoting their quiescence (Arai et al., 2004). Through chimeric studies, with mutant embryonic cells lacking Tie proteins (Tie1 and Tie2), it has been shown that Tie family is required for postnatal but not for fetal hematopoiesis (Puri and Bernstein, 2003). There are two possible mechanisms by which the Tie2–Ang-1 pathway blocks cell division. In a direct way, following Ang-1 binding, Tie2 phosphorylation results in activation of the phosphatidyl-inositol-3-kinase (PI3-K)–Akt signaling pathway in endothelial cells (Kim et al., 2000; Shiojima and Walsh, 2002), which in turn directly promotes HSC quiescence likely by p21 phosphorilation. Indirect effect of Tie2 is mediated by enhancing HSC cell adhesion properties to stromal cells *in vitro*, in a β1-integrin-dependent manner, and to the bone surface *in vivo* (Arboleda et al., 2003). The tight attachment of HSCs to stromal cells likely affects their cell cycle status (Suda et al., 2005).

Intracellular control of HSC dormancy is regulated by other signals such as TGFβ, well known negative regulator of HSC proliferation, at least *in vitro* (Yamazaki et al., 2009). The mechanism by which this occurs seems indirect, as TGFβ inhibits cytokine-

mediated lipid raft clustering, which is essential for enhancing cytokine signals over the threshold required for HSCs re-entering in the cell cycle.

Another example of HSC quiescence mediators is pre-B-cell leukaemia transcription factor 1 (Pbx1, see also §1.2), a global developmental regulator preferentially expressed in adult HSCs rather than in MPPs. It has been shown that Pbx1 promotes proliferation in several embryonic tissues while in the adult promotes HSC quiescence. Upon Pbx1 conditional deletion, quiescence is lost with a consequent loss of long term self-renewal capacity, as shown by failure in serial transplantation assays (Ficara et al., 2008). Another protein acting in HSC quiescence is the chromatin remodeling protein Mi-2b, which regulates both gene silencing and activation through association with histone deacetylases and acetyltransferases, respectively (Wilson et al., 2009). Mi-2b inactivation causes HSCs exit of quiescence, which is accompanied by and increased and faster stem cell cycling. Moreover Mi-2b mutant BM cells fail to reconstitute likely due to HSC apoptosis and/or stem cell exhaustion (Yoshida et al., 2008). Other important regulators of HSC dormancy are Egr1 (Min et al., 2008), a transcription factors member of the immediate early response gene family, HOXB4 (Antonchuk et al., 2002), Notch1 (Varnum-Finney et al., 2000), SHH (Bhardwaj et al., 2001), Wnt (Reya et al., 2003) and p53 (Liu et al., 2009), among others. In contrast to the above mentioned mechanisms, all of which involved in maintaining HSC quiescence, the oncogene Evi-1 (ecotropic viral integration site-1) does not restrict, but promotes HSC proliferation and likely self-renewal (Goyama et al., 2008).

The balance between cycling and dormant HSCs is critical in order to maintain a self-renewing stem cell pool. Decreasing cycling, enforcing quiescence and forcing HSCs in $G_0$, lead to an insufficient production of more committed progenitors and terminally differentiated cells, finally leading in hematopoietic failure. Conversely, promoting cycling of normally quiescent HSCs leads to a sustained production of downstream progeny at the expense of self-renewal, which finally results in the inability to reconstitute due to HSC exhaustion (Wilson et al., 2009).

## 1.1.4 Multipotent and lineage restricted progenitors

In addition to HSCs, the hematopoietic hierarchy is critically dependent on various progenitors, including the transiently reconstituting multipotent progenitors (MPPs), and the downstream lineage restricted progenitors, which are characterized by increasing lineage-restriction. All these intermediate progenitors can be identified through immunophenotype analysis. Similar to HSCs, MPPs and lineage restricted progenitors are negative for lineage markers, but they can be further distinguished using other combinations of specific markers. MPPs are, as previously mentioned, a heterogeneous population (Christensen and Weissman, 2001; Kiel et al., 2005; Osawa et al., 1996) and may be divided in at least three different subgroups. MPPs are phenotypically defined as LKS/CD34$^{+}$, and can be further divided into three fractions according to Flk2 expression: Flk2$^{-}$ MPPs, previously called short-term HSCs, Flk2-intermediate MPPs (Flk2$^{int}$) and Flk2$^{high}$MPPs. MPPs negative, or with lower expression of Flk2 are progenitors with robust myeloid maturation potential (Flk2$^{-}$MPPs and Flk2$^{int}$ MPPs) while MPPs with the higher expression of Flk2 are lymphoid-primed MPPs (Flk2$^{high}$, also known as LMPPs) (Mansson et al., 2007).

Regarding lineage committed progenitors, they can be identified with a combination of other markers. CLPs are identified as Lin$^{-}$ cells that express IL7 receptor and low level of cKit and Sca-1 (thus they are Lin$^{-}$/IL7R$^{+}$/cKit$^{low}$/Sca$^{low}$), and by their high level of expression of Flk2 (Karsunky et al., 2008; Kondo et al., 1997), while CMPs can be distinguished among the c-Kit positive, but Sca-1 negative population. Within this population CMPs can be further separated from downstream GMPs and MEPs, according to the different expression of CD34 and CD16/32 (FcRγII/III) markers. In detail, CMPs are Lin$^{-}$/cKit$^{+}$/CD34$^{int}$/CD16/32$^{int}$, GMPs are Lin$^{-}$/cKit$^{+}$/CD34$^{+}$/CD16/32$^{+}$, and finally MEPs are Lin$^{-}$/cKit$^{+}$/CD34$^{-}$/CD16/32$^{-}$ (Akashi et al., 2000) (For a representative scheme of the immunophenotypical analysis of these different populations see fig 1.1.3 §1.1.3.3). Recently the heterogeneity of GMPs and MEPs has been further highlighted, and other subpopulations with higher degrees of purity have been identified (Pronk et al., 2007), with CMPs generating Pre GM immediately upstream of GMPs, and with MEP now comprising a hierarchy having Pre MegE at the top, which give rise to Pre CFU-E and to MkP (Megakaryocyte Precursors).

Correct regulation of multi potent and lineage restricted progenitors is fundamental to guarantee a constant and adequate pool of undifferentiated cells which are able to

perform a rapid proliferative expansion in responses to peripheral stresses such as infection or bleeding. This rapid response is especially important in the myeloid lineage, given the short life span of granulocytes and monocytes, and the lack of 'memory' cells in contrast to the lymphoid lineage. Moreover it has been proposed that lineage-restricted progenitors may serve as targets for oncogenic transformation. In addition to their intrinsic proliferative capacity they might acquire upstream stem cell properties normally lost during differentiation, like unlimited self-renewal capacity, which ultimately confer them leukemia stem cell potential (Cano et al., 2008; Cleary, 2009; Krivtsov et al., 2006; Minami et al., 2008; Signer et al., 2010; Somervaille et al., 2009; Tremblay et al., 2010; Wojiski et al., 2009). Thus it is important to understand whether factors regulating HSC self-renewal, such as Pbx1, are also implicated in maintaining progenitor reservoirs.

### 1.1.5 Regulation of hematopoiesis

As a stem cell matures it undergoes changes that progressively limit its multipotency and make it closer to a specific cell type. All differentiation programs are tightly regulated both by external signals and lineage specific regulators. Regarding the external stimuli, three main factors stimulating production of committed stem cells, called colony-stimulating factors (CSFs), exist. They include granulocyte-macrophage CSF (GM-CSF), granulocyte CSF (G-CSF) and macrophage CSF (M-CSF), all of which are active on either progenitor cells or more mature cells. To drive myeloid progenitors towards the megakariocytic/erithroid lineage, erythropoietin is required for erythrocyte differentiation while thrombopoietin for megakaryocytes differentiation (specifically to obtaining thrombocyte-forming cells) (Harvey Lodish, 2012). Other relevant hematopoietic factors are the interleukins, a group of multifunctional cytokines, which act at different level of the hematopoietic hierarchy mainly driving lymphoid lineage differentiation and activation. Among them IL-3 exerts a pleiotropic activity supporting proliferation and differentiation of a wide spectrum of hematopoietic cells (Ihle, 1992). IL-3 stimulates the differentiation of multipotent hematopoietic stem cells into myeloid progenitor cells and, in combination with IL-7, into lymphoid progenitor cells. Moreover IL-7 in combination with other cytokines further modulates differentiation and activation of lymphoid progenitor cells into B and T lymphoid cells

(Ceredig and Rolink, 2012). These factors are added in cell culture media in the different *in vitro* differentiation assays.

Cytokines act through specific signal transduction pathways that activate lineage specific transcription factors (TFs) which in turn modulate proper gene expression pattern to drive differentiation. Several lineage specific TFs have been identified that regulate critical steps in hematopoiesis and their expression can be generally reconciled with the simple hierarchical hematopoietic tree. The key lineage-restricted TFs are endowed with the complementary roles of promoting their own lineage differentiation while simultaneously preventing other choices (reviewed in (Orkin and Zon, 2008). Numerous TFs acting in this alternative lineage programming mechanism have been described. For example GATA-1 and PU.1 promote erythroid/megakaryocytic/eosinophil and myeloid differentiation, respectively. The two proteins physically interact and antagonize each other (Galloway et al., 2005; Rhodes et al., 2005). One of the most striking example of lineage selection repression is provided by Pax5, a TF normally required for proper B-cell development (Adams et al., 1992; Nutt and Kee, 2007; Urbanek et al., 1994). Pax5-null B cell-progenitors assume a multipotential phenotype and fail to restrict their lineage choice (Nutt et al., 1999). Under appropriate growth factor conditions, mutant B cell progenitors develop into several hematopoietic cell types, including macrophages, osteoclasts, granulocytes T-, NK-, or dendritic cells and even erythroid precursors. So, commitment to B-cell development is driven by Pax5 and involves suppression of alternative lineage choices (Busslinger et al., 2000; Orkin, 2000).

Beyond their presence or absence, TFs can influence lineage choice and differentiation also in a concentration-dependent manner. The level of GATA-1 regulates lineage outcome in the transformed chicken progenitor system (Kulessa et al., 1995), with eosinophils formation at lower levels of GATA-1, and erythroid and megakaryocytic development at higher levels. These findings have been demonstrated also in mice (McDevitt et al., 1997). PU.1 also regulates differentiation in a concentration-dependent manner, since high levels of PU.1 favors macrophage development, while low levels B cells development (DeKoter and Singh, 2000; Orkin, 2000).

Besides TFs, an additional level of regulation is provided by microRNAs (miRNAs) (Shivdasani, 2006; Stadler and Ruohola-Baker, 2008) which have been demonstrated to play a central role in controlling all the different stage of hematopoiesis. Specific miRNAs are highly expressed in specific hematopoietic lineages and manipulation of

their levels correlates with strong defects in cellular properties or differentiation (Chen et al., 2004). For example, miR-150 regulates B cell differentiation (Xiao et al., 2007), whereas miR-155 is required for T helper cell generation and germinal center activity (Rodriguez et al., 2007; Thai et al., 2007). Detailed role of miRNAs in hematopoiesis is discussed in the specific session (§1.3.5 and §1.3.6), however in summary, TFs and miRNAs may regulate each other in a complex regulatory network acting in concert in lineage decisions, stem cell to progenitor transitions, and niche control.

# 1.2 The Pbx1 transcription factor

Pbx1 (pre-B-cell leukaemia transcription factor 1) is the product of a proto-oncogene originally discovered at the site of a chromosomal translocations in a pediatric B acute lymphoblastic leukaemia (B-ALL), where Pbx1 is fused with E2a leading to the formation of an oncogenic protein (Kamps et al., 1990; Nourse et al., 1990). Pbx1 is a transcription factor that binds DNA in complex with a wide subset of homeodomain proteins (like Hox, Meis and Prep, the last also known as PKnox), with which it forms hetero-oligomeric complexes (Moens and Selleri, 2006). In these dimeric and/or trimeric complexes, Pbx1 critically regulate developmental gene expression through modulation of Hox proteins binding and specificity to DNA, thus finely modulating their transcriptional effector functions in a context-dependent way (Saleh et al., 2000). It has recently been highlighted that Pbx1 also functions through other Hox-indipendent mechanisms to regulate gene expression. Moreover it may act marking specific genes for activation by penetrating repressive chromatin before other proteins that are later recruited as co-activators (Berkes et al., 2004). By modulating gene expression it regulates numerous embryonic processes, including morphologic patterning, axes specification and correct organogenesis. It is involved for example in skeletal patterning, pancreas development, nephrogenesis and ureteric branching in the developing kidney, and in hematopoiesis (DiMartino et al., 2001; Kim et al., 2002; Manley et al., 2004; Schnabel et al., 2003a; Schnabel et al., 2003b; Selleri et al., 2001). Pbx1 exerts different roles in development and adult life. During embryogenesis, it has been shown that Pbx1 promotes progenitor proliferation in multiple tissues (Moens and Selleri, 2006), including the hematopoietic system (DiMartino et al., 2001), while in the adult it positively regulates HSC quiescence (see §1.2.4).
As mentioned, Pbx1 was originally isolated as a proto-oncogene due to its disruption in a t(1:19) chromosomal translocations, in a subset of pediatric acute lymphoblastic leukemias. In detail, the t(1;19) rearrangement determines the fusion of the Pbx1 homeodomain with the transcriptional activation domains of the immunoglobulin enhancer–binding protein E2a (Kamps et al., 1990; Nourse et al., 1990). The derived E2a-Pbx1 chimeric oncoprotein retains the ability to bind DNA in complex with Hox, but not with other Pbx1 partners like Meis proteins (Chang et al., 1997), and causes aberrant proliferation of hematopoietic progenitors, finally leading to the leukemic

transformation by aberrant activation of Pbx1/Hox target genes (DiMartino et al., 2001; Moens and Selleri, 2006).

## 1.2.1 Pbx1 classification and structure

Pbx1 and the other Pbx proteins (Pbx2, Pbx3 and Pbx4) are mammalian homologues of the extradenticle (Exd) protein, first identified as cofactor for homeobox (Hox) transcription factors in Drosophila (Rauskolb et al., 1993). In addition to Hox, Pbx proteins form complexes with other homeodomain proteins like Meis and Prep, which have a role in controlling nuclear localization and promoting alternative DNA binding pattern (Berthelsen et al., 1999; Chang et al., 1997; Gonzalez-Crespo et al., 1998) (Figure 1.2.1).

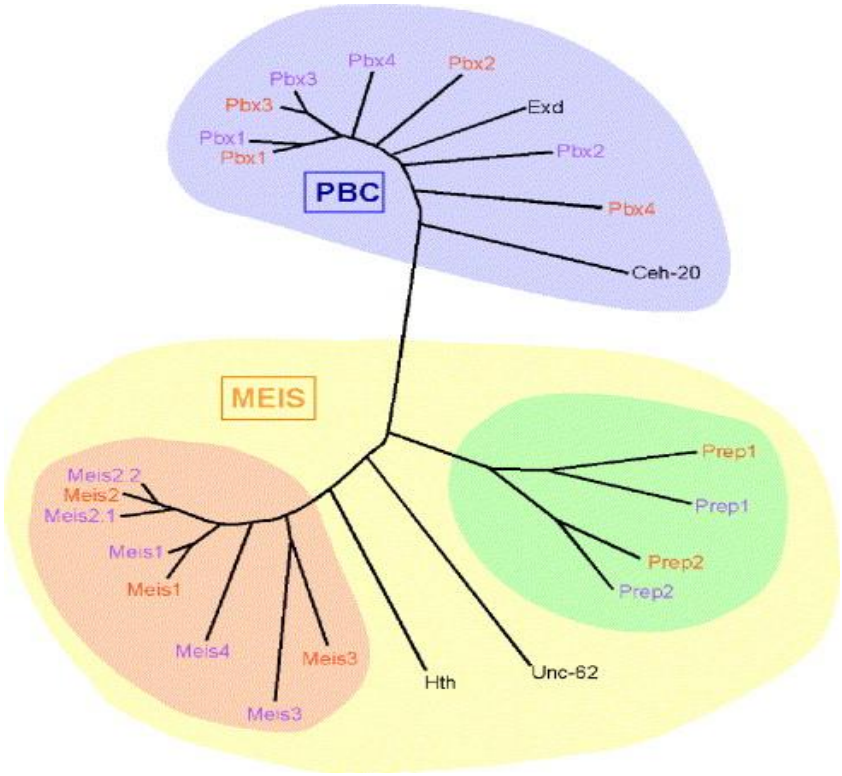


**Figure 1.2.1 Phylogeny of Hox cofactors**. TALE homeodomain proteins are divided into two groups: the PBC family, including the vertebrate Pbx proteins, fly Extradenticle and worm Ceh-20, and the MEIS family, including vertebrate Meis and Prep, fly Homothorax (Hth) and worm Unc-62. Orange letters indicate mouse proteins, purple lettering indicates their zebrafish orthologs (from Moens and Selleri, 2006).

Structurally Pbx1 belongs to the TALE (Three-Amino acid Loop Extension) superfamily of homeodomain transcription factor. Among this big TALE family, Pbx1 is further classified in a particular subclass designed as the PBC subfamily, due to a

conserved PBC motif which is N-terminal to the TALE homeodomain (Burglin, 1997, 1998) (Figure 1.2.1 and 1.2.2). The PBC subclass comprises the proteins Pbx1, Pbx2, Pbx3 (Monica et al., 1991) and Pbx4 in mammals (Wagner et al., 2001), Lazarus or Lzr in zebrafish (Popperl et al., 2000; Waskiewicz et al., 2001), as well as Extradenticle (or Exd) in Drosophila and Ceh-20 in *C. elegans* (Shanmugam et al., 1999; Shen et al., 1999) (reviewed in (Laurent et al., 2008).

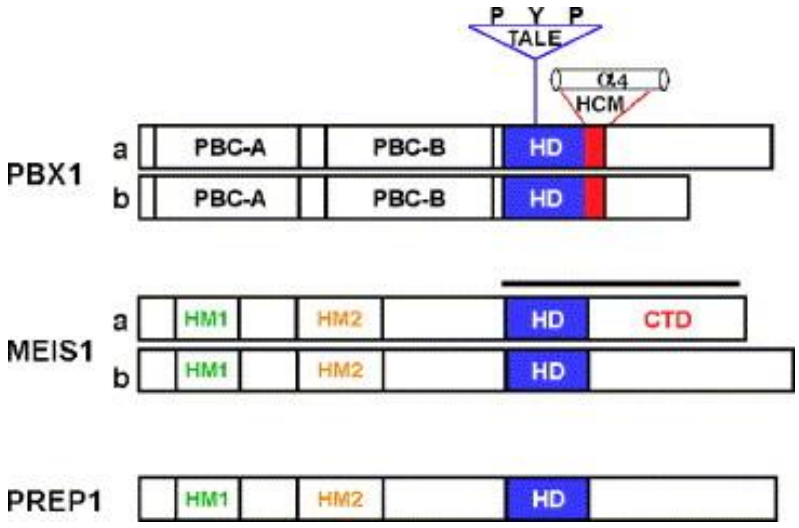


**Figure 1.2.2 Structure of TALE homeodomain proteins.** Prototype members of PBC and MEIS classes are shown here. ‘‘a’’ and ‘‘b’’ refer to splice isoforms of Pbx and Meis proteins. See text for details. (from (Moens and Selleri, 2006)).

All TALE homeodomain proteins are characterized by this divergent homeodomain (HD) composed by a 3 amino acid loop extension (TALE) located between the first and second a-helices. The TALE motif virtually always contains a proline (P)– tyrosine (Y)– proline (P) in positions 24– 26 (Burglin, 1997, 1998) (Figure 1.2.2), which is the domain responsible for the interaction with the hexapeptide motif of Hox proteins (Piper et al., 1999). The HD contains a DNA-binding motif and interacts with a subset of different Hox proteins, enhancing their DNA binding affinities and specificities. Tale proteins act together in a complex transcriptional regulatory network whose function *in vivo* is not fully understood, since most of the data about DNA sequence specificity of these factors are based on *in vitro* studies and on the analysis of a limited number of endogenous target sequences. The *in vivo* binding property of these proteins is more complex, since Pbx proteins and their partners have preferential functional interactions that also change their DNA binding site specificity (see also §1.2.3).

## 1.2.2 Pbx1 isoforms

Pbx2 and Pbx3 were discovered on the basis of their homology to Pbx1, while Pbx4 was first identified in zebrafish as a mutant in which Hox-dependent patterning events were disrupted (Popperl et al., 2000; Waskiewicz et al., 2002). Subsequently, Pbx4 gene has been identified in mammals. Pbx4 is expressed exclusively in the testis (Wagner et al., 2001) and is not orthologous to zebrafish pbx4 (Moens and Selleri, 2006). Pbx1, Pbx2, Pbx3 and Pbx4 genes encode products with high level of sequence identity. Alternative splicing of these genes leads either to larger (Pbx1a, Pbx2, Pbx3a and Pbx4) or shorter (Pbx1b, Pbx3b, Pbx3c and Pbx3d) isoforms (Milech et al., 2001; Monica et al., 1991; Wagner et al., 2001). The different Pbx proteins and isoforms can be discriminated on the basis of biochemical studies, either by their DNA binding properties or their dimerization capacity. First, Pbx proteins show different DNA binding properties. Indeed, although *in vitro* they recognize the same DNA consensus sequence, Pbx1 is not able to bind DNA without partners, while Pbx2 and Pbx3 can do it. Second, there are some differences in the homo dimerization ability of Pbx proteins. Some studies demonstrated that homodimerization is only a Pbx3 capability (Neuteboom and Murre, 1997), while others reported it also for Pbx1a and Pbx1b (Calvo et al., 1999). However, all these studies are based only on *in vitro* approaches and the results remain controversial. Nevertheless the Pbx homodimerization could be important for gene regulation through a competitive mechanism between Pbx itself and various partners for binding to specific gene promoters (Laurent et al., 2008).

Regarding the functions of these different Pbx genes, the early studies reported in zebrafish suggested that the functional differences between Pbx isoforms are likely due to differences in their expression rather than in their activities (Popperl et al., 2000). Consistent with this observation, the *in vitro* DNA-binding properties of different Pbx proteins appear very similar (Chang et al., 1996). Nevertheless in mammals the situation appears more complex and there are several evidences of functional differences among the different Pbx isoforms. Indeed with the differential splicing Pbx proteins loose functional domains leading to proteins with different function and dimerization capabilities (Ferretti et al., 1999).

Another example of divergent properties between different Pbx isoforms comes from studies on interaction between Pbx1 and the pancreatic specific homeodomain factor Pdx1 (Peers et al., 1995). The dimer Pdx1/Pbx1b acts as a transcriptional activator through the Pdx1 activation domain, while the other dimer Pdx1/Pbx1a acts as a

transcriptional repressor complex. The difference is due to different capability of co-repressors recruitment. Indeed, the Pbx1a isoform possesses a C-terminus domain that binds co-repressor proteins SMRT and NcoR, while the Pbx1b isoform lacks this domain and is consequently unable to recruit these factors (Asahara et al., 1999). In addition to their different biochemical properties, Pbx isoforms exhibit also some specificity in expression pattern both in a tissue specific and developmental specific manner. For example Pbx1a isoform is restricted to the brain, whereas Pbx1b is expressed in the whole body. Furthermore, Pbx1b is the major embryonic isoform while Pbx1a is found mostly during adulthood (Schnabel et al., 2001). Moreover, expression of some Pbx isoforms seems to be preferential in certain pathologic contexts. Indeed, expression of Pbx3d is observed in normal cells, whereas Pbx3c expression is mostly found in leukaemia cells (Milech et al., 2001) (reviewed in (Laurent et al., 2008).

## 1.2.3 Pbx1 partners

***Hox proteins***

The best known class of Pbx1 partners is the Hox protein family. Hox proteins form a family of transcription factors, characterized by a very highly conserved DNA-binding homeodomain (HD), that specify antero-posterior identities during development throughout the animal kingdom. In mammalians there are 39 Hox genes, classified in 13 paralog groups within four separate clusters (A, B, C and D). Although these proteins regulate developmental programs in a very specific manner, they all bind *in vitro* to a TAAT core sequence which is very frequent along the DNA and occurs approximately once every 500 base pair within the genome (Galant et al., 2002). Chromatin Immunoprecipitation (Calvi et al.) experiments performed *in vivo* to search Hox target genes confirmed that these proteins bind DNA in a widespread fashion on TAAT sequences (Carr and Biggin, 1999; Walter et al., 1994; Williams et al., 2005). Moreover the binding affinity is not very high. To explain this apparent paradox between the low DNA specificity and the high specificity in regulating distinct developmental programs of these proteins, a “quantitative model” was hypothesized, according to which the level of Hox proteins could be more important rather than their nature (Duboule, 2000). This theory is consistent with some elegant experiments in which the coding sequence of mouse Hoxa3 and Hoxd3 genes were exchanged, showing a total functional equivalence between the two paralogs (Greer et al., 2000). However, other data clearly demonstrate

that the quantitative model is not exhaustive and that there are specific differences in the biochemical properties of Hox proteins, which specifically regulate their function. For example mice in which the Hoxa11 HD has been exchanged with the Hoxa13 HD exhibit an abnormal development, resulting from a Hoxa13 posterior mediated phenotype (Zhao and Potter, 2001). These data demonstrate that, despite the HD is highly conserved and some Hox proteins could have overlapping functions, there are some differences which lead nevertheless to a different regulation of genetic programs. Another explanation for the low Hox DNA binding specificity is that it increases and changes according to recruitment of different cofactors. Indeed, oligomerization with TALE cofactors increases Hox DNA binding specificity since Hox/Pbx DNA sites occur once every 8,200 base pair and Hox/Pbx/Meis once every 420,000 base pairs (Laurent et al., 2008).

***Meis and Prep***

Another class of TALE homeodomain proteins, which regulates both Hox and Pbx activities, is the Meis/Prep subclass (Berthelsen et al., 1998; Burglin, 1998; Chang et al., 1997; Chen and Capecchi, 1997; Knoepfler et al., 1997; Moskow et al., 1995). The MEIS class includes Homothorax (Hth) in flies and the Meis and Prep proteins in vertebrates (Figure 1.2.1). Meis/Prep proteins interact directly with Pbx proteins and are important for the DNA binding of the Pbx/Hox complex, recognizing a specific sequence on the regulatory regions of target genes (Ebner et al., 2005; Ferretti et al., 2000; Jacobs et al., 1999; Mann and Affolter, 1998; Ryoo et al., 1999). Moreover, Meis/Prep proteins are involved in nuclear targeting (Abu-Shaar et al., 1999; Berthelsen et al., 1999; Jaw et al., 2000; Mercader et al., 1999; Rieckhof et al., 1997) and stability (Jaw et al., 2000; Longobardi and Blasi, 2003; Waskiewicz et al., 2001) of Pbx proteins (reviewed in (Moens and Selleri, 2006). As mentioned above, Pbx1 interacts with Meis1/pKnox1 predominantly with the N-terminal domain. The architecture of the Pbx1/Meis1–DNA complex is similar to that of Pbx/Hox–DNA complexes but with some differences. Meis1, like Hox proteins, is thought to bind 3’ of the TGAT Pbx1 half-site but DNA-binding specificity and stability of Pbx/Meis complexes are very different from those of Pbx/Hox complexes, since they equally recognize some DNA motif while specifically some others. Therefore Pbx/Meis and Pbx/Hox complexes could regulate either distinct or overlapping subsets of genes (Knoepfler et al., 1997).

Both Prep1 and Meis1 dimerize with Pbx and recognize similar DNA sequences *in vitro* but there are some functional differences in the region where they bind. While Prep1 interacts preferentially with promoters and nearby regions, Meis shows preferential binding for intergenic and intragenic regions away from transcription starting site regions. Prep could thus be directly involved in regulating promoter, while Meis sites coincides with enhancers functions. In addition, Prep mostly participates in dimer formation with Pbx, while Meis is predominantly found in trimeric complexes together with Pbx/Hox (Penkov et al., 2013).

Since Pbx1 is also able to bind to Meis/Prep proteins but in interaction surfaces independent from those of Hox, it can form trimers with Prep or Meis and Hox, thus further modulating the DNA-binding selectivity of the individual proteins (Ferretti et al., 2000; Jacobs et al., 1999; Penkov et al., 2013; Ryoo et al., 1999).

While earlier work on *in vitro* Pbx1-Hox binding sites suggested that the sequence specificity of a given Pbx/Hox complex was defined (Chan et al., 1997; Ryoo et al., 1999), more recent evidences have indicated that the sequence requirements for DNA binding by Hox complexes are difficult to predict (Ebner et al., 2005). The complexity is based not only on the multiple possible combinations between Pbx and the numerous members of the Hox family, but also on the existence of various isoforms of Pbx proteins. Indeed, most of the studies on Hox/Pbx interactions were performed with Pbx1, or the drosophila analogue Exd, while other PBC proteins were assumed to behave identically (Laurent et al., 2008).

***Other Pbx1 binding proteins***

Increasing evidences showed that Pbx function is not restricted to partnership with Hox or other homeodomain proteins. A recent two-hybrid screen revealed that only 6% of putative Pbx1 partners correspond to homeodomain proteins and only 18% are transcription factors. For example other Pbx interacting proteins are involved in cytoskeleton assembly and/or regulation (Huang et al., 2003). The increasing amount of non-homeodomain Pbx1 partners points out that Pbx proteins exert some of their roles in development via still unexplored Hox-independent pathways (Laurent et al., 2008).

## 1.2.4 Pbx1 in hematopoiesis

In the hematopoietic system Pbx1 shows different roles in the embryo compared to the adult. During murine development Pbx1 is expressed in hematopoietic progenitors, where it promotes their proliferation, and its absence results in severe anemia and embryonic lethality at embryonic day 15 (E15) or E16 (DiMartino et al., 2001). Conversely, in the adult it is preferentially expressed in HSCs compared MPPs (Forsberg et al., 2005; Kiel et al., 2005), and positively regulates their quiescence. Postnatal hematopoiesis is profoundly perturbed in the absence of Pbx1, with severe reduction of HSCs due to an extreme self-renewal defect leading to non-functional stem cells (Ficara et al., 2008). Indeed, using two Pbx1 conditional knockout mouse models, it was demonstrated that its absence in postnatal HSCs causes their excessive proliferation and premature differentiation, ultimately leading to their exhaustion, an effect possibly mediated by perturbation of the TGFβ pathway. In addition to the HSC defect, Pbx1 conditional knockout mice also exhibit significant reductions in multi-potent and lineage-restricted progenitors, both common myeloid progenitors (CMPs) and common lymphoid progenitors (CLPs) (Ficara et al., 2008). The role of Pbx1 in multi-potent and lineage restricted progenitors will be the object of the result section (§3.1).

## 1.2.5 Pbx1 knock-out (KO) mouse models

The study of Pbx functions takes advantage from several mouse models in which individual Pbx proteins are constitutively or conditionally deleted.

Constitutive KO for Pbx1, 2 and 3 have been generated (Rhee et al., 2004; Selleri et al., 2001; Selleri et al., 2004). Some of these mice show partially overlapping phenotypes, indicating some redundant Pbx functions. In addition, while Pbx1 KO mice (especially those with no Pbx1 or Pbx3) exhibit some overlapping features with Hox deficient mice, thus highlighting the role of Pbx proteins as Hox cofactors, they do not perfectly phenocopy single or multiple mutants for Hox genes, showing also Hox-indipendent Pbx functions (Laurent et al., 2008).

Constitutive Pbx1 KO mice die at E15.5/16.5, displaying severe hypoplasia (lungs, liver, stomach, gut, kidneys and pancreas), ectopia (thymus and kidneys) or aplasia of multiple organs (spleen, adrenal gland), as well as widespread skeletal malformations

(Selleri et al., 2001). Pbx3-deficient mice die a few hours after birth from central respiratory failure due to abnormal activity of inspiratory neurons where Pbx3 is highly expressed (Rhee et al., 2004). In contrast with the premature death of Pbx1 or Pbx3 KO mice, Pbx2-deficient mice are viable and display no evident phenotype, despite the widespread expression of the gene during embryogenesis (Selleri et al., 2004). This suggests that loss of Pbx2 is compensated by other Pbx members.

Since Pbx1 KO mice are embryonic lethal, to study its function in the adult it is necessary to conditionally inactivate it. For the experiments described in the Results session two Pbx1-conditional KO mouse models were used, $Tie2Cre^{+}.Pbx1^{-/f}$ mice and $Mx1Cre^{+}.Pbx1^{-/f}$ mice. To generate both models Floxed-Pbx1 ($Pbx1^{f/f}$) mice are intercrossed with mice expressing Cre recombinase under a specific promoter able to induce Pbx1 deletion starting from HSCs (Joseph et al., 2013).

In the $Tie2Cre^{+}.Pbx1^{-/f}$ mice, that we used in the present study, Pbx1 deletion occurs specifically in HSCs and endothelial cells starting early during development, in the AGM region. In detail, these mice are obtained by intercrossing homozygous Pbx1 floxed mice ($Pbx1^{f/f}$), in which Pbx1 gene is flanked by Lox-P sites, with $Tie2Cre^{+}.Pbx1^{+/-}$ mice, harboring a heterozygous deletion in the Pbx1 allele (Selleri et al., 2001) and the Cre recombinase under the control of the Tie2 promoter (Figure 1.2.3). $Tie2Cre^{+}.Pbx1^{+/-}$ mice are obtained in our animal house by crossing $Tie2Cre^{+}$ with $Pbx1^{+/-}$ mice (see matherials and meyhods, §5.1).

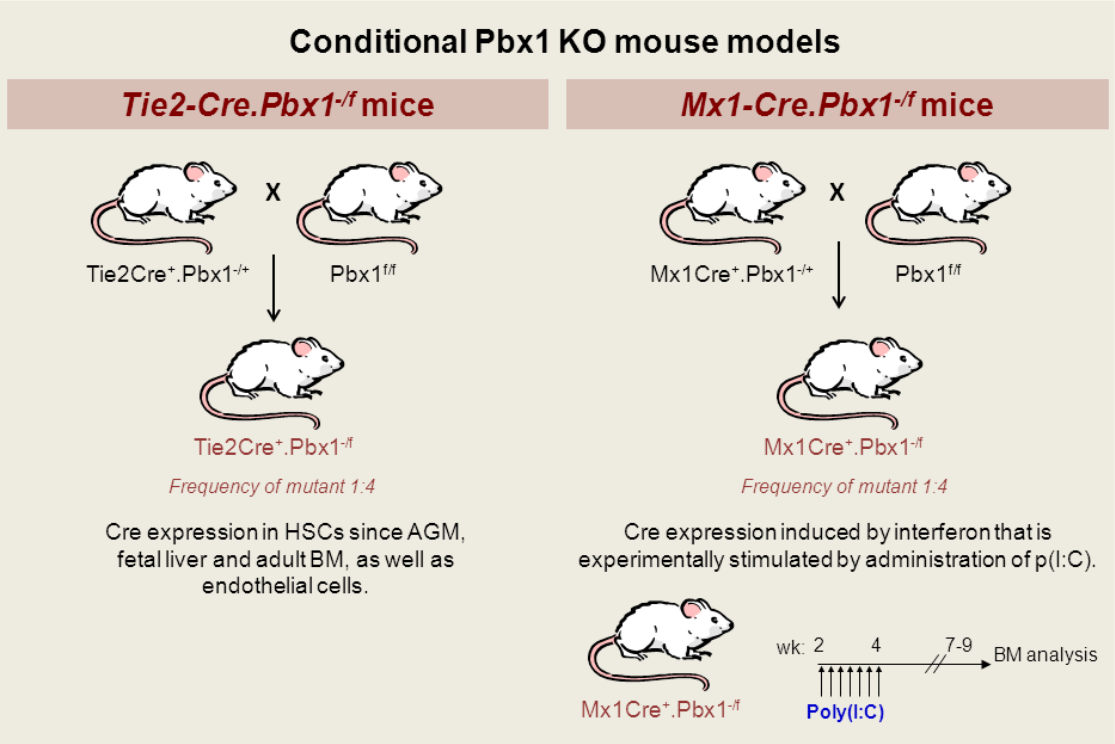


**Figure 1.2.3 Crossing scheme to generate Pbx1 conditional KO mice.** Mutant mice are generated by crossing $Pbx1^{f/f}$ mice with mice expressing Cre recombinase under a specific promoter able to induce Pbx1 deletion in HSCs. Bottom right: schematic representation of pharmacological Cre induction by poly(I:C) treatment in $Mx1Cre^{+}.Pbx1^{-/f}$ mice. $Tie2Cre^{+}.Pbx1^{+/-}$ and $Mx1Cre^{+}.Pbx1^{+/-}$ breeders are not commercially available and need to be generated by crossing $Cre^{+}$ mice with $Pbx1^{+/-}$ mice. Those lines are then maintained by intercrossing with C57BL/6 *wt* mice.

*Tie2* encodes a tyrosine kinase receptor specific to angiopoietin which is expressed both by endothelial cells, where it is important for angiogenesis (Maisonpierre et al., 1997; Schnurch and Risau, 1993), and by hematopoietic cells, where it plays a critical role in HSC quiescence (Arai et al., 2004; Takakura et al., 1998). Consistent with the role of Tie2 in angiogenesis and hematopoiesis, Cre-recombinase under the control of the Tie2 promoter (as in Tie2Cre mice) specifically drives Cre expression in endothelial cells and HSCs (Chang et al., 2004; Constien et al., 2001; Kisanuki et al., 2001; Tang et al., 2010). In our model, one Pbx1 allele is constitutively deleted while the other is floxed. In this way Cre-mediated Pbx1 inactivation is more efficient. When Cre recombinase is expressed, tissue-specific inactivation of Pbx1 is achieved, due to deletion of exon 3 of the floxed allele. With this crossing scheme (Figure 1.2.3, left) 25% of mutant mice are obtained. $Tie2Cre^{+}.Pbx1^{-/f}$ mice are viable but display a short life span and die of unknown causes between 3 and 7 weeks of age.

Another Pbx1 KO mouse model is the $Mx1Cre^{+}.Pbx1^{-/f}$ inducible KO (Figure 1.2.3, right). In this model $Pbx1^{f/f}$ mice are crossed with the inducible $Mx1Cre^{+}$ line in which the Cre expression is driven by the Myxovirus resistance-1 (Mx1) promoter. Mx1 is a

component of the defense mechanism against viruses and its expression can be highly induced in response to type I interferon. Cre recombinase under the control of the Mx1 promoter can be pharmacologically activated by the administration of Poly(I:C), a synthetic analog of double-stranded RNA (dsRNA) (Kuhn et al., 1995). Poly(I:C) is recognized by toll like receptor 3 (TLR3) and mimics a viral infection leading to the activation of NF-kB and the production of cytokines, which in ultimate activate the interferon-inducible Mx promoter and, in this case, the consequent deletion of the Pbx1 gene.

The two models are equivalent in term of the resulting HSC phenotype (Ficara et al., 2008), although in The Mx1-Cre models in a minority of cells Pbx1-deletion does not occur. Despite this functional equivalence there are advantages and disadvantages in using these two mouse models, which make them more useful for some experiments than others. Mice with complete deletion of Pbx1, like in the $Tie2Cre^{+}.Pbx1^{+/f}$ model, display severe defects in lineage restricted progenitors (CLPs and CMPs) in addition to HSCs (Ficara et al., 2013; Ficara et al., 2008), and therefore, even if they are more difficult to manage, due to their precocious death and the fact that their BM have fewer cells, represent the ideal system for studying Pbx1 function not only in the HSC compartment but also in their downstream progenitors. Conversely, the $Mx1Cre^{+}.Pbx1^{-/f}$ model gives the advantage, being inducible, to delete Pbx1 when mice are adult enabling an easier management of the mouse colony and, more important, a higher number of cells, since Pbx1-null HSCs can be analyzed prior to their exhaustion (that occurs as a consequence of Pbx1 deletion). On the other hand, even if Pbx1 deletion is quite efficient in HSCs from the inducible model, the very few un-deleted cells have a selective advantage in generating downstream progeny. Thus this model is not suited for the experiments performed with progenitors downstream to HSCs.

# 1.3 Micro-RNAs

MicroRNAs (miRNAs) are small (18-24 nucleotides) endogenous single-stranded non-protein coding RNA molecules that have emerged as crucial transcriptional and posttranscriptional regulators of gene expression. They act by binding messenger RNA (mRNA) sequences through an imperfect match, mostly in the 3'UTR of the transcript (Ambros, 2004; Chen and Rajewsky, 2007). Their binding to the mRNA target leads either to mRNA degradation or to the inhibition of its translation into protein, ultimately resulting in gene silencing (Baek et al., 2008; Bartel, 2004; Rana, 2007).

The first miRNAs were identified in the early 1990s in *C. elegans* (Lee et al., 1993). However they were not recognized as a distinct class of biological regulators with conserved functions until 2001, when the term "microRNA" was used for the first time. Indeed at that time this mechanism of gene regulation was thought to be restricted to nematodes rather than to be a broad evolutionary conserved process. Since their discovery a lot of progresses have been made in studying miRNA expression and in understanding their function and mechanisms of action, and thousands of miRNAs have been found in many other organisms, from plants to mammalians. In plants and animals, although core components of the microRNA pathway are highly conserved, there are some differences in miRNA function and biogenesis, suggesting that they arose independently in the two kingdoms. Plant miRNAs usually have perfect or near-perfect pairing with their mRNA targets and induce gene repression through degradation of their target transcripts (Brodersen et al., 2008; He and Hannon, 2004). Moreover plant miRNAs may bind their targets both in coding regions and untranslated regions (He and Hannon, 2004). In contrast, animal miRNAs typically have only partial complementarity to their target, and induce their down regulation both by inhibition of translation and mRNA degradation. In addition, most of the animal miRNAs bind to the 3'UTR of their targets. Regarding prokaryota, whilst short RNA sequences (50 – hundreds of base pairs) of a broadly comparable function occur in bacteria, bacteria lack true microRNAs (Fahlgren et al., 2010).

By finely affecting gene regulation, miRNAs are likely to be involved in several biological processes, starting from development to adult life. It is now well established that they are involved in the proper function of different organs and tissues (Brennecke et al., 2003; Chen et al., 2004; Cuellar and McManus, 2005; Harfe et al., 2005; Lagos-Quintana et al., 2002; Lim et al., 2005; Poy et al., 2004; Wilfred et al., 2007) and that

they are key regulators in several critical cellular processes including proliferation, cell cycle progression, metabolism, survival, apoptosis and response to changes in environment (Bartel, 2009). Moreover, miRNAs have been shown to be important regulators of stem cell development by playing a critical role both in their maintenance and differentiation (Yi and Fuchs, 2011).

As transcription factors, different sets of miRNAs are expressed in different cell types and tissues, and misregulation of their expression is also associated with several diseases including cancer where miRNAs could have tumour suppressive or tumour promoting functions depending on the nature of their target mRNAs (Calin and Croce, 2006). Regarding the role of miRNAs in disease, there are also new emerging miRNA-based therapies under investigation (Trang et al., 2008).

According to Sanger miRNA registry (miRBase version 20), 1186 precursors and 1908 mature miRNAs have been identified in the mouse genome to date, which may target about 60% of the genes (Friedman et al., 2009; Lewis et al., 2005), making them one of the most abundant class of gene-regulatory molecules in animals. Each miRNA could repress the expression of many, perhaps hundreds, of target genes, and one gene could be regulated by several miRNAs, thus leading to a widespread change in gene expression and highlighting the extent of this form of regulation in mammals (Berezikov et al., 2005; Selbach et al., 2008).

### 1.3.1 Nomenclature

There is a standard nomenclature system for miRNAs, strictly regulated by the miRBase Registry on the basis of established guidelines (Ambros et al., 2003). In order to minimize gaps and misunderstanding in the naming scheme, and to guarantee the validity of submitted miRNAs through a peer review process, names are assigned by the Registry after a manuscript describing their discovery is accepted for publication. Official gene names should be incorporated into the final version of the manuscript. The nomenclature guidelines require that novel miRNA genes are experimentally verified by cloning or with evidence of expression and processing (except for homologous miRNAs from related organisms identified by sequence analysis methods, the name of which can be assigned without further experimental evidence) (Ambros et al., 2003; Griffiths-Jones et al., 2006; Griffiths-Jones et al., 2005). According to these rules, microRNA are named with the prefix "mir" followed by a dash and a number which often indicates progressive order of naming. The uncapitalized "mir" refers to the pre-miRNA, while a

capitalized "miR-" refers to the mature form. An additional lower case letter following the main identification number identifies miRNAs with nearly identical sequences except for one or two nucleotides. For example, miR-123a would be closely related to miR-123b. Regarding the precursors, pre-miRNAs that give rise to identical mature miRNAs but are located in different sites in the genome are indicated with an additional dash-number suffix, always following the main identification number. For example, the pre-miRNAs mir-194-1 and mir-194-2 lead to an identical mature miRNA (miR-194) but are located in different genome regions. When two different mature microRNAs arise from the two opposite arms of the same pre-miRNA, they are identified with a -3p or -5p suffix, and when the relative expression levels of the two forms are known, an asterisk following the name indicates the miRNA expressed at lower levels relative to the miRNA in the opposite arm of a hairpin. For example, miR-123 and miR-123* would share a common pre-miRNA hairpin, but miR-123 would be found higher expressed. The species of miRNAs origin is designated with a prefix of three-letter, e.g., mmu-miR-123 is a mouse (*Mus musculus*) miRNA and hsa-miR-123 is a human miRNA. There are also other common prefixes including 'v' for viral, which are miRNA encoded by a viral genome, and 'd' for Drosophila miRNA.

## 1.3.2 miRNA biogenesis and mechanisms of action

Mature miRNAs are generated by multiple processing steps of sequential endonucleolytic cleavages (Figure 1.3.1), which occur in part into the nucleus and in part into the cytoplasm. Micro-RNA genes are encoded by genomic DNA and can be found either within protein coding genes, both in introns and exons, or transcribed from their own genes in intergenic regions. The majority of characterized miRNA coding sequences are intergenic or oriented antisense to neighboring genes. However, as much as 40% of miRNA coding sequences may lie in the introns of protein and non-protein coding genes or even in exons of long non protein-coding transcripts (Lau et al., 2001). In the latter case the microRNA sequence could be transcribed together with its host gene leading to a coupled regulation of miRNA and protein-coding gene. Other miRNA genes show a common promoter and their transcription gives rise to a polycistronic unit containing multiple discrete loops, from each of which mature miRNAs are processed (Reinhart et al., 2000; Rodriguez et al., 2004). The common promoter does not necessarily imply that mature miRNAs of a family will be homologous in structure and/or function. Moreover, from the common transcript only part of the individual

miRNAs may be finally processed. Alternatively, certain miRNAs, such as the miR-17–92 family, which are grouped in clusters on a single unprocessed transcript, are expressed together.

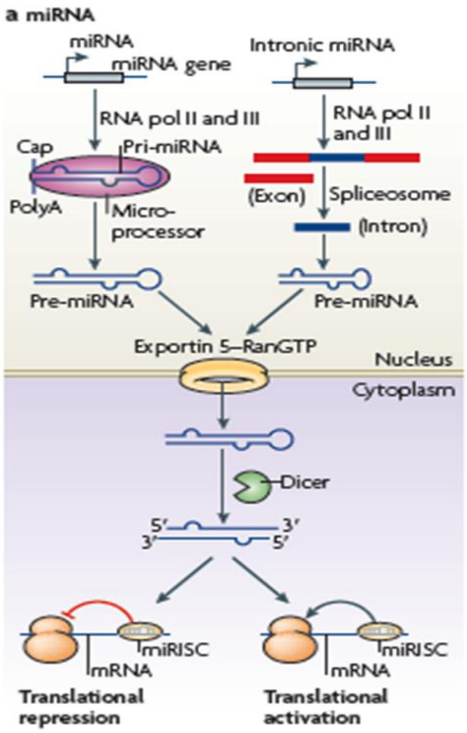


**Figure 1.3.1 miRNA biogenesis.** Canonical and non-canonical pathways of miRNA biogenesis are shown. See text for details. (from (Gangaraju and Lin, 2009))

Micro-RNAs are mostly transcribed in the nucleus by RNA polymerase II, even if a small contribution by RNA polymerase III has also been described (Borchert et al., 2006), and regulation of transcription is performed by the same transcription factors that control transcription of coding genes (Cai et al., 2004; Lee et al., 2004). The first product of the transcription is a large RNA primary transcript, called pri-miRNA, which is thousands nucleotide long and contains a characteristic hairpin stem loop structure. As the traditional messenger RNAs, Pri-miRNAs are capped with modified nucleotides at the 5’ end and polyadenlylated with multiple adenosines (poly(A) tail) at the 3’ end (Lee et al., 2004; Reinhart et al., 2000). A single pri-miRNA may contain from one to six miRNA precursors. As mentioned above, the transcription of some miRNAs is mediated by RNA polymerase III although this mechanism is less represented. RNA polymerase III (Pol III) indeed transcribes only some miRNAs, especially those with upstream Alu sequences, transfer RNAs (tRNAs), and mammalian wide interspersed repeat (MWIR) promoter units (Weber, 2005). In the canonical pathway, pri-miRNAs

are then processed in the nucleus into an intermediate structure, called pre-miRNAs, by a microprocessor complex, which contains the RNase III enzyme Drosha and the double-stranded RNA-binding protein DiGeorge syndrome critical region gene 8 (DGCR8; also known as Pasha in invertebrates) (Denli et al., 2004; Kim and Kim, 2007; Lee et al., 2003). Recent data suggest that this processing occurs co-transcriptionally (Morlando et al., 2008). In this complex, DGCR8 recognizes the double-stranded RNA structure in the hairpins of the pri-miRNA and correctly orients the catalytic RNase III domain of Drosha in order to cleave the hairpins from pri-miRNAs. The resulting product is a shorter 60–70 nucleotides hairpin structure precursor with a two-nucleotide overhang at its 3’ end (Figure 1.3.2).

An alternative miRNA biogenesis pathway has been recently reported (Figure 1.3.1). Specifically, some miRNAs, called “mirtrons” (since they are embedded within an intron of a gene) have been shown to be generated directly from the intron by spliceosome and a debranching enzyme that yields a short hairpin structure ready for further processing. Thus following this alternative splicing pathway they bypass the Microprocessor complex processing (Ruby et al., 2007). In both the canonical and mirtron pathways, pre-miRNA hairpins are then subsequently translocated from the nucleus into the cytoplasm by the nucleo-cytoplasmic shuttle Exportin-5-Ran-GTP (Bartel, 2009). Exportin-5, which is a member of the karyopherin family, recognizes the two-nucleotide overhang left by Drosha at the 3' end of the pre-miRNA hairpin and mediates the transport to the cytoplasm through GTP bound to the Ran protein (Bohnsack et al., 2004; Gregory et al., 2006).

Upon reaching the cytoplasm, the pre-miRNA hairpin is further processed by another RNase III enzyme, Dicer. This endoribonuclease interacts with the 3' end of the hairpin and cuts away the single stranded loop yielding a shorter imperfect paired double-stranded miRNA (miRNA duplex) about 22 nucleotides long with 2 nt overhangs on the 3′ end. Overall hairpin length and loop size influence the efficiency of Dicer processing, and the imperfect nature of the miRNA duplex also affects cleavage (Berezikov et al., 2007; Kawahara et al., 2008). The duplex is unwound by Dicer and one strand is then loaded, again by Dicer, into the multicomponent ribonucleoprotein complex called RISC (RNA-induced silencing complex) (Ambros, 2004; Bartel, 2009), which is the cellular machinery for ultimate gene regulation. RISC contains an Argonaute-subfamily member, which binds to the miRNA and guides RISC towards the mRNA target. Argonaute proteins are essential to RISC function. They contain two conserved RNA

binding domains: one of them, a PAZ domain, binding the single stranded 3' end of the mature miRNA, and the second one, a PIWI domain, that interacts with the 5' end of the guide strand. These two domains act together in order to bind the mature miRNA and properly orient it for subsequent interaction with the mRNA target. Although both strands of the duplex may potentially act as miRNAs, only one strand is usually functional and incorporated into the RISC, on the basis of its thermodynamic instability and weaker base-pairing relative to the other strand (Ji, 2008; Lelandais-Briere et al., 2010). Indeed, the strand of the duplex with a less thermodynamically stable 5' end, called the guide strand miRNA, is preferentially embedded with (RISC) (Schwarz et al., 2003). The other strand, called the passenger strand and denoted with an asterisk (miRNA*), is released and degraded (Krol et al., 2010). However, in some cases both strands of the duplex may be incorporated into RISC and function as miRNAs that target different mRNA populations (Schwarz and Zamore, 2002). The mature miRNA associated to the RISC interacts with the mRNA target mostly through an imperfect match between the miRNA and the 3'UTR (the sequence located downstream of the stop codon) or, in few cases, the coding region of the target mRNA leading to inhibition of translation and/or a decrease in mRNA stability (Chekulaeva and Filipowicz, 2009; Filipowicz et al., 2008; Rigoutsos, 2009). mRNA cleavage occurs when the complementarity is perfect while inhibition of protein translation when complementarity is imperfect (Ambros, 2004; Bartel, 2009). A critical miRNA sequence is responsible for target recognition. This sequence, called "seed sequence" is composed by nucleotides 2–8 (counted from the 5' end) and is the part of the mature miRNA that hybridizes nearly perfectly with the target mRNA (Bartel, 2009; Lai, 2002). As previously described, the mechanism by which miRNAs regulate gene target silencing depends on the degree of complementarity between the miRNA and the target mRNA (Figure 1.3.2). If complementarity is perfect, miRNA induces degradation of the target mRNA through endonuclease activity of Ago2. This mechanism is frequent in plants but rare in mammalian cells (Yekta et al., 2004). Conversely, imperfect pairing results in repression of target mRNA translation. This occurs either at the initiation step or at the elongation step, and/or by sequestration of target mRNAs into cytoplasmic processing bodies (P-Bodies) where mRNA targets will be degraded through deadenylation pathways (Guo et al., 2010a). However these mechanisms are not entirely understood. Regardless of the mechanism, the final outcome is a reduction in protein levels.

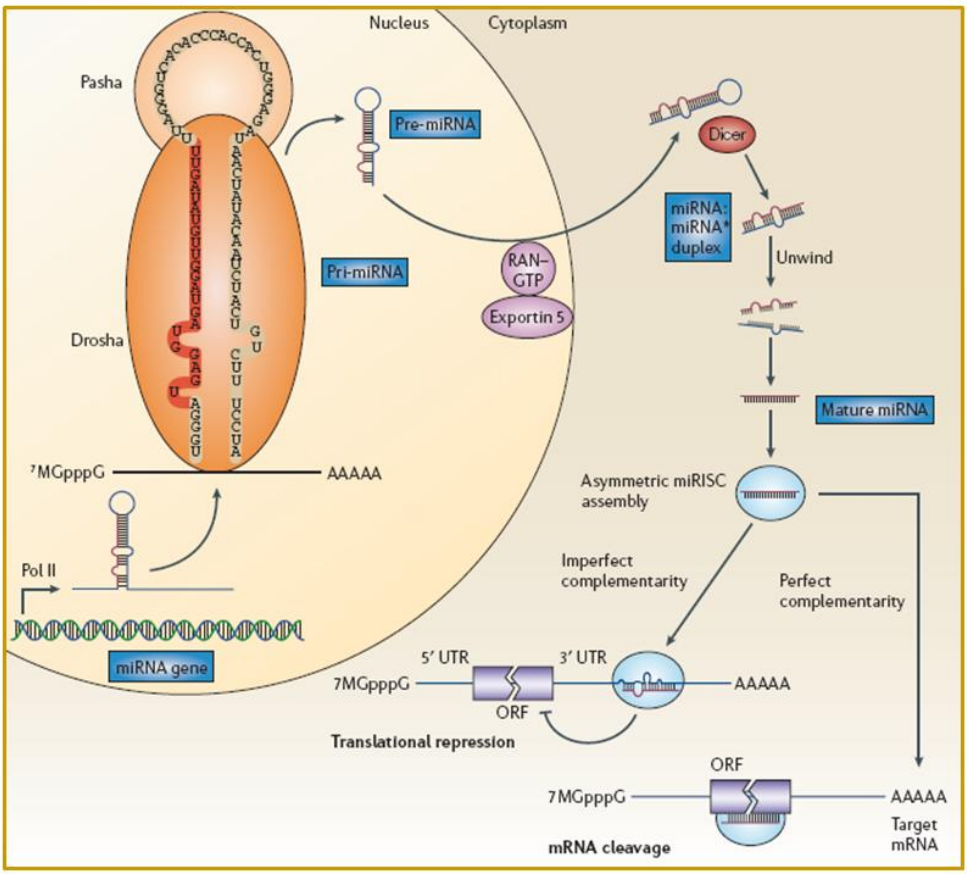


**Figure 1.3.2 complementarity on miRNA/mRNA drives mechanism of gene repression.** See text for detail (from (Esquela-Kerscher and Slack, 2006))

Although the main conventional miRNAs function is to silence gene expression, it has been shown that miRNAs could occasionally work by activating the translation of its targets and regulating their stability (Vasudevan et al., 2007). However additional experiments are needed to better understand this phenomenon.

The degree of downregulation of a single target is quantitatively modest (generally less than 50%), therefore miRNAs can induce subtle changes and fine tune gene expression (Baek et al., 2008). Nevertheless there is a strong synergistic effect since a single miRNA can potentially target hundreds of different target genes simultaneously and, at the same time, multiple miRNAs can target a single mRNA (Ambros, 2004; Bartel, 2009). The outcome of this complex network is a widespread gene expression regulation by miRNAs.

### 1.3.3 Regulation of miRNA

miRNA biogenesis is subject to tight regulation at multiple levels, since a defined spatiotemporal pattern of miRNA expression is very important for their proper function. In this regard, regulatory mechanisms by which cells control miRNA production and function have recently come into light (Davis-Dusenbery and Hata, 2010; Krol et al., 2010). The regulation of miRNA expression and function mainly occurs at three levels: transcription, processing and subcellular localization. miRNAs are initially regulated at the transcriptional level by transcription factors, which regulate the expression of different pri-miRNAs in a cell type- or development-dependent way or in response to different environmental stimuli. The transcription itself is regulated in a similar manner to the protein coding genes, with several mechanisms including DNA methylation and histone modification of the miRNA promoter. A second level of regulation occurs during miRNA processing, where several post-transcriptional regulatory mechanisms have been recently identified. These mechanisms function at various stages of miRNA processing, starting from the initial primary transcript to the delivery of mature, single stranded miRNAs to the target mRNAs. Thus, miRNAs coming from the same polycistronic transcript can be expressed differently (Tsuchida et al., 2011). Examples of factors involved at this level are the small mother against decapentaplegic (SMAD) proteins. These transcription factors, upon activation by TGF-β and bone morphogenic protein signaling, enhance processing of pri-miRNAs, such as mir-21, which in turn regulate cell differentiation (Davis et al., 2008). Another example is the tumour suppressor protein p53, which has an important role in miRNA processing following the onset of DNA damage. p53 forms a complex with Drosha and induces increased maturation of pri-miRNAs to pre-miRNAs, especially those miRNAs that suppress cell growth (Suzuki et al., 2009). Both mechanisms (mediated by SMAD and p53) involve binding to an RNA helicase (p68) that boosts microprocessor function. Moreover, after transport into the cytoplasm, some pre-miRNAs are subjected to post-transcriptional modifications catalysed by terminal uridylyltransferase 4 (TUT4). For example lin-28, which is one of the let-7 targets, can physically interact with the pre-let-7 in the cytoplasm of embryonic stem cells, promoting its polyuridylation. This modification directly inhibits Dicer processing and induces degradation of pre-let-7, thus preventing its further processing and inhibiting its function (Hagan et al., 2009; Heo et al., 2008; Heo et al., 2009). Regulation of miRNAs can also be mediated by subcellular localization mechanisms. For example on reaching maturation, delivery of the RISC

containing fully processed miRNA guide strand to target mRNA has been shown to involve importin 8 (Weinmann et al., 2009).

Another non canonical level of regulation is RNA editing, although only a small fraction of pre-miRNAs may be altered through this mechanism (Blow et al., 2006; Luciano et al., 2004). RNA editing is the site-specific modification of RNA sequences which leads to products that are different from those encoded by their DNA. It occurs most commonly through adenosine deaminases enzymes acting on RNA (ADARs) which catalyze adenosine to inosine transitions.

The last level of miRNA regulation is their turnover. Despite miRNAs are highly stable molecules, with a half-life of hours or even days (Krol et al., 2010), turnover of mature miRNAs is needed to allow the rapid changes in their expression profiles, which is in turn necessary to regulate the developmental and differentiation status of the cells where they act. Often these processes must occur rapidly and miRNA levels should change accordingly. Thus, miRNA decay needs to be tightly regulated and recent studies have identified specific exonucleases regulating miRNA turnover in plants and worms (Chatterjee and Grosshans, 2009; Ramachandran and Chen, 2008). Decay of mature miRNAs in *C. elegans* is mediated by the 5´-to-3´ exoribonuclease XRN2, also known as Rat1p (Chatterjee et al., 2011), while in plants, SDN (small RNA degrading nuclease) family members degrade miRNAs in the opposite (3'-to-5') direction. Similar enzymes are encoded in animal genomes, however a specific role for miRNAs turnover control in mammals is under investigation (Krol et al., 2010).

Finally miRNA function could be also regulated by controlling levels and activity of the key processing proteins, like Drosha, Dicer and their partners (Davis-Dusenbery and Hata, 2010). For example, during immune responses, cytokines such as interferons have been shown to inhibit Dicer expression, decreasing the processing of pre-miRNAs (Wiesen and Tomasi, 2009). This mechanism could also be employed to accumulate several pri-miRNAs, without being fully processed, until the right developmental or environmental stimuli arise (Thomson et al., 2006).

## 1.3.4 Strategies for identifying miRNA targets

Common strategies for identifying miRNA targets include the use of different bioinformatics predictive tools, which allow prediction of putative miRNA targets on the basis of the complementarity (perfect o near perfect) between miRNA and mRNA

sequences, mostly in the 3'UTR. These predictive tools may be combined with mRNA microarray data obtained from cells in which a particular miRNA is overexpressed or knocked down. Another powerful use of these bioinformatics predictive tools is the comparison of a miRNA profile obtained from a specific tissue or cell population with the mRNA microarray obtained on the same samples, as described in the present thesis (§3.2.4). This tool allows to search for those miRNAs whose expression inversely correlate with the expression of mRNA that is predicted to be one possible target. Although these methods have been successfully used to analyze miRNA function and to identify important miRNA targets, they have limitations (reviewed in (Navarro and Lieberman, 2010)). Bioinformatics algorithms typically predict hundreds or even thousands of targets of a single miRNA and have high false positive rates. Algorithms that rely on 3'UTR miRNA seed sequences seem to work better, but they still fail to predict biologically relevant targets, which have been experimentally proven such as Ras for let-7 and E2F2 and Myc for miR-24 (Johnson et al., 2005; Lal et al., 2009). Importantly they fail to analyze seedless miRNA binding sites or sites in the coding region or 5'UTR of genes that, even if less frequent, can mediate recognition of biologically relevant miRNA targets (Lal et al., 2009; Tay et al., 2008). Beyond these observations, a major caveat in using gene microarrays to study miRNA function is that often the changes in mRNA levels due to their miRNAs targeting are modest and not detectable by the microarray hybridization techniques. Moreover, this method does not distinguish direct mRNA targets from those transcripts whose change in expression is indirectly mediated by miRNAs and, most importantly, misses targets that are regulated primarily through translational inhibition. To overcome these limitations, other alternative biochemical approaches, based on proteomic analysis coupled with radiolabeling of the proteins or immune precipitation techniques, have been recently developed (Easow et al., 2007). However all of them show several limitations due either to their technical complexity or to the need of a large amount of samples (which is not always possible) or to their high costs, which strongly limit their use.

## 1.3.5 miRNAs in hematopoiesis

A key role for miRNAs in regulating the multiple cell-fate decisions governing hematopoietic differentiation is currently emerging: miRNAs can act together with lineage-specific TFs to finely regulate gene expression during hematopoietic

differentiation. They can also target TFs, and can be themselves regulated by TFs, giving multiple levels of regulation. In general the overall miRNA expression increases with cell differentiation, suggesting that miRNAs might play a role in shutting down genetic programs that are required for maintaining alternative cell fates or that prevent differentiation more generally (Mathieu and Ruohola-Baker, 2013).

MicroRNAs are differentially and dynamically expressed during hematopoiesis and regulate hematopoietic differentiation in almost every stage. They show different roles in different population in the hematopoietic hierarchy, inhibiting or promoting a specific lineage, and their aberrant expression has been associated with many diseases, including hematological malignancies, where microRNAs can act as oncogenes or tumor suppressors by mechanisms not yet completely understood. The first study demonstrating the relationship between microRNAs and hematopoiesis was published in 2004 (Chen et al., 2004). In this study, Chen and colleagues cloned 150 microRNAs from mouse bone marrow and found that three microRNAs (mir-181, mir-223 and mir-142) were preferentially expressed in hematopoietic cells. Further characterization revealed that miR-181 was highly expressed in the murine thymus and differentiated B lymphocytes, whereas it was detectable at lower levels in undifferentiated progenitor cells; miR-223 expression was confined to myeloid cells and miR-142 expression was highest in B-lymphoid tissues (Chen et al., 2004). Ectopic expression of miR-181 in hematopoietic stem and progenitor cells resulted in B lymphocyte proliferation *in vitro*. Consistent with the *in vitro* data, subsequent transplantation of these cells into lethally irradiated mice resulted in a significant increase of the B-cell lineage ($CD19^+$ cells), with a substantial decrease of T cells (especially $CD8^+$ T cells) also *in vivo*. However, ectopic expression of miR-142 or miR-223 did not induce any obvious phenotype (Chen et al., 2004). Following this pioneer study, many groups have investigated the expression and function of miRNAs during hematopoiesis. Notably, Ramkinssoon et al., studying expression profiles of mir-142, mir-181, mir-223 and mir-155, founded substantial differences in expression patterns between human and mouse hematopoietic cells (Ramkissoon et al., 2006).

The essential requirement for miRNAs during hematopoietic differentiation was further demonstrated with the complete inactivation of miRNA formation by conditionally deleting Dicer in specific hematopoietic compartments. As Dicer knockouts are embryonic lethal (Bernstein et al., 2003), the *in vivo* role of Dicer in adult hematopoiesis can only be studied by conditional knockouts. Targeted deletion of Dicer

in the thymus blocks peripheral $CD8^+$ T cell development and reduces the $CD4^+$ T cell compartment (Muljo et al., 2005). Moreover Dicer-deficient $CD4^+$ T cells show reduced cell proliferation, increased apoptosis, and a skewing toward the Th1 lineage. Targeted deletion of Dicer at early stages of B cell differentiation blocks B cell development at the pro- to pre-B cell transition, with a pronounced increase in pre-B cell apoptosis (Koralov et al., 2008). However, if Dicer is conditionally deleted at an early stage of T-cell development, it does not seem to be essential for CD4/CD8 lineage commitment (Cobb et al., 2005). Likewise, embryonic stem cells deficient for Dgcr8 accumulate in the $G_1$ phase of the cell cycle and exhibit defective differentiation (Wang et al., 2008; Wang et al., 2007). Furthermore, conditional inactivation of Ago2 led to severe hematopoietic defects in the lymphoid and erythroid precursors (O'Carroll et al., 2007).

Up to date, a number of different miRNAs have been associated with the regulation of hematopoietic development and differentiation, as reviewed by (Bissels et al., 2011a; Havelange and Garzon, 2010). Below there is a brief summary of relevant miRNAs in the different branches of hematopoietic differentiation (Figure 1.3.3).

A combined approach involving miRNA profiling of human stem-progenitor cells from bone marrow and mobilized peripheral blood, coupled to microarray analysis and bioinformatics prediction of mRNA targets, revealed that distinct miRNA signatures fine regulate almost every step of hematopoiesis, including HSCs and MPPs. For example, miR-128 and miR-181 are expressed in early progenitor cells and prevent the differentiation of all haematopoietic lineages. mir-146 impairs differentiation of multipotent progenitor cell (MPP) into common lymphoid progenitors (CLP), while mir-155, mir-24a and mir-17 may inhibit the differentiation of MPP into common myeloid progenitor (CMP). miR-16, miR-103 and miR-107 may inhibit the differentiation of CMP into granulocytic macrophage progenitor (GMP) whereas miR-221, miR-222 and miR-223 control the terminal differentiation pathways (Georgantas et al., 2007; Starczynowski et al., 2011) (reviewed in (Gangaraju and Lin, 2009))

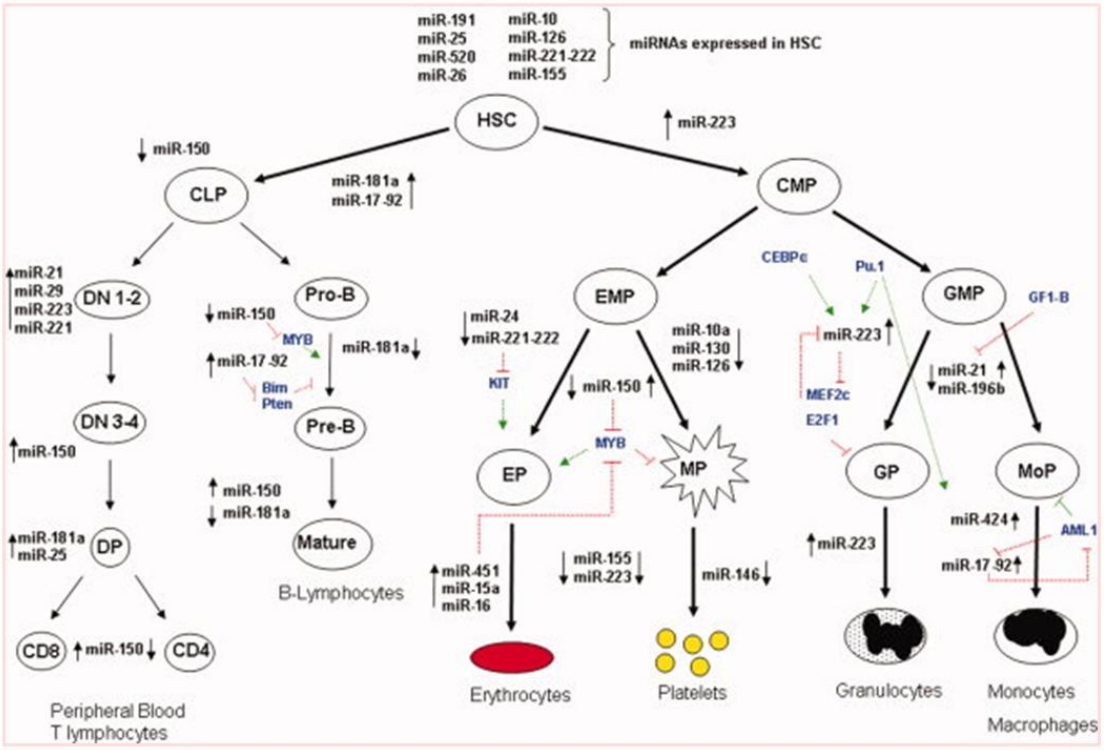


**Figure 1.3.3 Expression levels and regulatory networks of miRNAs during hematopoiesis.** CLP, common lymphoid progenitor; CMP, common myeloid progenitor; DN, double negative T-cell precursors; DP, double positive ($CD4^+CD8^+$ T cells); EMP, erythrocyte-megakaryocyte precursor; EP, erythrocyte precursor; GMP, granulocyte-monocyte precursor; GP, granulocyte precursor; HSC, hematopoietic stem cells; MP, megakaryocyte precursor. Dashed green arrows means positive regulation; Red dashed lines means negative regulation; Black thick arrows follows hematopoiesis development and differentiation hierarchy; Small black arrows (up or down) means miRNA expression during a specific hematopoietic stage. MiRNA targets or transcription factors involved in the regulation of miRNAs are shown using blue letters (from (Havelange and Garzon, 2010)).

Analyzing in detail one of the first lineage-specific decision during hematopoiesis, which is the differentiation of multi potent progenitor cells into either common lymphoid or common myeloid progenitors, it has been shown that miR-223 and miR-181 are expressed less abundantly in the progenitor cells and are upregulated upon differentiation into the myeloid and lymphoid lineages, respectively (Chen et al., 2004). However, less is known about miRNA acting upstream to multipotent progenitors and only very recently their specific role in HSCs is beginning to be elucidated (Guo et al., 2010; Ooi et al., 2010) (see § 1.3.6).

Like in other systems, lineage-specific TFs can also regulate the levels of some lineage-specific miRNAs thus indirectly determine the fate of those stem cells. For example, PU.1, a TF that is essential for monocytic differentiation, activates miR-424, which in turn targets the TF nuclear factor I/A (NfI-A) and induces monocytic differentiation (Rosa et al., 2007).

## 1.3.6 miRNA in Stem cells

Recently, the stem cell and miRNA fields have converged with the identification of stem-cell-specific miRNAs (Houbaviy et al., 2003), and it is now clear that miRNAs provide a new dimension to the regulation of stem cell functions. Due to their role in gene silencing and to their fast mechanism of action, miRNAs seem to regulate stem cell fate and behaviour by fine-tuning the protein levels required for stem cell or niche cell functions. Earlier evidences demonstrating essential requirement for miRNAs in stem cells came from studies on complete inactivation of miRNA formation in humans and mice ES cells, through generation of DGCR8 and Dicer mutants, respectively.

Dicer is essential for early mouse development since its absence is embryonic lethal (Bernstein et al., 2003). However, embryonic lethality does not seem to be due to the absence of ES cells. Dicer-null mouse ES cells are viable, although they show severe defects in growth and differentiation. Dicer-null ES cells fail to express endodermal and mesodermal differentiation markers, even under specific differentiation conditions, and have prolonged $G_1$ and $G_0$ phases of the cell cycle (Kanellopoulou et al., 2005). DGCR8-deficient human ES cells show similar defects, since they also exhibit delayed differentiation, reduced expression of differentiation markers and delayed kinetics of cell cycle progression (Wang et al., 2007). Most DGCR8-deficient ES cells are arrested in the $G_1$ phase, which indicates that the main function of the miRNA pathway is to promote the ES cell cycle at the $G_1$–S-phase transition. In addition, DGCR8-null ES cells fail to silence the expression of self-renewal markers, such as Oct4, Rex1, Nanog and Sox2, and do not produce teratomas in xenotransplantation assays as wt ES cells normally do (Wang et al., 2007), highlighting a differentiation defect also *in vivo*. The similar phenotype of DGCR8 and Dicer mutants further confirms that the predominant function of miRNAs is to regulate cell cycle progression during stem cell differentiation (Gangaraju and Lin, 2009). Micro-RNA function has also been intensively explored in somatic tissue stem cells, highlighting multiple roles of miRNAs in almost each adult stem cell populations. For the purposes of our study we focus on miRNAs involved in regulation of HSC and how they control their proper self-renewal and differentiation.

***miRNAs in HSCs***

Emerging evidences demonstrate that miRNAs regulate self-renewal and proliferation of HSCs and of their downstream multipotent progeny (Laine et al., 2012). For instance, increased expression of miR-125a (Guo et al., 2010) or miR-125b (Ooi et al., 2010) in mouse HSCs was reported to enhance HSC function and expand them *in vivo*. Both

miRNAs probably act by suppressing multiple proapoptotic genes, like Bak1, a direct target of miR-125a, or Bmf and Klf13, targets of miR-125b. A similar regulatory function has been suggested for miR-33, since it was found to inhibit the expression of p53 tumor suppressor protein, thus promoting mouse HSC self-renewal (Herrera-Merchan et al., 2010). Furthermore, in HSCs high expression of miR-29a has been associated with their self-renewal capacity. In detail, miR-29a was shown to be highly expressed in normal HSCs and primary human AML, and down-regulated in more committed hematopoietic progenitors. An analogous expression pattern is demonstrated in mouse hematopoietic populations. Ectopic expression of miR-29a in mouse hematopoietic stem and progenitor cells leads to increased myeloid differentiation and proliferation at the level of MPP, with concomitant acquisition of self-renewal capacity by more committed myeloid progenitors. Moreover, enforced miR-29a expression reveals a biased myeloid differentiation, and the development of a myeloproliferative disorder that progresses to acute myeloid leukemia (AML), which is serially transplanted by miR-29a-expressing myeloid progenitors. These findings suggest miR-29a as a possible oncomir able to transform myeloid progenitors into self-renewing leukemik stem cells (LSCs). Although the direct targets of this miRNA are unknown, it seems that miR-29a positively regulates progenitor proliferation by expediting $G_1$ to $S/G_2$ cell cycle transitions (Han et al., 2010). Another recently HSC-associated miRNA is miR-126, which is involved in control of HSC pool size in human and mice (Gentner et al., 2009; Gentner et al., 2010; Lechman et al., 2012). miR-126 is expressed and functionally active in human and mouse HSCs and early progenitors, but not in more committed progeny where it is progressively down regulated. miR-126 expression can be used also as a marker to prospectively isolate human HSCs with xenograft repopulating potential (Gentner et al., 2010). Gain- and loss-of-function studies demonstrate that miR-126 regulates HSCs and early progenitor cells. In detail, lentiviral mediated miR-126 knockdown (using a lentiviral “sponge”) led to increased cell-cycle progression and *in vivo* HSC expansion, without exhaustion. Conversely, enforced expression of miR-126 impaired cell-cycle entry and resulted in increased HSC quiescence followed by reduced hematopoietic output. Thus, miR-126 may play a key role in maintaining HSC quiescence by restricting cell-cycle progression. Mechanisms through which miR-126 can exert these functions likely involve the PI3K/AKT/GSK3β pathway, where several miR-126 targets are reported (Lechman et al., 2012).

It is well known that HSC function is tightly controlled not only by intrinsic cellular signals but also by their cellular microenvironment, the HSC niche, which has a direct impact on hematopoiesis (Schofield, 1978; Wilson and Trumpp, 2006). In this regard, it is interesting that miRNAs could also have a role in modulating HSC microenvironment. To support this notion there is evidence that secretion of the chemo-attractant stromal derived factor 1 (SDF1 or CXCL12) is also influenced by miR-886-3p, which specifically targets the 3´UTR of SDF1 mRNA, thereby modulating the expression of this chemokine that plays a critical role in hematopoietic regulation (Bissels et al., 2011a; Pillai et al., 2010).

The role of miRNAs in the regulation of self-renewal and of the early steps of HSC differentiation has not yet been clearly understood in part due to technical problems relative to HSC isolation (Bissels et al., 2011a). MiRNA expression profiling in HSCs is hampered by the low number of available cells and by the wide spectrum of surface marker combinations that are normally used for their enrichment. Moreover, expression of miRNAs in human and mouse has been analyzed in different populations, obtained from different sources (such as bone marrow, peripheral blood, mobilized peripheral blood and cord blood) and with different combination of markers. These populations are not always properly enriched neither comparable to each other. Indeed, a comparison of the available miRNA profiles of primitive human hematopoietic cell populations [data of (Bissels et al., 2011b; Han et al., 2010; Jin et al., 2008; Liao et al., 2008; Merkerova et al., 2009)], reveals considerable variation in miRNA expression profiles of HSCs in different studies that can be attributed to the different stem cell fractions used for comparison. Like for ES cells, improving methods to separate specific cell populations and homogeneous starting material will overcome, at least in part, these problems, thus increasing knowledge about miRNA expression in HSCs (Bissels et al., 2011a).

As described in §1.2.4, Pbx1-null HSCs have a profound self-renewal defect. Therefore, in the second part of this thesis (§3.2), we employed Pbx1 conditional KO mice as a model for studying if miRNAs play a role in balancing self-renewal *versus* differentiation in HSCs. Our interest in characterizing the role of miRNAs in this model arises from the fact that they have been extensively linked to the main processes that are defective in Pbx1-null HSCs (differentiation and self-renewal). Moreover self-renewal itself, which is the main characteristic of stem cells, is progressively lost in the normal HSC-to-MPP transition, making also the characterization of miRNA in the

physiological transition an important issue to address. Importantly, the transcriptional profile previously performed on HSCs (Ficara et al., 2008) revealed that in the absence of Pbx1 there is a premature up-regulation of Dgcr8 transcript. These observations lead to the hypothesis that Pbx1 loss in HSCs may result in altered expression of Dgcr8 and miRNAs, and prompted the investigation of a possible link between self-renewal regulation and miRNAs in HSCs, similarly to what has been proposed for ES cells (Wang et al., 2007). In support to this hypothesis, direct link between Dgcr8, miRNAs and HSC defect has been recently demonstrated in *Xenopus* models during embryonic development. *Xenopus* Dgcr8 morfant embryos fail to correctly specify HSCs and display early hematopoietic differentiation defects (Nimmo et al., 2013).

# 2. AIMS OF THE STUDY

Hematopoiesis is highly regulated at each step of differentiation. For a constant supply of short-lived terminally differentiated blood cells, as well as for rapid response to several hematopoietic stresses, HSCs are endowed with the ability to continuously provide more mature progenitors while properly maintaining their pool size, without exhaustion, throughout life. This equilibrium is finely maintained on one hand by precisely balancing self-renewal and differentiation in HSCs, and on the other hand by regulating proliferation and differentiation also of their downstream progenitors, including lineage choice.

Pbx1 was shown to be a negative regulator of HSC differentiation by affecting their quiescence. Postnatal hematopoiesis is profoundly perturbed in the absence of Pbx1, with a severe reduction of HSCs both in number and functionality (Ficara et al., 2008), and severe reduction of committed lymphoid and myeloid progenitors. However, the precise molecular mechanisms through which Pbx1 exerts its function in HSCs and its role in progenitor biology are two issues still unexplored. In particular, it is not known whether Pbx1 function is also mediated by micro-RNAs, crucial new players in the regulation of proliferation and differentiation in several tissues.

We speculate that Pbx1 regulates the balance between self-renewal *versus* maturation not only in HSCs but also in downstream progenitors, and we want to address whether it does so also through micro-RNAs, at least in HSCs. Taking advantage of Pbx1 conditional KO mice, in the present thesis we addressed these issues through the following specific aims:

**Aim1.** To understand if Pbx1 plays a role in multipotent and lineage committed progenitors, by analyzing the capacity of Pbx1-mutant progenitors to proliferate and differentiate toward myeloid, erhythroid and lymphoid cells.

**Aim2.** To establish if microRNAs are part of the program downstream of Pbx1 that regulates self-renewal *versus* differentiation in HSCs. This aim will be pursued on one hand by comparing the micro-RNA expression profile of Pbx1-conditional KO HSCs (which have a self-renewal defect) *versus wt* HSCs, and on the other hand by comparing the micro-RNA expression profile of wt HSCs and wt Flk2$^-$ multipotent progenitors (Flk2$^-$MPPs), where loss of self-renewal occurs for the first time in the hematopoietic hierarchy.

# 3. RESULTS

## 3.1 Pbx1 role in multipotent and lineage restricted progenitors

### 3.1.1 Experimental background

Three main experimental evidences suggest that, in addition to HSCs, Pbx1 may play important roles in lineage-restricted progenitors.

#### *3.1.1.1 Pbx1-null lineage restricted progenitors are reduced*

Pbx1 conditional knockout mice ($Tie2Cre^{+}.Pbx1^{-/f}$, see §1.2.5) exhibit significant reduction of common myeloid progenitors (CMPs) and a drastic reduction of common lymphoid progenitors (CLPs), as shown by multicolor FACS analysis of total BM ((Ficara et al., 2008) and Figure 3.1.1A-B). Quantification of the data reveals a 90% reduction of CLPs and 50% of CMPs in mutant mice compared to control (analysis from 14 and 15 control and mutant mice respectively; *p=0.05) (Figure 3.1.1C).

However, although lymphocytes are reduced in the BM and in the thymus, mature myeloid cell numbers are unaffected despite significant CMP reduction. This contrasts with several mouse models carrying mutations in genes implicated in maintaining HSC self-renewal and/or cell cycle properties. In these models, either no phenotypes in the myeloid progenitor compartment are observed (Galan-Caridad et al., 2007), or they are characterized by myeloproliferative-like diseases (Metcalf et al., 2006; Santaguida et al., 2009; Tothova et al., 2007; Viatour et al., 2008; Yilmaz et al., 2006b) as a consequence of the HSC defect. This difference with our model suggests a specific role for Pbx1 in progenitors.

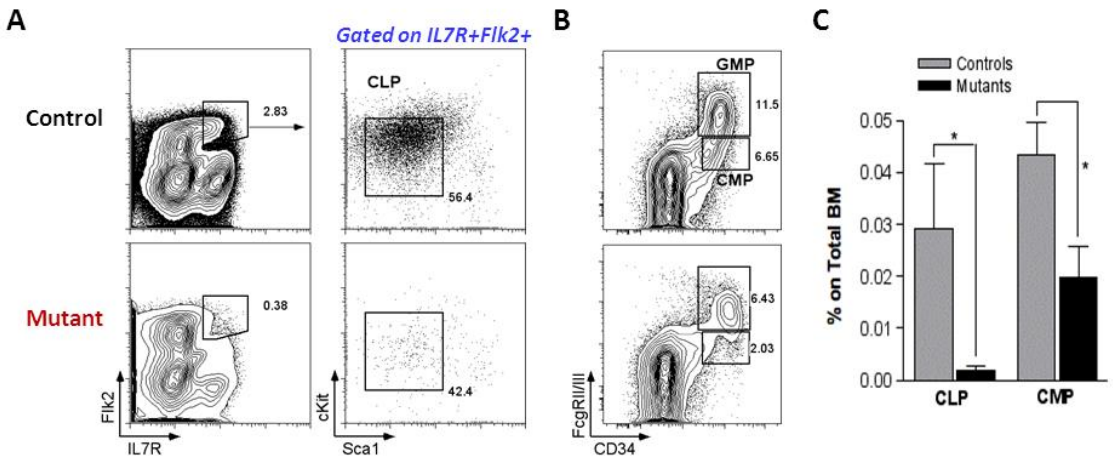


**Figure 3.1.1 Pbx1-null progenitors are reduced.** (A) Representative FACS analysis of CLPs from control (Tie2Cre-.Pbx1+/f) or mutant (Tie2Cre+.Pbx1-/f) mice. Contour plots on the left are referred to the Lin- gate. Percentages are relative to the parent gate. (B) Representative FACS analysis of CMPs and GMPs from control or mutant mice. Contour plots are referred to the Lin-cKit+Sca1+ gate. Percentages are relative to the parent gate. (C) Quantitative data from FACS analysis shown in (A) and (B). Histograms represent the average CLP and CMP percentage within the BM of control or mutant mice (n=14 and 15, respectively; *P<0.05) (from (Ficara et al., 2013))

### *3.1.1.2 Pbx1-null common myeloid progenitors (CMPs) have a higher proliferation rate*

Data from Dr. Cleary's laboratory at Stanford University revealed that the CMP reduction observed *in vivo* did not correlate with a reduction of their proliferation capacity. Conversely, prospectively isolated Pbx1-null CMPs, placed in liquid culture and exposed to growth factor stimulation (SFC, IL6 and IL3), displayed a higher proliferation rate compared to controls (Figure 3.1.2).

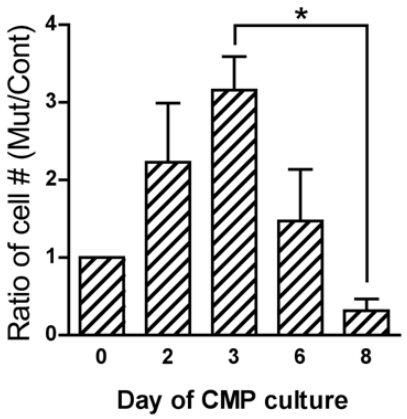


**Figure 3.1.2 CMP proliferation rate.** Liquid culture of prospectively isolated CMPs (2000–10,000 cells), in presence of cytokines. The graph shows the ratio of Pbx1-null cell number *versus* control at different time points (n=3, *P=0.003) (from (Ficara et al., 2013)).

This higher proliferation rate is massive during the first three days of culture, but decreases at later time points. In other words, the number of Pbx1-null cells increased at a much lower rate compared to controls toward the end of the culture period, resulting in an inverted ratio of mutant CMPs *versus* wild-type CMPs at day 8 (Ficara et al., 2013). The observed phenotype could not be ascribed to increased cell death, since Annexin V assays previously performed in Cleary's lab did not reveal any alteration in apoptosis process (not shown).

Hence, the reduced number of Pbx1-null CMPs is not due to an intrinsic defect in proliferation, but rather to their aberrantly higher proliferation rate, leading to the hypothesis that, in the absence of Pbx1, progenitors exhaust faster in the myeloid lineage.

### *3.1.1.3 Transcriptional profile of Pbx1-null CMPs suggests premature maturation toward the GMP stage*

To explain this aberrant myeloid phenotype we took advantage of the transcriptional profiling performed in Cleary's lab on Pbx1-null CMPs, in order to find Pbx1-dependent genes potentially involved in the CMP defect. Microarray analysis was performed on prospectively isolated CMPs and their immediate downstream progenitors GMPs, both from mutant and control mice. Analyzing first the normal CMP-to-GMP transition, statistical analysis of microarray (SAM) shows 592 non-redundant differentially expressed (DE) transcripts. This gene set of DE transcripts was compared to the one obtained from the transcriptome analysis of mutant *vs* wild-type CMPs. As schematically shown in Figure 3.1.3 by Venn diagrams, this analysis reveals that 123/305 (40%) non-redundant DE transcripts in mutant *vs* wild-type CMPs were also differentially regulated in the normal CMP-to-GMP transition.

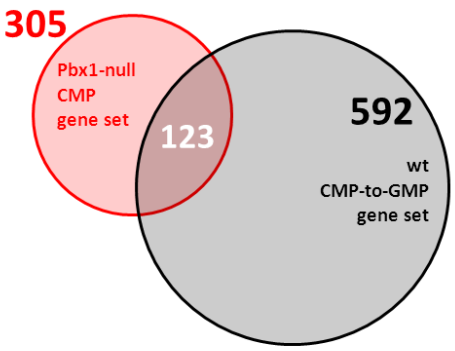


**Figure 3.1.3 Overlap between the Pbx1-null CMP gene set and the gene set defining the normal CMP-to-GMP transition** (from (Ficara et al., 2013)).

The gene set defining the normal CMP-to-GMP transition was compared to gene set of mutant *vs* wild-type CMP DE transcripts also by employing Gene set enrichment analysis (GSEA) (Mootha et al., 2003; Subramanian et al., 2005). Transcripts down regulated in mutant CMPs were highly enriched for normal CMP-specific genes, whereas transcripts upregulated in mutant CMPs correlated with normal GMP genes (Ficara et al., 2013).

Thus, in the absence of Pbx1, phenotypically defined CMPs prematurely express a subset of genes typical of their downstream GMP progeny, making them more similar to GMPs than to CMPs, at least from a transcriptional point of view.

### 3.1.2 Faster kinetics of myeloid differentiation in Pbx1-null CMPs

Since the described data suggested that Pbx1 may maintain common myeloid progenitor number and identity, possibly by restraining proliferation and differentiation, in the present thesis we tested the *in vitro* differentiation ability of Pbx1-null CMPs toward myeloid and erythroid cells.

In order to assess whether the increased proliferation observed in Pbx1-null CMPs in short-term culture is associated with a normal or aberrant differentiation capacity, we plated FACS-sorted CMPs in liquid culture in 96 multi well (MW) plates in medium supplemented with cytokines (SCF, IL3 and IL6), and analysed them by FACS at two different time points (one and three days later), to check for the expression of a typical myeloid marker (Mac-1) and/or the concomitant loss of their immature phenotype, revealed by the expression of cKit.

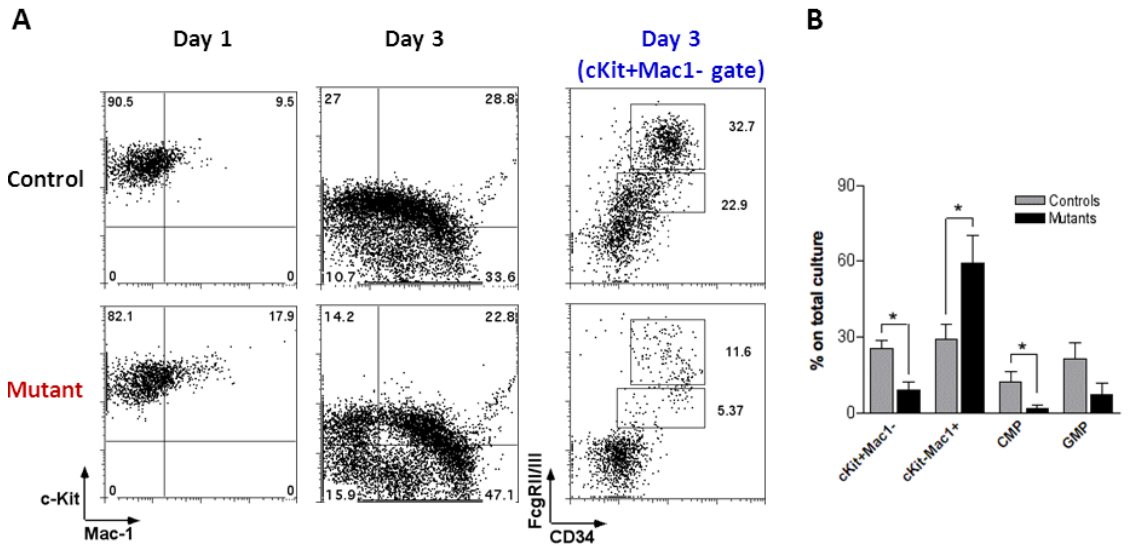


**Figure 3.1.4 Premature differentiation of Pbx1-null CMPs.** (A) Representative FACS analysis of the progeny of CMPs prospectively isolated from control or mutant mice (representative of five). Dot plots on the right are relative to the c-Kit+Mac-1- gate at day 3. Percentages are relative to the parent gate. (B) Histograms summarize data shown in (A), day 3 (n=5, *P<0.05) (from (Ficara et al., 2013)).

After only one day of culture, a higher proportion of Pbx1-null CMPs had acquired Mac-1 expression compared to controls (Figure 3.1.4A). This faster differentiation tendency became more evident at the next time point. At day three cultures derived from mutant CMPs contained a smaller proportion of immature c-Kit$^{+}$Mac-1$^{-}$ cells, and a higher fraction of differentiating c-Kit$^{-}$Mac-1$^{+}$ cells. We then analyzed more in detail the immature fraction of cells (c-Kit$^{+}$Mac-1$^{-}$) for the expression of FcγRII/III and CD34 markers, which allow to distinguish CMPs (FcγRII/III$^{int}$ and CD34$^{int}$, middle gate) and GMPs (FcγRII/III$^{high}$ and CD34$^{high}$, upper gate). Representative FACS analysis shows that mutant CMPs loose their immature phenotype more rapidly than their wt counterparts (Figure 3.1.4). Quantification of these data shows a more evident reduction of all the immature fraction of cells (c-Kit$^{+}$Mac-1$^{-}$ and CMPs), with a concomitant increase of the differentiating (Mac-1$^{+}$) fraction. Concomitant FACS analysis for CFSE and Mac-1 after 2 days of culture showed that cells that had acquired Mac-1 had also diluted CFSE (not shown), indicating that the observed premature differentiation by Pbx1-null CMPs was not due to an absence of proliferation. Overall, these data demonstrate that Pbx1-null CMPs differentiate more rapidly. This can account for the partial transcriptional overlap between mutant CMPs and wt GMPs (Figure 3.1.3).

We then performed colony-forming-cell assays on CMPs from mutant and control mice to test their clonogenic and differentiation capability. After 7 days of culture, we counted colonies and scored them for myeloid and erythroid differentiation. Pbx1-null

and control cells gave rise to a similar number of colonies (Figure 3.1.5A). However colonies from Pbx1-null CMPs tended to be smaller compared to wt (not shown) and, after pooling all colonies, a lower number of total cells was obtained (Figure 3.1.5B). This is in agreement with the previous mentioned results of liquid culture at day 8 (Figure 3.1.2), at which time point the number of Pbx1-null cells is lower compared to controls. In addition, in cultures of mutant CMPs there was an inversion in the relative proportion of myeloid and erythroid colonies, with a significant reduction in erythroid colonies and a concomitant increase of the myeloid ones (Figure 3.1.5C).

We then harvested a pool of Pbx1-null colonies and performed a cytospin preparation to check if the cellular composition of the colonies was altered. May-Grunwald/Giemsa staining of the spotted cells clearly shows a lower proportion of 'blast-like', not terminally differentiated cells in the cytospin preparations from pooled mutant colonies compared to controls with a number of blast-like cells per field of 11.5+/- 1.25 and 1.2+/-0.57 in control and mutant respectively (n=10, P<0.0001) (Figure 3.1.5D).

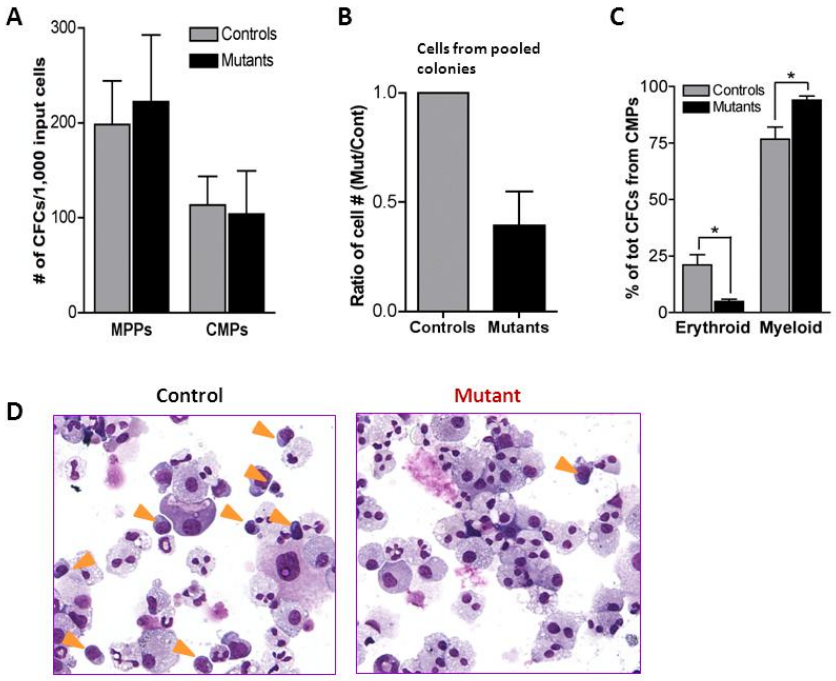


**Figure 3.1.5 Premature differentiation of Pbx1-null CMPs.** (A) Methylcellulose CFC assay from prospectively isolated CMPs and MPPs (average of four independent assays, each performed in duplicate (*P≤0.02). (B) and (C) Methylcellulose CFC assays from prospectively isolated CMPs. Histograms represent the average of four and two independent assays, respectively, each performed in duplicate (*P≤0.02). (D) Cytospin and May-Grunwald and Giemsa staining of pooled colonies from A and B. Arrowheads on cytospin images indicate blast-like, not terminally differentiated cells (from (Ficara et al., 2013)).

Overall, these data indicate that in Pbx1-null CMPs there is an accelerated maturation to the next stage of the hematopoietic hierarchy with a concomitant loss of their adequate

self-renewal capacity and a preferential skewing towards the myeloid (granulocytic-monocytic) lineage respect to the erythroid one.

This premature myeloid differentiation likely contributes to the observed reduction of CMPs in the absence of Pbx1, despite the unaffected mature myeloid cell numbers, since they differentiate more rapidly.

### 3.1.3 Pbx1-null Common Lymphoid Progenitors (CLPs) show reduced differentiation capacity toward B cells

Pbx1 conditional knockout mice exhibit not only alteration in CMPs but also, and with an even more severe phenotype, in CLPs. In this case there is also a severe reduction of differentiated lymphocytes in the BM and in the thymus. To test whether a faster and aberrant differentiation could account also for the CLP defect, we performed lymphoid differentiation assays to assess the capacity of mutant lymphoid progenitors to differentiate toward B cells (Figure 3.1.6). One thousand prospectively isolated CLPs from control or mutant mice were seeded on OP9 stromal cell layers plated the day before, in medium supplemented with cytokines (SCF, Flt3 and IL-7). In these conditions lymphoid progenitors differentiate towards B cells in around 10 days and develop visible colonies of hematopoietic cells growing on the stroma. This progeny was harvested and analyzed by FACS at two time points (four and eleven days) for the presence of B220 and CD19, typical B cell markers. Figure 3.1.6 shows representative contour plots of the two time points. The plots are referred to the hematopoietic gate. Any residual stromal cells were excluded on the basis of their light scatter characteristics, and lack of expression of B cell markers (Ficara et al., 2013).

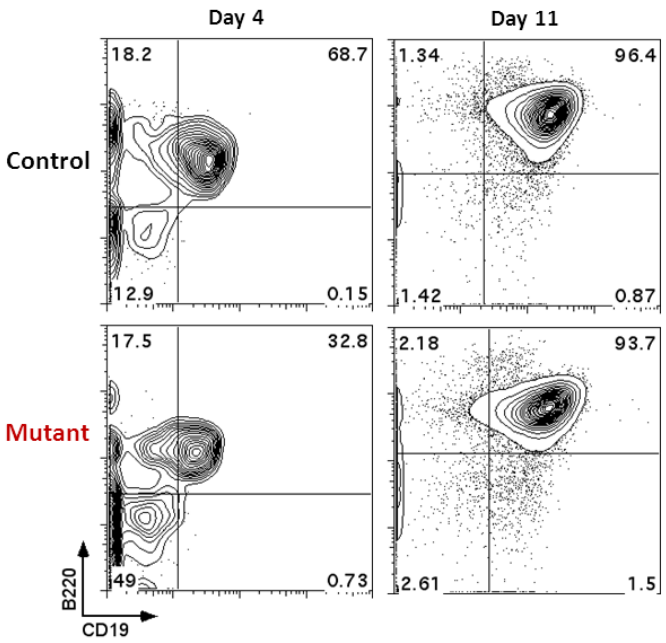


**Figure 3.1.6 Differentiation of Pbx1-null CLPs.** Representative time course FACS analysis of differentiation assays at two time points (day 4 and day 11) from control (upper lane) or mutant (bottom lane) CLPs. Percentages are relative to the parent gate (from (Ficara et al., 2013)).

Both Pbx1-null and control CLPs differentiated into $B220^{+}CD19^{+}$ cells *in vitro*, without detectable differences. This is in contrast with what observed in the myeloid lineage, in which there was an evident accelerated differentiation, as mentioned above (see Figure 3.1.4). However, data from Cleary's lab indicated that the *in vivo* lymphoid outputs from Pbx1-null CLPs were lower compared to wt (not shown), suggesting that Pbx1 may maintain lymphoid potential. Since our *in vitro* experiments were performed on bulk cultures, in which potential differences might be missed, we repeated the *in vitro* B-cell differentiation assays in limiting dilution, to highlight potential defects not detectable with bulk cultures.

Limiting dilution analysis aims to determine the frequency of cells having a particular function that are present in a mixed population of cells. Freshly isolated CLPs were seeded in limiting dilution in 96 MW plates on OP9 stromal cells plated the day before, in medium supplemented with cytokines as described. In this way, if there is at least one bona fide lymphoid progenitor in the cell population, it will differentiate developing a colony of B cells. Since cells were plated at limiting dilution conditions, we also expected a fraction of negative wells, in which no visible colonies are formed. After 10 days we selected the positive wells (the ones with visible hematopoietic colonies), harvested them and analyzed them individually by FACS for the presence of B220± and CD19± surface markers. To definitively exclude positive wells we checked the

remaining wells three days later, harvesting cells from additional wells in which small colonies were non evident before. Due to the drastic CLP phenotype in mutant mice (Figure 3.1.1), we could plate Pbx1-null cells only at three different concentrations (the minimum to have statistical significance). We plated different concentrations of control and mutant cells (3, 10 and 30 cells/well for control, 10, 30 and 90 cells/well for the mutant) to have an informative read out. In fact preliminary experiments, performed to set up the assay, had suggested a reduced frequency of these progenitors in the mutant mice. For each condition we seeded a high number of wells (summary table in Figure 3.1.7 is representative of one experiment) to reach statistical significance, with higher number of wells for the lower cell doses. However, for Pbx1-null CLPs, the number of wells was limited by the number of cells that we were able to obtain from mutant mice. Figure 3.1.7 shows the gating strategy used for the analysis, with representative plots from FACS analysis of different wells.

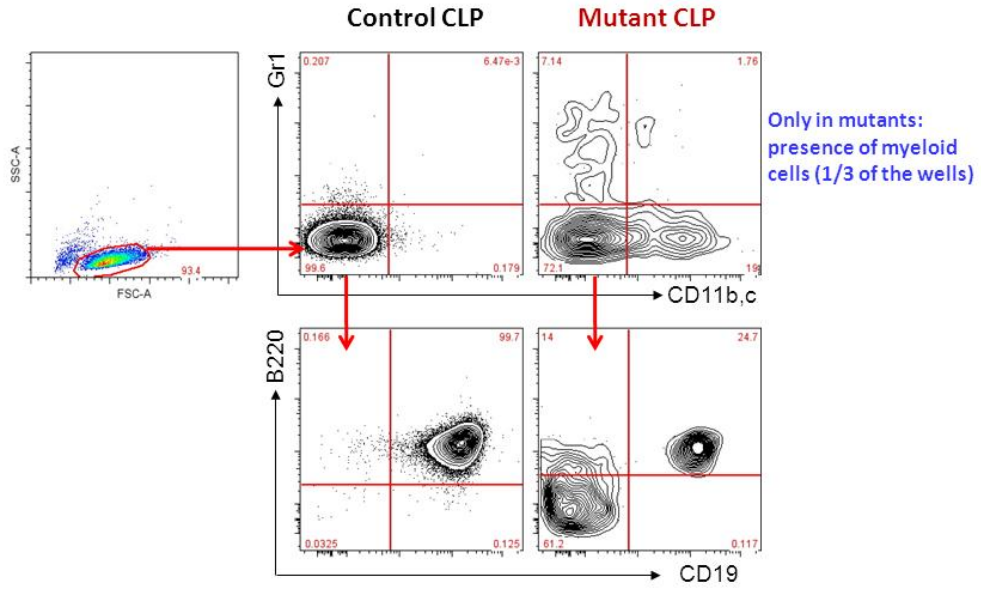


| | | | |
|---|---|---|---|
| Mutant CLP | 10 cells/well | 30 cells/well | 90 cells/well |
| | 40 | 14 | 5 |
| Control CLP | 3 cells/well | 10 cells/well | 30 cells/well |
| | 48 | 12 | 12 |

**Figura 3.1.7 Differentiation of Pbx1-null CLPs in limiting dilution.** Representative FACS analysis of the progeny of prospectively isolated CLPs from control or mutant mice, cultured in limiting dilution in presence of cytokines. Percentages are relative to the parent gate. Summary table in the bottom shows the number of wells in one experiment for each condition (representative of two).

From this experiment different progenies can be expected, with great variability from well to well. Indeed this differentiation assay will favor lymphoid differentiation while

the myeloid differentiation is prevented. Nevertheless these populations, although purified, represent an enrichment, since cells unable to differentiate toward B lineage can be found. Thus myeloid "contaminating" cells can be obtained, especially when lymphoid progenitors are only a small fraction of the plated cells. Therefore, we set the staining including antibodies for myeloid (Gr1 and Mac-1) and dendritic (CD11c) cell markers, in addition to B-lymphoid markers, in order to exclude them from the analysis. In detail, the scatters plot (representing physical parameters) shows that the hematopoietic population is homogeneous and separated from stromal cells. On the gate of "live" cells, we first excluded cells expressing myeloid and/or dendritic cell markers, and we then analyzed the expression of the lymphoid markers B200 and CD19. B220 is expressed from the earliest stages of the B cell development (Pre-pro B cells), while CD19 expression defines a more mature differentiation stage (from Pro B to mature B cells). In our experiments, the vast majority of B cells were double-positive for B220 and CD19, as expected after 10 days of culture since we plated a committed lymphoid progenitor. Importantly, both mutant and control cells generated $B220^{+}CD19^{+}$ cells, indicating that the reduced number and frequency of Pro- and Pre-B cells observed *in vivo* (Ficara et al., 2008) is not due to an intrinsic differentiation defect from CLPs. Interestingly, the progeny of control CLPs contained only B cells. Conversely, after plating mutant CLPs we found several wells containing myeloid cells, some of them without the presence of B cells. In detail, myeloid cells were detected in about 1/3 of the wells. On one hand, this may be due to the fact that the shortage of mutant CLPs renders the sorting less accurate, thus we might have plated a less pure cell population (purity of mutant CLPs was never assessed due to the low number of cells obtained after sorting). However our favored hypothesis is that phenotypically defined CLPs from mutant mice might not be all true functional CLPs, as it happens for HSCs. In other words, the $Lin^{-}IL7R^{+}Flk2^{+}Sca1^{low}cKit^{low}$ cell population from mutant mice likely contains fewer lymphoid progenitors than wt.

After analyzing all samples we calculated the negative fraction ($F_0$), i.e. the fraction of wells without CD19 positive cells, and then we plot this data in a semi logarithmic graph, in function of the plated cell dose for each culture (Figure 3.1.8).

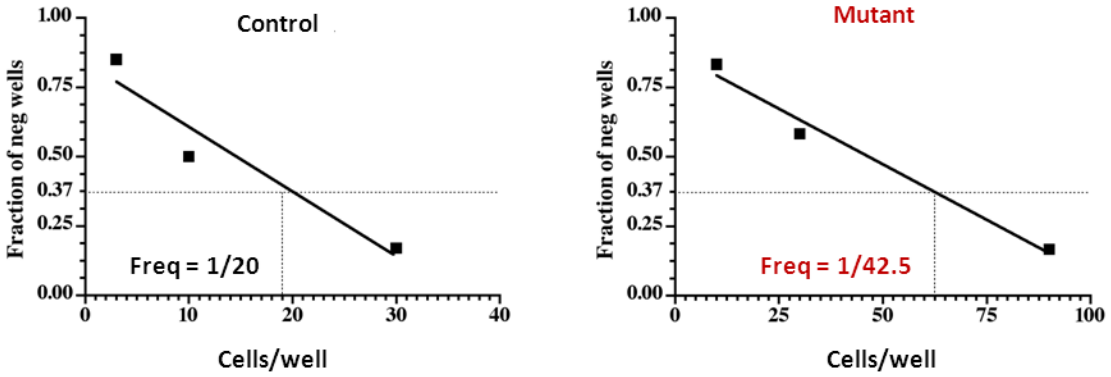


**Figure 3.1.8 CLP limiting dilution analysis.** Plots of limiting dilution analysis (representative of two) show the frequency of control or mutant CLPs able to develop into $CD19^+$ B cells in co-culture with OP9 stromal cells ($R^2$=0.92 and 0.96, respectively) (from (Ficara et al., 2013)).

A straight line is obtained by linear regression from which, interpolating at $F_0 = 0.37$, we obtained the cell dose in which there is one cell with the function we are analyzing, in this case the frequency of lymphoid progenitors in each population. The rationale beside this calculation rely on the Poisson Distribution (Szilvassy et al., 1990; Szilvassy et al., 1989; Taswell, 1981), which assumes in a simplified manner, that you have the same probability to plate one cell or zero cell (or even more than one cell) when plating an ideal single cell suspension. This probability is mathematically calculated at 37%. Since you start from a mixed population, you cannot discriminate if the experimental read out comes from only one cell or more than one, but you can count the negative read outs, you make a function of these negative fractions. Whichever dilution of cells giving rise to 37% of negative read outs represents the frequency of the cells you are looking for (in this case the frequency of lymphoid progenitor in each population). The semilogaritmic plots show a lower frequency of functional CLPs from Pbx1-null mice (1/20 in the control mice vs 1/42.5 in the Pbx1-null in this example) (Figure 3.1.8). Therefore, the *in vivo* CLP reduction cannot be ascribed to a faster and aberrant differentiation capacity, but rather to their decreased frequency.

Thus, in absence of Pbx1, both myeloid and lymphoid progenitors are able to differentiate into mature progeny but with a premature kinetic (a higher efficiency) for the myeloid lineage and a decreased efficiency in the lymphoid (and erythroid) lineage.

## 3.1.4 Pbx1 drives lineage choice from MPPs

These data led us to hypothesize that Pbx1 may drive lineage choice in hematopoietic progenitors. We investigated this aspect further at the level of multi potent progenitors

(LMPPs and MPPs), to study if a possible lineage choice defect in Pbx1-null mice is already present up-stream of CLPs and CMPs. For this purpose mutant and control MPPs were flow-sorted into three fractions according to Flk2 expression (Figure 3.1.9 and Table 1.1.1) and analyzed by FACS. As described in §1.1.4, MPPs are phenotypically defined as LKS $CD34^{+}$, and can be further divided into three fractions according to Flk2 expression: $Flk2^{-}$MPPs, frequently called "short-term" HSCs, Flk2-intermediate MPPs ($Flk2^{int}$) and $Flk2^{high}$ MPPs. MPPs negative or with low expression of Flk2 are progenitors with robust myeloid maturation potential ($Flk2^{-}$MPPs and $Flk2^{int}$MPPs) while MPPs with higher expression of Flk2 are lymphoid-primed MPPs ($Flk2^{high}$, also known as LMPPs) (Mansson et al., 2007). Figure 3.1.9 shows representative FACS analysis of MPPs from control and mutant mice (contour plots are relative to the LKS gate) with the relative quantification of the FACS data, in term of percentage and absolute numbers per mouse.

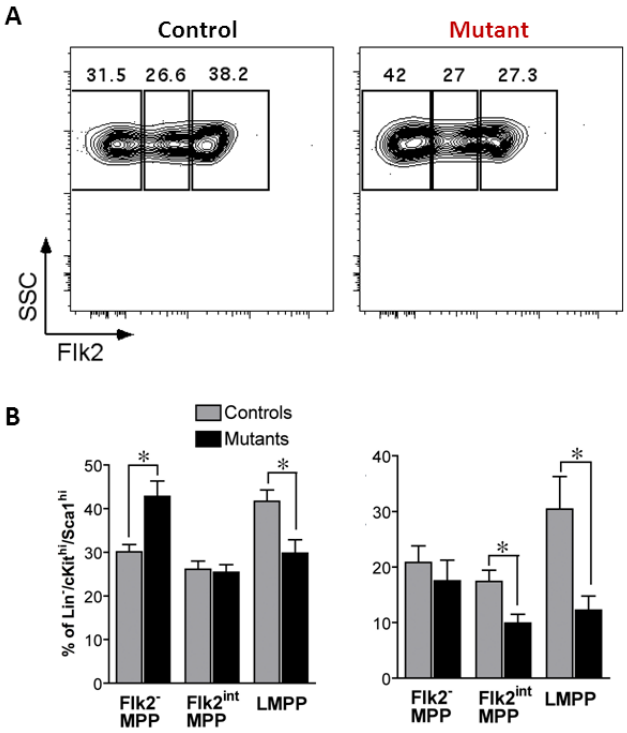


**Figure 3.1.9 Evaluation of multi-potent progenitors in Pbx1-conditional knockout mice.** (A) Representative FACS analysis of MPPs from control or mutant mice, relative to the LKS gate. (B) Quantitative data from FACS analysis shown in (A). Histograms show the percentage of Flk2-negative, Flk2-intermediate and Flk2-high MPPs within the LKS (left) or their absolute numbers per mouse (right); *P=0.01, n=8 (from (Ficara et al., 2013)).

The analysis of these MPP subsets revealed a significant decrease, both in the percentage and in the absolute number, of LMPPs in mutant mice compared to control (Figure 3.1.9 B). Of note, the mean fluorescence intensity was similar in mutants and

controls, indicating that the reduction in progenitor subpopulations was not due to an altered expression of the markers used to define them (Ficara et al., 2013). Moreover, in addition to the already observed decrease in CMPs ((Ficara et al., 2008) and Figure 3.1.1), here we also observed an associated reduction of the absolute number of their $Flk2^{int}$ progenitors (Figure 3.1.9 B). These data strongly support the hypothesis that the lineage choice defect in Pbx1-null mice potentially arises at the level of multi potent progenitors. Thus, in addition to HSCs and restricted progenitors, Pbx1 may serve important roles in maintaining the normal MPP frequencies. To assess if Pbx1 regulates the ability of multi potent progenitors to differentiate into down-stream progeny, we tested the differentiation capability of $Flk2^{+}$MPPs (including both $Flk2^{int}$ MPPs and LMPPs) towards both myeloid and in lymphoid lineage *in vitro*, through the same assays previously performed with CMPs and CLPs.

To test the myeloid differentiation capacity, $Flk2^{+}$MPPs were prospectively isolated for methylcellulose colony assays. Colonies were counted and scored at day 9 for their myeloid *versus* erythroid output.

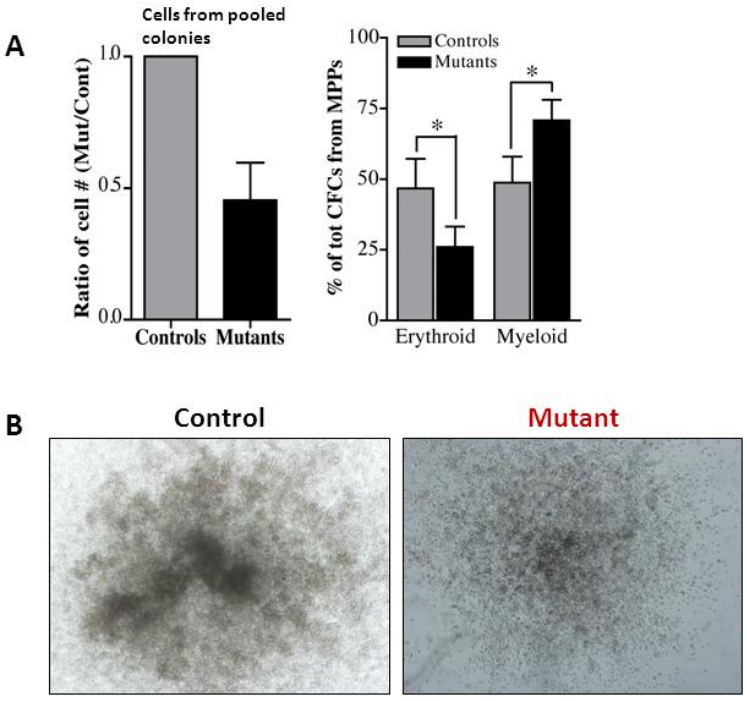


**Figure 3.1.10 Myeloid differentiation ability of Pbx1-null multi-potent progenitors.** (A) Methylcellulose colony assay of prospectively isolated Flk2+MPPs. Erythroid and myeloid colonies were counted 9 days after plating. The histogram on the left represents pooled colonies from three independent experiments. The histogram on the right represents the average of four independent assays, each performed in duplicate (*P≤0.04). (B) Pictures of representative myeloid colonies (CFU-GM) taken with the same magnification (from (Ficara et al., 2013)).

Similarly to what observed with CMPs, there is no statistical difference between the number of colonies arising from Pbx1-null and control MPPs (Figure 3.1.5A). However, similarly to CMPs, the relative proportion of erythroid and myeloid colonies was inverted (Figure 3.1.10 A, right). Moreover, colonies were smaller (Figure 3.1.10 B), and when they were collected in pool at the end of the assay, they yielded a reduced number of total cells (Fig 3.1.10 A, left).

We then plated the same type of prospectively isolated MPPs in liquid culture in presence of cytokines for several days to analyze their progeny for myeloid markers expression by FACS (Figure 3.1.11).

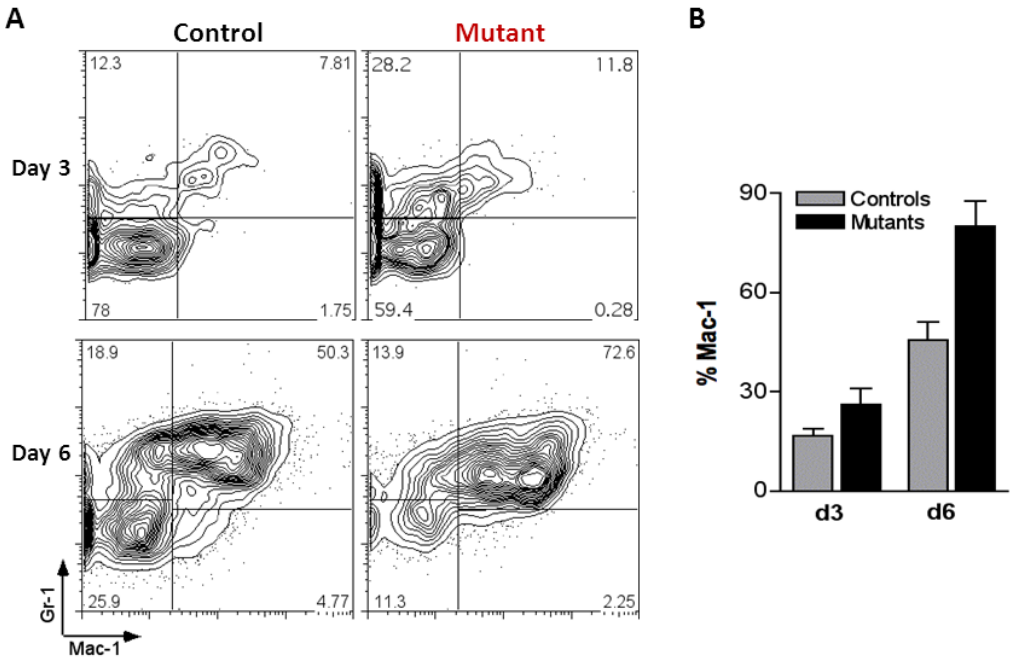


**Figure 3.1.11 Myeloid differentiation ability of Pbx1-null multi-potent progenitors.** (A) Time-course FACS analysis (representative of four) was performed on prospectively isolated MPPs from control or mutant mice, cultured in the presence of serum and cytokines for 3 or 6 days. Contour plots show events within the live/forward and side light scatter gate. (B) Histograms show quantitation of average percentage of Mac-1+ cells in (A) (from (Ficara et al., 2013)).

FACS analysis demonstrated that Pbx1-deficient cells up-regulated the expression of myeloid markers Mac-1 and Gr-1, and furthermore they were prone to do it with a faster kinetics compared to wt cells (Figure 3.1.11). Moreover, if we analyze the immature fraction of cells, looking at the expression of cKit and Sca1 on the $Gr1^{-}Mac\text{-}1^{-}$ gate, we can note that mutant MPPs extinguished their immature phenotypes ($cKit^{+}Sca1^{+}$ population) earlier compared to controls (not shown). Thus, as in CMPs, there is an accelerated myeloid differentiation in Pbx1-deficient MPPs suggesting that Pbx1 may normally restrain MPP differentiation along the myeloid lineage (Ficara et al., 2013).

To test the *in vitro* lymphoid differentiation ability of multipotent progenitors we prospectively isolated LMPPs (LKSF$^{high}$) from control and mutant mice. Similarly to what described for CLPs, we investigated the lymphoid differentiation potential of control and Pbx1-null LMPP in limiting dilution *in vitro* B-cell differentiation assays. We plated freshly sorted control LMPPs at 3, 10 and 30 cells/well and Pbx1-null LMPPs at 10, 30 and 90 cells/well. For each condition we seeded a very high number of wells (summary table in Figure 3.1.12 is representative of one experiment), and after 10 days we selected the positive wells to analyze them by FACS for the presence of B220 and CD19. As in the previous limiting dilution experiments, we also included CD11b, CD11c and Gr1 markers to identify also myeloid and/or dendritic cells. At day 13 we checked again the plates to make sure not to exclude positive wells with colonies too small for being evident after 10 days. Figure 3.1.12 shows representative FACS analysis of different wells.

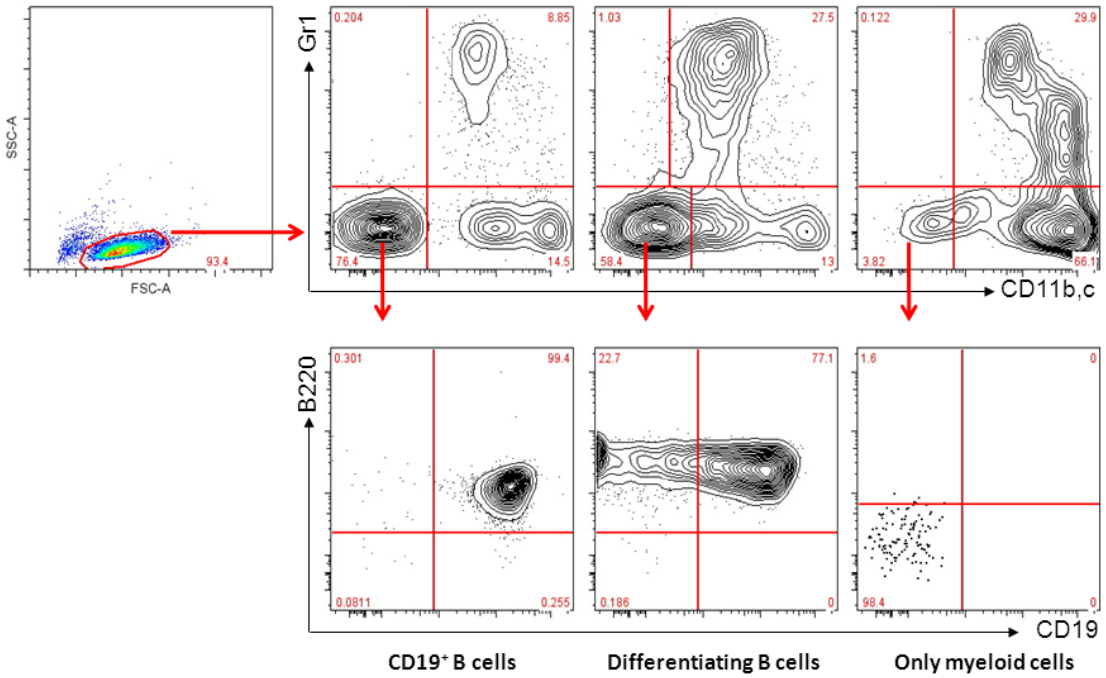


| | | | |
|---|---|---|---|
| Mutant LMPP | 10 cells/well | 30 cells/well | 90 cells/well |
| | 96 | 48 | 24 |
| Control LMPP | 3 cells/well | 10 cells/well | 30 cells/well |
| | 72 | 24 | 12 |

**Figure 3.1.12 Pbx1-null LMPPs differentiation in limiting dilution.** Representative FACS analysis of progeny of prospectively isolated LMPPs from control or mutant mice, cultured in limiting dilution in presence of cytokines. Percentages are relative to the parent gate. Summary table in the bottom shows the number of wells in one experiment for each condition (representative of two).

As described for CLPs, after gating on "live" cells, we first excluded cells expressing myeloid and dendritic cell markers. On the negative fraction we analyzed the expression of the lymphoid markers B220 and CD19. LMPPs gave rise to three different progenies. In the first column of Figure 3.1.12 there is an example of a more differentiated B cell population, expressing both B220 and CD19. In the second column there is an example of partial B cell differentiation in which there are Pre-Pro B cells expressing B220 but not yet CD19. Finally, in the last column, an example of a positive well (i.e. a well with cells grown on the stroma), but in which all the cells are myeloid, without any B cells. The greater variability of LMPP outputs in this assay compared to CLPs highlights the more immature state of the former population. LMPPs are lymphoid-primed (not restricted) MPPs, still harboring some myeloid potential, while CLPs are lymphoid committed cells. This variability underlines the importance of performing limiting dilution analysis as opposed to bulk cultures. The semi logarithmic plot obtained after the analysis shows that there is a markedly lower frequency of B cell progenitors from Pbx1-null LMPPs compared to control LMPPs, meaning that the frequency of bona fide lymphoid progenitors is 3 fold higher in the control compared to Pbx1-null LMPPs (1/19 vs 1/62.5) (Figure 3.1.13). In contrast, *in vitro* myeloid output from Pbx1-null LMPPs was increased compared to controls.

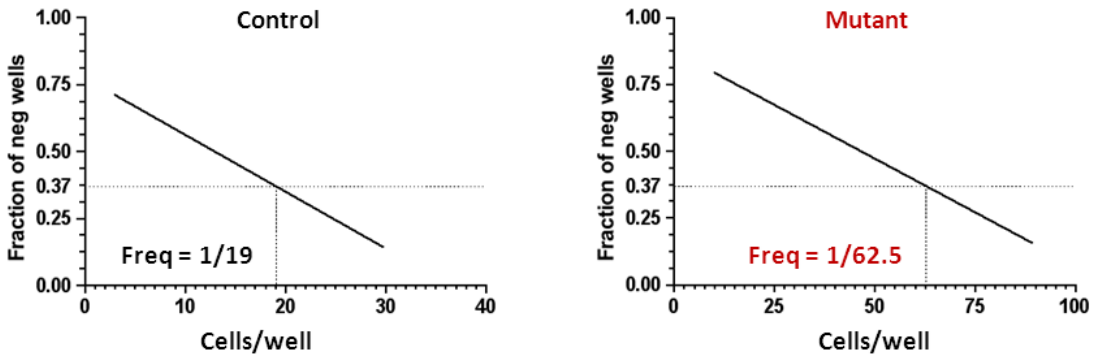


**Figure 3.1.13 LMPP limiting dilution analysis.** Plots of limiting dilution analysis (representative of two) show the frequency of control or mutant LMPPs able to develop into $CD19^+$ B cells in co-culture with OP9 stromal cells ($R^2$=0.91 and 0.98, respectively) (from (Ficara et al., 2013)).

The difference between control and mutant cells is more pronounced than the one observed in the CLP population (see Figure 3.1.8), in accordance with the hypothesis that in Pbx1-null mice the CLP reduction is mainly due to up-stream defects.

Taken together, we can conclude that Pbx1 affects lineage choice of MPPs by restraining myeloid differentiation and allowing lymphoid differentiation.

Notably these experiments, together with other previous data obtained in Cleary's lab, led to the publication of the following paper:

**"Pbx1 restrains myeloid maturation while preserving lymphoid potential in hematopoietic progenitors."**

Francesca Ficara[1,2], **Laura Crisafulli[1,2]**, Chenwei Lin[3], Masayuki Iwasaki[4], Kevin S. Smith[4], Luca Zammataro[5]and Michael L. Cleary[3,4].

J Cell Sci. 2013 Jul 15;126(Pt 14):3181-91.

http://www.ncbi.nlm.nih.gov/pubmed/23660001

[1]Milan Unit, Istituto di Ricerca Genetica e Biomedica, Consiglio Nazionale delle Ricerche, Milan, Italy; [2]Humanitas Clinical and Research Center, via Manzoni 56, 20089 Rozzano (Mi), Italy; [3]Department of Pediatrics – Cancer Biology, Stanford University School of Medicine, Stanford, CA 94305; [4]Department of Pathology, Stanford University School of Medicine, Stanford, CA 94305; [5]Computational Research Unit, Center for Genomics Science@SEMM, Istituto Italiano di Tecnologia, Via Adamello 16, 20139 Milano, Italy

# 3.2 microRNAs in Pbx1-null hematopoietic stem cells (HSCs) and multipotent progenitors (MPPs)

In the secon part of this thesis we took advantage of Pbx1-conditional KO mice first to identify miRNAs involved in the maintenance of self-renewal, and secondly to study whether they are modulated by Pbx1 or if they regulate Pbx1-dependent pathways. To address these questions we performed a miRNA profiling of HSCs and their immediate downstream progenitors Flk2$^-$MPPs from both mutant and control mice, and combined it with the transcriptional profile of the same populations previously performed on these mice.

## 3.2.1 miRNA profiling of wt and Pbx1-null HSCs and MPPs

To perform the miRNA profiling, highly purified HSCs (LKS$^+$Flk2$^-$CD34$^-$) and their immediate downstream progeny (LKS$^+$Flk2$^-$CD34$^+$, also called ST-HSCs, here Flk2$^-$ MPPs os simply MPPs) were prospectively isolated from poly(I:C)-treated Pbx1-conditional KO mice crossed with the inducible Mx1Cre$^+$ line ((Ficara et al., 2008) and Figure 1.2.3). This is another Pbx1 conditional KO mouse model in which the expression of the Cre recombinase is induced by the administration of the polyinosinic-polycytidylic acid (poly(I:C) (see §1.2.5). This experiment was conducted in collaboration with Cleary's lab, since in our Institute we only maintain the Tie2Cre$^+$.Pbx1$^{-/f}$ conditional KO mice line. As described in §1.2.5, we choose to use those mice since the MxCre model gives the advantage, being inducible, to delete Pbx1 when mice are adult enabling us to obtain a higher number of cells.

HSCs and Flk2$^-$MPPs were sorted, as previously mentioned, from the bone marrow of 5 Pbx1 mutant and 4 control individual mice. The number of cells obtained was 1600 on average for HSCs (ranging from 1400 to 2000), and 6000 for Flk2$^-$MPPs, which was sufficient for the miRNA profiling purpose performed with the PreAmplification strategy (see below), without pooling RNA from different mice.

RNA was extracted from the sorted samples with a method that specifically preserves small RNAs together with the longer RNA transcripts and the MegaPlex TaqMan®

Assays system was used to perform the microRNA profiling (see materials and methods §5.5). MegaPlex TaqMan® Assays system is a highly sensitive and specific technology, based on real-time PCR, which enables analysis of small number of cells and allows simultaneous detection of more than 300 different miRNAs, including those expressed at low level, as opposed to other technologies with lower sensitivity like fluorescent-based miRNA microarrays. Moreover, the inclusion of a PreAmplification step in the protocol further enhances miRNA profiling sensitivity, which is particularly useful in our case since the paucity of the cells. For profiling purpose the RT step was performed in Multiplex fashion, in which all the mature miRNAs are simultaneously reversed transcribed into cDNAs in one reaction using a specific pool of miRNA-stem looped RT primers designed to detect and quantitate up to 380 miRNAs. The same RT step can be performed with individual TaqMan miRNA Assays for single analysis purposes, performed later for validation of the profiling (see §3.2.5). We performed 14 rounds of PCR amplification, according to the manufacture protocol. Preamplified cDNA was loaded in a 384 MW plate in which 376 TaqMan miRNA and 8 different control assays were preloaded (in collaboration with Dr. Yuley Wang in Applied Biosystem).

Of the profiled miRNAs 45% (177 on 384 including controls) was expressed within at least one group and were further analyzed, whereas the remaining 207 were filtered out (Ct level $\geq$ 35).

## 3.2.2 Selection of the normalization strategy

On the 177 expressed miRNAs we had to choose the correct normalization method before performing complex bioinformatics analysis. This is crucial since the normalization strategy strongly impacts the final results. For this part we collaborated with the Bioinformatics group of the Center for Advanced Studies, Research and Development in Sardinia (CRS4).

The most appropriate normalization strategy has been selected on the basis of the smallest variation among replicates, measured by the coefficient of variation (CV = standard deviation/mean) (Deo et al., 2011). CV indicates to which extent the expression of an individual miRNA varies among samples.

In detail, we compared three normalization strategies:

1. Endogenous control normalization
2. Quantile normalization
3. Median normalization

Regarding the endogenous control, we applied several algorithms (normFinder, gNorm, Delta CT and BestKeeper) to facilitate the identification of an endogenous normalizer consistently stably expressed across all samples. Among the endogenous controls present in the array, the most stable controls, after comprehensive ranking of all four methods, were MammU6 and snoRNA202 that were used for further comparison with the other normalization strategies.

Looking then at the overall signal distribution, we also compared the distribution of normalized values for each sample with the distribution of not normalized data (Figure 3.2.1). This analysis reveals that the quantile normalization method generates the most homogeneous distribution.

Finally, for each normalization strategy, we calculated the CV based on the set of the filtered miRNAs (Table 3.2.1). After applying the normalization, a lower CV indicates a good performance of the normalization method. Quantile and median normalization show the best performance, since both of them reduce variability across the replicates.

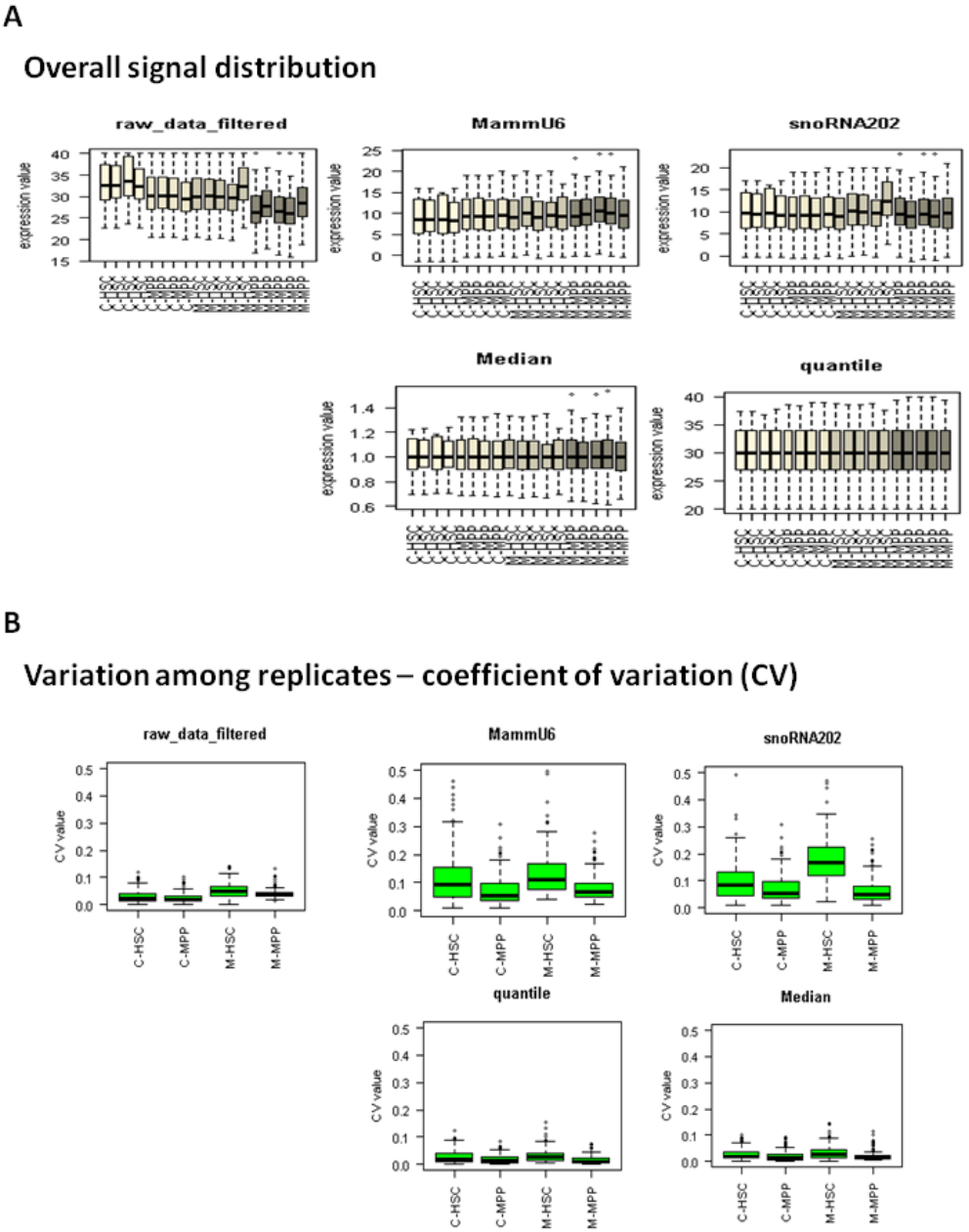


**Figure 3.2.1 Choice of the best normalization strategy.** (A) Overall signal distribution. Distribution of normalized values for each sample compared to the distribution of not normalized data. (B) Variation among replicates. The boxplots show the distribution of the coefficent of variation (CV) of the normalized *versus* raw data. Quantile and Median normalization show the best performance (see text for details). Raw data filtered: not normalized data; MammU6: endogenous normalization using mammU6; snoRNA202: endogenous normalization using snoRNA202; quantile: quantile normalization; median: median normalization

**Median value of coefficient of variation (CV)**

| | C-HSC | C-MPP | M-HSC | M-MPP |
|---|---|---|---|---|
| **raw_data** | 0.030 | 0.026 | 0.053 | 0.042 |
| **MammU6** | 0.141 | 0.141 | 0.187 | 0.443 |
| **snoRNA202** | 0.106 | 0.141 | 0.236 | 0.100 |
| **quantile** | 0.030 | **0.019** | **0.033** | **0.016** |
| **Median** | **0.028** | 0.022 | 0.036 | 0.020 |

The **quantile** method has the lowest CV in 3 out of 4 sample groups

**Table 3.2.1** Summary table of coefficient of variation (CV) median values (from CV graphically showed in fig 3.2.1)

Looking at the CV within the single experimental groups we realized that quantile normalization outperforms median normalization since it has the lowest CV in 3 out of 4 sample groups. Thus, quantile normalization shows the overall best performance compared to all the other methods and was therefore chosen for the analysis of the miRNA profile. The complete list of normalized data is shown in Appendix A.

### 3.2.3 Global miRNA analysis: hierarchical clustering and differential expression (DE) analysis

After filtering and normalization, we performed a thorough bioinformatics analysis of the miRNA profiling data of wt and Pbx1-null highly purified HSCs and Flk2$^-$MPPs, which allowed drawing different conclusions.

A global analysis through unsupervised hierarchical clustering, using Pearson's correlation as distance measure and average linkage as agglomerative algorithm, indicates for the first time a clear distinction between HSCs and Flk2$^-$MPPs at the level of miRNA expression (Figure 3.2.2), suggesting that miRNAs might regulate the first transition step in the adult hematopoietic development.

Within each group, mutant and control cells clustered separately, suggesting that Pbx1 directly or indirectly regulates miRNA expression in those populations.

A differential expression analysis through SAM (Statistical Analysis of Microarray) (Tusher et al., 2001) revealed that in the absence of Pbx1 several miRNAs are differentially expressed (DE) in HSCs and Flk2$^-$MPPs compared to their relative wt controls, with putative targets in the list of Pbx1-dependent mRNAs (see later).

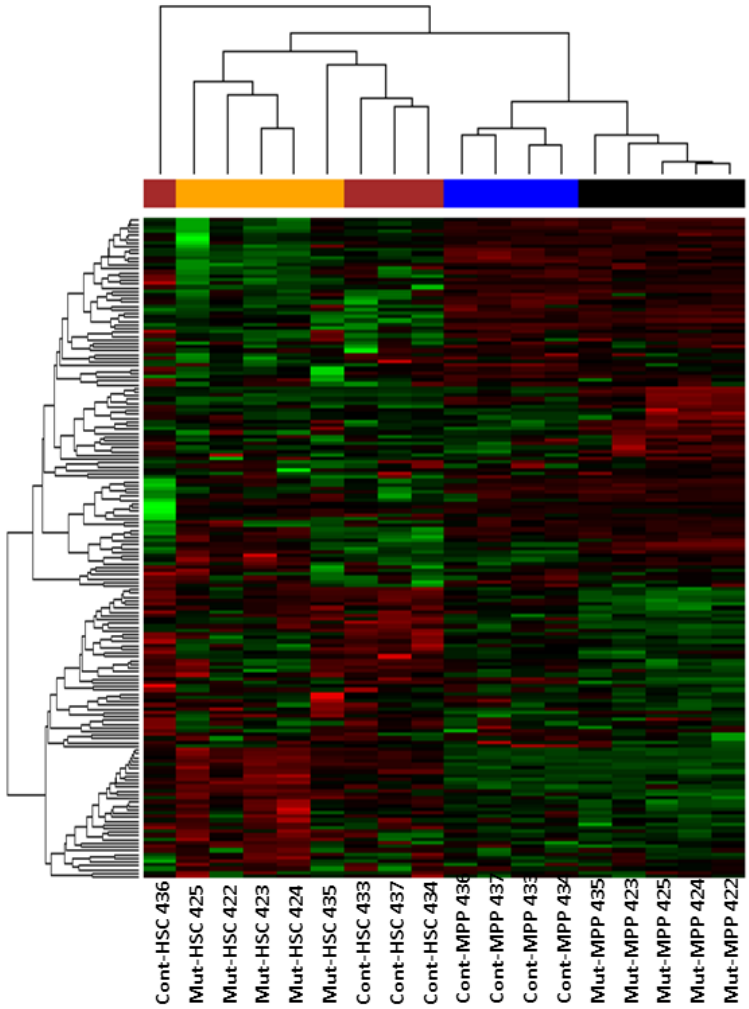


**Figure 3.2.2** Heat map showing the hierarchical clustering of HSC and Flk2-MPP relative miRNA expression. The color scale represents Z-score transformed signal intensity (see text for details).

In detail, focusing first on the HSC group, we found 48 DE miRNAs in Pbx1-null HSCs compared to controls (q-value < 0.1), of which 25 were down-regulated and 23 up-regulated. Importantly, the expression of most of the DE miRNA changes more than two fold (Figure 3.2.3 and Table 3.2.2). Similarly, concentrating on the MPP group, 67 DE miRNAs were found in Pbx1-null Flk2-MPPs compared to their controls, of which 38 were down-regulated and 29 up-regulated (Figure 3.2.3 and Table 3.2.3).

The two lists of DE miRNAs in Pbx1-null HSCs and in Pbx1-null Flk2$^-$MPPs, both compared to their relative controls, only partially overlap, with about 50% of the DE miRNAs in Pbx1-null HSCs which is different from the DE miRNAs in Pbx1 null Flk2$^-$ MPPs (Figure 3.2.3 B). This suggests that Pbx1 may have different roles in different cell subpopulations and motivates us to profile additional downstream progenitors in the future, to search for additional role of Pbx1 and miRNAs during the later steps of

hematopoietic differentiation. In this regard, we already collected and stored RNA from wt and mutant LMPPs (three pools of 2000-5000 cells each), which we know are defective in generating lymphocytes in the absence of Pbx1, as demonstrated in §3.1.

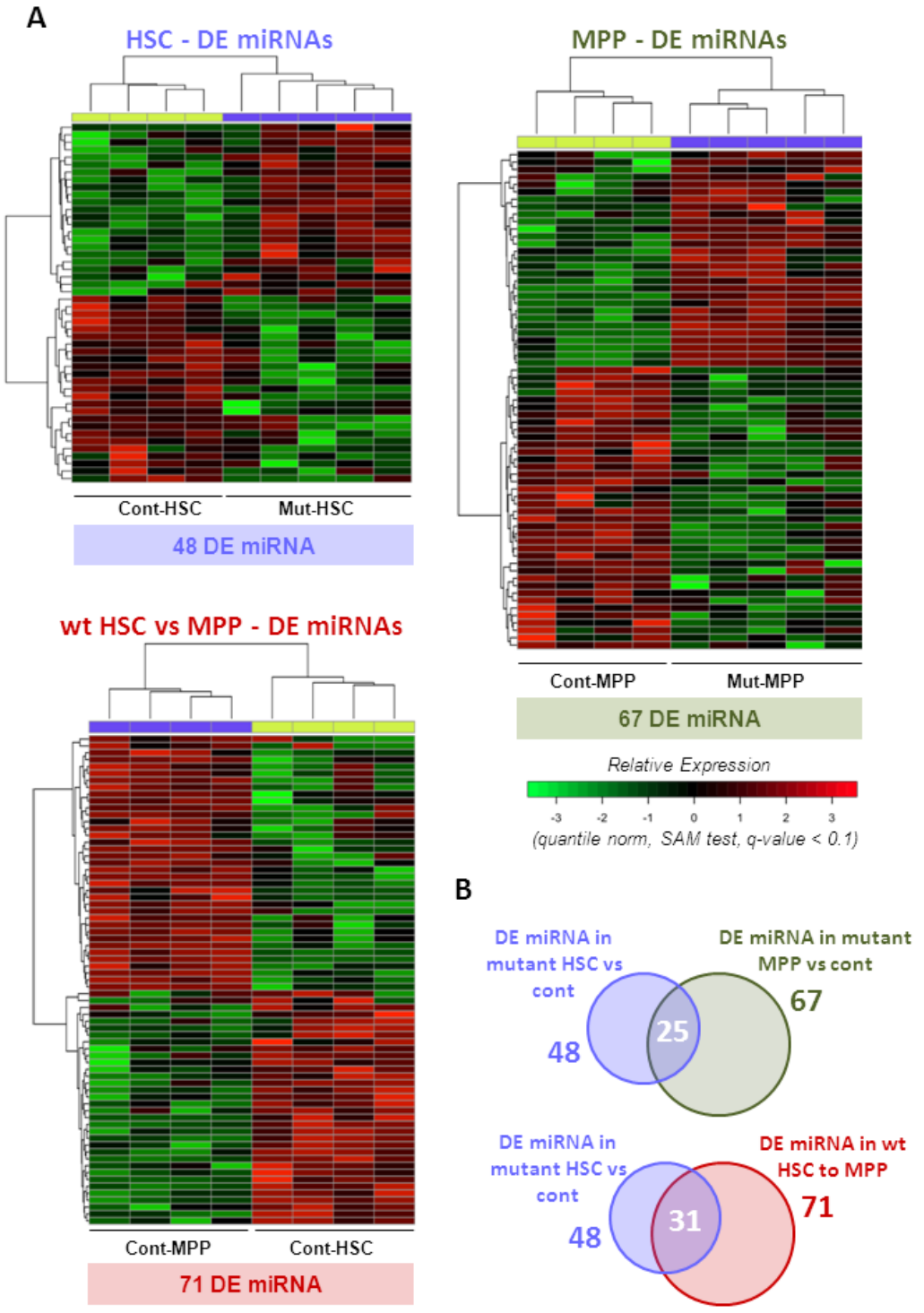


**Figure 3.2.3 Results of miRNA differential expression analysis.** (A) Hierarchical cluster dendrogram of relative expression of differentially expressed miRNAs. The color-scale represents Z-score transformed signal intensity (i.e. number of standard deviation from the miRNA average value). (B) Overlap of deregulated miRNAs in different conditions. The significance of the overlap has been computed by hypergeometric test: top, p-value 0.014; bottom, p-value 5e-05.

On the other hand, the fact that the other half of the DE miRNAs in Pbx1-null HSCs are also DE in Pbx1-null MPPs compared to their relative controls suggests that Pbx1 might be responsible, directly or indirectly, for their regulation. To support this hypothesis, we performed a promoter analysis through TRANSFAC® (a database on Transcription Factor Binding Sites which collects data on eukaryotic transcription factors, their experimentally-proven binding sites, consensus binding sequences and regulated genes) and MAST algorithm (Bailey and Gribskov, 1998), searching for Pbx1 binding sites in different regions upstream of the miRNA start sites (5000bp, 10000bp and 15000bp). The binding sequence selected for applying MAST algorithm is the matrix containing both the Pbx1 core binding site motif (TGAT) and a general Hox core binding site motif that is conserved across the Hox family (TGAT). This because using Pbx1 binding site alone, which is only four base long, would generate high quantity of non specific results and, however, Pbx1 normally acts as heterodimer, mostly with Hox proteins (see Introduction, §1.2.3). Promoter analysis revealed the presence of putative Pbx1-Hox binding sites in DNA regions up-stream of the coding region of a few miRNAs common to the two lists. However, those miRNAs are either expressed at a very low level, or change less than 2-fold in Pbx1-null HSCs compared to control, and will not be further investigated, even if this analysis would suggest a possible direct regulation by Pbx1-Hox binding. However, since Pbx1 can form complexes also with other homeodomain proteins, like Meis and Prep, and the binding specificity of the complexes is different according to the proteins involved, we will improve this analysis checking also for different binding site combinations (see Discussion, §4).

This miRNA profiling gave us the opportunity to analyze miRNAs specifically expressed during the physiological transition from HSCs to the first MPP stage, thus generating for the first time a list of DE miRNAs in the more primitive stages of normal hematopoietic differentiation. Comparison of miRNA profiling of control HSCs *versus* control Flk2$^-$MPPs revealed 71 DE probes, 37 of them up regulated and 34 down regulated during this differentiation step (Figure 3.2.3 and Table 3.2.4). By comparing this list with the previous one of 48 DE miRNAs in Pbx1-null HSCs *versus* wt, we found that 65% (31/48, hypergeometric p-value = 5e-05) of the DE miRNAs in Pbx1-null HSC are also DE in the normal HSC-to-MPP transition (Figure 3.2.3 B). This is similar to what occurs at the transcriptional level, where Pbx1-null HSCs exhibit a transcriptional profile typical of their immediate downstream progeny, making mutant HSCs more similar to the first MPP stage than bona fide HSCs (Ficara et al., 2008).

This observation is in accordance with our hypothesis that Pbx1 might control miRNAs involved in HSC differentiation.

## HSC mutant vs wt

### Up regulated miRNAs

| miRNA name | FD | Av lower Ct | Putative PT |
|---|---|---|---|
| **mmu-miR-532-5p** | 18,1 | 30 | Y (19) |
| mmu-miR-182 | 14,3 | 33 | Y |
| mmu-miR-200c | 13,2 | 34 | Y |
| **mmu-miR-324-3p** | 9,0 | 34 | Y |
| **mmu-miR-224** | 8,9 | 32 | Y |
| mmu-miR-680 | 7,2 | 32 | Y (17) |
| mmu-miR-34a | 6,7 | 32 | Y (23) |
| **mmu-miR-15a** | 6,4 | 31 | Y (one experimentally tested) |
| mmu-miR-124 | 5,3 | 34 | Y |
| **mmu-miR-146a** | 3,3 | 22 | Y (32) |
| mmu-miR-139-5p | 3,2 | 28 | Y (36) |
| **mmu-miR-342-3p** | 2,8 | 27 | Y (32) |
| **mmu-let-7e** | 2,7 | 26 | Y (29) |
| **mmu-let-7i** | 2,7 | 27 | Y (29) |
| **mmu-miR-148a** | 2,6 | 26 | Y (25) |
| mmu-miR-194 | 2,6 | 31 | Y |
| **mmu-miR-150** | 2,5 | 23 | Y |
| **mmu-miR-671-3p** | 2,4 | 31 | N |
| mmu-miR-29c | 2,4 | 31 | Y (31) |
| mmu-miR-126-5p | 2,3 | 28 | Y (36) |
| **mmu-let-7g** | 2,1 | 28 | Y (29) |
| **mmu-miR-365** | 2,0 | 28 | Y |
| **mmu-miR-331-3p** | 1,7 | 29 | Y |

### Down regulated miRNAs

| miRNA name | FD | Av lower Ct | Putative PT |
|---|---|---|---|
| **mmu-miR-127** | 91,95 | 31 | Y (2) |
| **mmu-miR-411** | 13,11 | 34 | Y (9) |
| **mmu-miR-1** | 12,95 | 31 | Y (2) |
| **rno-miR-1** | 11,80 | 29 | Y (2) |
| **mmu-miR-682** | 8,18 | 34 | N |
| mmu-miR-872 | 6,09 | 31 | Y (7) |
| **mmu-miR-34b-3p** | 5,99 | 30 | Y (9) |
| **mmu-miR-434-3p** | 4,73 | 32 | N |
| **mmu-miR-203** | 3,27 | 25 | Y (3) |
| **mmu-miR-188-5p** | 2,65 | 27 | Y (1) |
| mmu-miR-27a | 2,64 | 29 | Y (14) |
| mmu-miR-125b-5p | 2,61 | 28 | Y (1) |
| **mmu-miR-99b** | 2,55 | 29 | N |
| mmu-miR-19b | 2,54 | 20 | Y (2) |
| **mmu-miR-667** | 2,40 | 31 | N |
| **mmu-miR-223** | 2,32 | 24 | Y (12) |
| mmu-miR-25 | 2,29 | 27 | Y (7) |
| rno-miR-381 | 2,08 | 32 | N |
| **mmu-miR-197** | 1,94 | 29 | N |
| mmu-miR-376b | 1,87 | 26 | Y (1) |
| **mmu-miR-101a** | 1,70 | 28 | Y (13) |
| **mmu-miR-19a** | 1,57 | 25 | Y (2) |
| **mmu-miR-140** | 1,50 | 26 | Y (2) |
| **mmu-miR-93** | 1,49 | 25 | N |
| mmu-miR-24 | 1,42 | 24 | N |

**Table 3.2.2 DE miRNAs in Pbx1-null HSCS.** List of miRNAs DE in mutant *versus* wt HSCs as assessed by SAM analysis. In bold miRNAs which are common with the DE miRNAs in the normal HSC-to-MPP transition. In boxes miRNAs which are common with DE miRNAs in mutant *versus* wt MPPs. miRNAs highlighted in yellow are of potential interest for this study (Abbreviations: FD=Fold Difference; Av= Average; PT= Predicted Target; Y=presence of PT among the DE mRNAs, with the number of PT specified for some; N=absence of PT).

## MPP mutant vs wt

### Up regulated miRNAs

| miRNA name | FD |
|---|---|
| mmu-let-7a | 67,82 |
| mmu-miR-34a | 49,71 |
| mmu-let-7f | 45,90 |
| mmu-miR-687 | 9,75 |
| mmu-miR-532-5p | 9,14 |
| mmu-miR-425 | 7,25 |
| mmu-miR-676 | 5,39 |
| mmu-miR-685 | 4,97 |
| mmu-miR-200c | 4,67 |
| mmu-miR-339-5p | 3,66 |
| mmu-miR-126-5p | 3,34 |
| rno-miR-532-5p | 3,10 |
| mmu-miR-503 | 2,88 |
| mmu-miR-674 | 2,64 |
| mmu-miR-31 | 2,58 |
| mmu-miR-126-3p | 2,57 |
| mmu-miR-221 | 2,47 |
| mmu-miR-652 | 2,37 |
| mmu-miR-345-5p | 2,35 |
| mmu-miR-15a | 2,05 |
| mmu-miR-146b | 1,83 |
| mmu-miR-29c | 1,80 |
| mmu-miR-450a-5p | 1,76 |
| mmu-miR-10a | 1,69 |
| mmu-miR-139-5p | 1,59 |
| mmu-miR-150 | 1,54 |
| mmu-miR-146a | 1,44 |
| mmu-miR-21 | 1,27 |
| mmu-miR-222 | 1,26 |

### Down regulated miRNAs

| miRNA name | FD |
|---|---|
| mmu-miR-34b-3p | 24,57 |
| mmu-miR-1 | 15,18 |
| mmu-miR-375 | 9,46 |
| mmu-miR-133a | 9,26 |
| rno-miR-1 | 8,35 |
| mmu-miR-434-3p | 7,08 |
| rno-miR-381 | 6,85 |
| mmu-miR-337-5p | 5,61 |
| mmu-miR-182 | 5,15 |
| mmu-miR-544 | 4,57 |
| mmu-miR-127 | 4,39 |
| mmu-miR-383 | 4,34 |
| mmu-miR-350 | 4,25 |
| mmu-miR-188-5p | 3,01 |
| mmu-miR-376b | 2,89 |
| mmu-miR-409-3p | 2,46 |
| mmu-miR-872 | 2,01 |
| mmu-miR-667 | 1,98 |
| mmu-miR-181c | 1,95 |
| mmu-miR-223 | 1,94 |
| rno-miR-351 | 1,73 |
| mmu-miR-19a | 1,54 |
| mmu-miR-19b | 1,54 |
| mmu-miR-142-5p | 1,53 |
| mmu-miR-671-3p | 1,53 |
| mmu-miR-181a | 1,51 |
| mmu-miR-320 | 1,50 |
| mmu-miR-138 | 1,50 |
| mmu-miR-340-3p | 1,49 |
| mmu-miR-574-3p | 1,49 |
| mmu-miR-93 | 1,47 |
| mmu-miR-301b | 1,38 |
| mmu-miR-340-5p | 1,31 |
| mmu-miR-195 | 1,29 |
| mmu-let-7d | 1,28 |
| mmu-miR-744 | 1,24 |
| mmu-miR-26a | 1,19 |
| mmu-miR-16 | 1,19 |

**Table 3.2.3. DE miRNAs in Pbx1-null MPPs.** List of miRNAs DE in mutant *versus* wt MPPs. In boxes miRNAs which are common with DE miRNAs in mutant *versus* wt HSCs (Abbreviations: FD=Fold Difference; Av= Average).

**wt HSC-to-MPP**

| Up regulated miRNAs | |
|---|---|
| **miRNA name** | **FD** |
| mmu-miR-221 | 591,41 |
| mmu-miR-107 | 12,63 |
| mmu-miR-467a | 10,88 |
| rno-miR-207 | 10,12 |
| mmu-miR-23b | 9,70 |
| **mmu-miR-532-5p** | 8,93 |
| mmu-miR-450a-5p | 8,66 |
| mmu-miR-18a | 7,66 |
| **mmu-miR-224** | 7,52 |
| **mmu-miR-671-3p** | 6,96 |
| **mmu-miR-15a** | 6,89 |
| **mmu-miR-324-3p** | 6,84 |
| mmu-miR-339-5p | 5,86 |
| **mmu-miR-223** | 5,48 |
| mmu-miR-340-3p | 5,10 |
| rno-miR-351 | 5,09 |
| mmu-miR-652 | 5,06 |
| mmu-miR-322 | 4,21 |
| mmu-miR-542-3p | 3,48 |
| **mmu-let-7i** | 3,44 |
| mmu-let-7b | 3,20 |
| mmu-miR-100 | 3,07 |
| **mmu-let-7e** | 3,05 |
| mmu-miR-181c | 2,89 |
| mmu-miR-103 | 2,83 |
| mmu-miR-20b | 2,51 |
| **mmu-miR-93** | 2,27 |
| mmu-miR-744 | 2,17 |
| mmu-miR-196b | 2,02 |
| **mmu-let-7g** | 1,96 |
| **mmu-miR-19a** | 1,94 |
| rno-miR-196c | 1,77 |
| mmu-miR-222 | 1,67 |
| mmu-miR-130a | 1,53 |
| mmu-miR-92a | 1,34 |
| mmu-let-7d | 1,33 |
| **mmu-miR-331-3p** | 1,22 |

| Down regulated miRNAs | |
|---|---|
| **miRNA name** | **FD** |
| **mmu-miR-127** | 49,75 |
| mmu-miR-184 | 38,88 |
| **mmu-miR-411** | 21,05 |
| **mmu-miR-434-3p** | 10,66 |
| **mmu-miR-146a** | 8,01 |
| **mmu-miR-682** | 7,40 |
| **mmu-miR-1** | 7,14 |
| **mmu-miR-197** | 7,12 |
| mmu-miR-451 | 6,55 |
| mmu-miR-133a | 6,52 |
| **rno-miR-1** | 6,19 |
| **mmu-miR-148a** | 5,73 |
| mmu-miR-7a | 5,60 |
| **mmu-miR-34b-3p** | 5,51 |
| mmu-miR-145 | 5,21 |
| **mmu-miR-188-5p** | 4,73 |
| **mmu-miR-342-3p** | 3,73 |
| **mmu-miR-667** | 3,45 |
| mmu-miR-409-3p | 3,21 |
| mmu-miR-152 | 3,11 |
| **mmu-miR-203** | 3,05 |
| mmu-miR-31 | 2,89 |
| mmu-miR-128a | 2,83 |
| **mmu-miR-150** | 2,76 |
| **mmu-miR-365** | 2,48 |
| **mmu-miR-99b** | 2,19 |
| mmu-miR-193b | 1,91 |
| mmu-miR-29a | 1,59 |
| mmu-miR-26b | 1,58 |
| **mmu-miR-101a** | 1,51 |
| mmu-miR-191 | 1,40 |
| **mmu-miR-140** | 1,38 |
| mmu-miR-30e | 1,26 |
| mmu-miR-484 | 1,24 |

**Table 3.2.4. DE miRNAs in wt HSC-to-MPP transition.** List of miRNAs DE in wt HSCs *versus* MPP. In bold miRNAs which are common with the DE miRNAs in mutant *versus* control HSCs (Abbreviations: FD=Fold Difference; Av= Average).

## 3.2.4 mRNA-miRNA integrated analysis

The miRNA profile was then compared to the previously published transcriptional profile data relative to mutant and wt HSCs (Ficara et al., 2008), searching for miRNA predicted targets whose change in expression inversely correlates with those of miRNAs. (Figure 3.2.4).

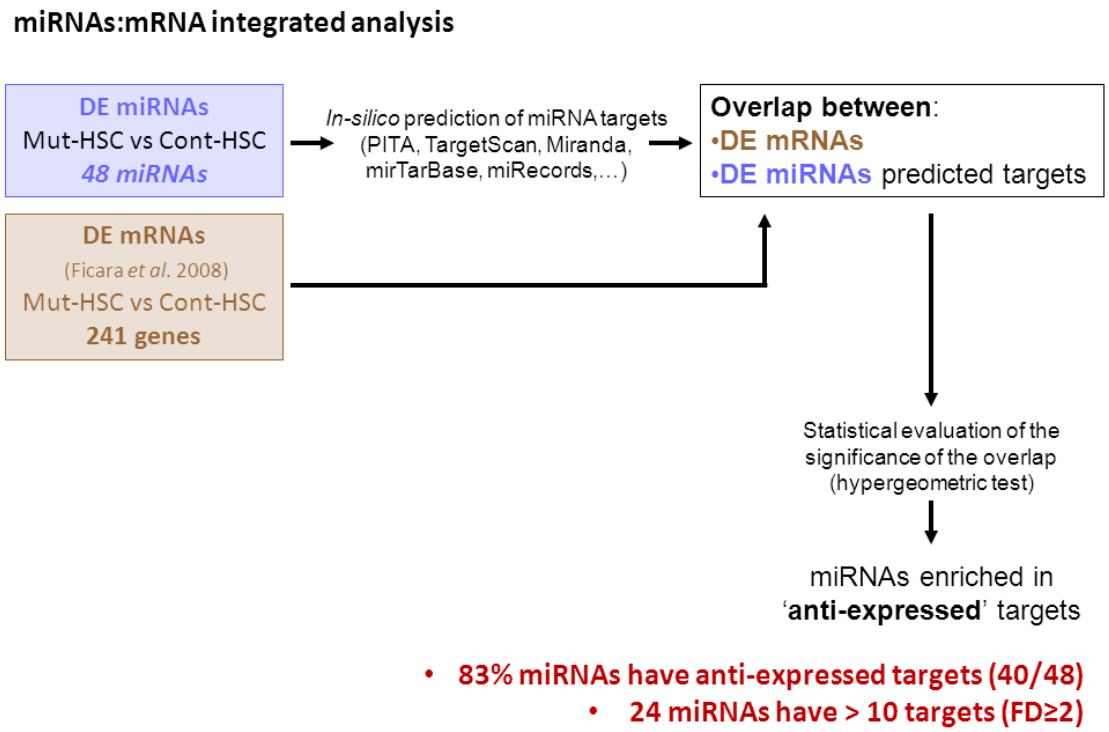


**Figure 3.2.4 Schematic representation of miRNA:mRNA integrated analysis.** See text for details.

On the DE miRNAs we performed an *in-silico* prediction of their targets, which relyes on a combination of multiple algorithms, (PITA, TargetScan, miRanda, mirTarBase, miRecords, DianaMicroT, MirTarget2, picTar, starBase) also combined with experimental reports. This multiple combinatorial algorithm was developed by our bioinformatics collaborators and allows the simultaneous and interactive combination of the outputs of the different tools. Putative predicted targets were then compared with the transcriptional profile data searching for overlaps between DE mRNA and DE miRNA predicted targets whose expression inversely correlates with those of miRNAs. A hypergeometric test was applied for statistical evaluation of the significance of the overlap.

Focusing first on the comparison between mutant and control HSCs, 40 out of 48 miRNAs were found to have predicted anti-correlated targets within the list of DE mRNAs (p 0.1). Of these, 24 have more than 10 predicted targets and change more than 2-fold compared to controls. In addition to providing anti-correlated miRNA-mRNA pairs, we also identified genes co-targeted by different miRNAs and functionally related genes within the same pathway. These analyses suggest that the same transcripts might be target of several miRNAs at the same time, and *vice versa* that the same miRNA can

target different DE genes (Table 3.2.5). Genes with multiple miRNA target site could be subjected to a stronger regulation and therefore could be potential important regulators of the mutant phenotype. The most targeted genes are Usp24 and Msi2, targets of 15 DE miRNAs, and Hlf, target of 11 DE miRNAs (Figure 3.2.5 A). Sheme of co-target analysis of the top targeted transcripts is summarized in Table 3.2.5.

This combined multiple analysis (co-targeting) is particularly useful since the regulatory miRNA effect could be mediated by simultaneous action of different miRNAs rather than by a single miRNA:mRNA interaction.

We also performed a gene set enrichment analysis (GSEA) of anti-expressed targets to search if in our gene set there is enrichment for genes common to other published gene sets from microarray studies which, in turn, can suggest biological and/or pathological function as well as molecular pathways possibly involved. This analysis revealed that anti-expressed targets common to different miRNAs are enriched for typical HSC genes, and for genes involved in differentiation, cell cycle, and immune system, among others (Figure 3.2.5 B). These findings nicely correlate with the phenotype of Pbx1-null HSCs, which display reduced self-renewal and aberrant differentiation.

**Cotargeting analysis**

**A**

**Top genes co-targeted by multiple miRNAs (≥10)**

| Gene | N. of regulatory miRNAs |
|---|---|
| Usp24 | 15 |
| Msi2 | 15 |
| Pbx1 | 13 |
| Ocrl | 12 |
| Hlf | 11 |
| Camkk2 | 11 |
| Zpf608 | 10 |
| Mlt3 | 10 |
| Nfatc2 | 10 |
| Pabpc1 | 10 |
| Nfia | 10 |

**B**

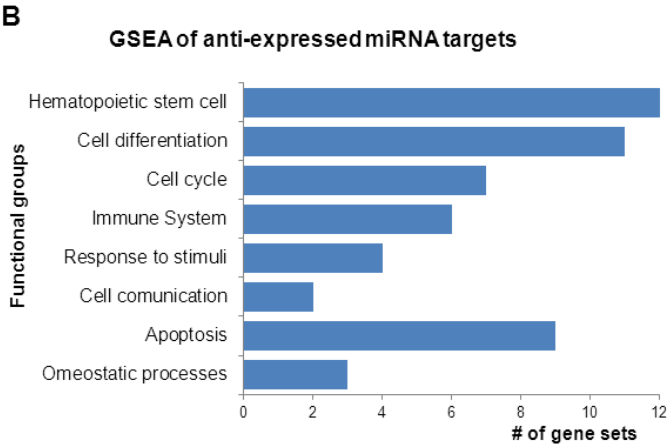


**Figure 3.2.5 Cotargeting analysis.** (A) Summary of the top genes targeted by ≥ 10 miRNAs highly expressed in Pbx1-null HSCs. (B) Summary of GSEA of anti-expressed miRNA targets. Bar graph shows the number of gene sets belonging to different functional groups that are enriched in the anti-expressed predicted targets (PT) of miRNAs up-regulated in the absence of Pbx1. Only miRNAs with ≥5 PT were included in the analysis (n=19 miRNAs).

**Co-targeting analysis**

| Target gene name | Target gene name (abbreviation) | number of regulatory miRNAs | mmu-let-7e-5p | mmu-let-7g-5p | mmu-let-7i-5p | mmu-miR-124-3p | mmu-miR-126-5p | mmu-miR-139-5p | mmu-miR-146a-5p | mmu-miR-148a-3p | mmu-miR-150-5p | mmu-miR-15a-5p | mmu-miR-182-5p | mmu-miR-194-5p | mmu-miR-200c-3p | mmu-miR-224-5p | mmu-miR-29c-3p | mmu-miR-324-3p | mmu-miR-331-3p | mmu-miR-342-3p | mmu-miR-34a-5p | mmu-miR-365-3p | mmu-miR-680 | mmu-miR-532-5p |
|---|---|---|---|---|---|---|---|---|---|---|---|---|---|---|---|---|---|---|---|---|---|---|---|---|
| ubiquitin specific peptidase 24 | **usp24** | 15 | | | | | | | | | | | | | | | | | | | | | | |
| Musashi homolog 2 (Drosophila) | **msi2** | 15 | | | | | | | | | | | | | | | | | | | | | | |
| pre B-cell leukemia transcription factor 1 | pbx1 | 13 | | | | | | | | | | | | | | | | | | | | | | |
| oculocerebrorenal syndrome of Lowe | ocrl | 12 | | | | | | | | | | | | | | | | | | | | | | |
| hepatic leukemia factor | **hlf** | 11 | | | | | | | | | | | | | | | | | | | | | | |
| calcium/calmodulin-dependent protein kinase kinase 2, beta | camkk2 | 11 | | | | | | | | | | | | | | | | | | | | | | |
| nuclear factor of activated T-cells, cytoplasmic, calcineurin-dependent 2 | **nfatc2** | 10 | | | | | | | | | | | | | | | | | | | | | | |
| nuclear factor I/A | nfia | 10 | | | | | | | | | | | | | | | | | | | | | | |
| zinc finger protein 608 | zfp608 | 10 | | | | | | | | | | | | | | | | | | | | | | |
| myeloid/lymphoid or mixed lineage-leukemia translocation to 3 homolog | **mllt3** | 10 | | | | | | | | | | | | | | | | | | | | | | |
| poly A binding protein, cytoplasmic 1 | pabpc1 | 10 | | | | | | | | | | | | | | | | | | | | | | |
| claudin 12 | cldn12 | 9 | | | | | | | | | | | | | | | | | | | | | | |
| myosin, light polypeptide kinase | **mylk** | 9 | | | | | | | | | | | | | | | | | | | | | | |
| follistatin-like 1 | fstl1 | 9 | | | | | | | | | | | | | | | | | | | | | | |
| zinc finger and BTB domain containing 20 | zbtb20 | 9 | | | | | | | | | | | | | | | | | | | | | | |
| myeloid ecotropic viral integration site 1 | **meis1** | 8 | | | | | | | | | | | | | | | | | | | | | | |
| Kruppel-like factor 4 (gut) | **Klf4** | 7 | | | | | | | | | | | | | | | | | | | | | | |
| homeo box A5 | **hoxa5** | 7 | | | | | | | | | | | | | | | | | | | | | | |
| cyclin D1 | **ccnd1** | 6 | | | | | | | | | | | | | | | | | | | | | | |
| phosphatidylinositol 3-kinase, regulatory subunit, polypeptide 1 (p85 alpha) | **pik3r1** | 6 | | | | | | | | | | | | | | | | | | | | | | |

**Table 3.2.5. Cotargeting analysis.** The matrix shows top genes targeted by multiple miRNAs and miRNAs which regulate multiple genes. Gene in bold were selected for future luciferase validation assays. Predicted miRNA:mRNA interactions are shown by red boxes. Experimentally validated target is shown in yellow box.

We focused our analysis on miRNAs which have anti-correlated targets among the DE transcripts but, we don't exclude *a priori* other miRNAs with no predicted targets among the DE genes, especially those with the highest level of fold difference, since mRNA-miRNA pairing may result in inhibition of translation rather that mRNA degradation (see introduction). Unfortunately we don't have proteomic profiling data on Pbx1-null HSCs (it would be technically challenging).

Since miRNA can be either intragenic or extragenic we also studied their genomic position. Intragenic miRNAs are expected to change concordantly with the host gene, however none of the DE miRNAs in mutant HSCs or Flk2$^-$MPPs and their corresponding controls is located within a transcript detected in the microarray.

## 3.2.5 Validation

To validate some of the profiling data, we sorted HSCs and Flk2$^-$MPPs from adult wt mice to extract RNA and perform Multiplexed RT and PreAmplifications. Of note, for validation we could purify miRNA and mRNAs from the same sample, although these populations are extremely rare. The possibility of comparing miRNAs and transcripts

within the same sample greatly improves our confidence on the results of the miRNA:mRNA integrated analysis.

We were able to obtain enough HSCs and MPPs for reliable detection of miRNAs and mRNAs (Figure 3.2.6) from the same sample only by pooling BM of two-three mice.

First, we assessed that the cDNA pre-amplification procedure, that we used also for mRNA, did not artificially alter transcript expression levels (Figure 3.2.6 B).

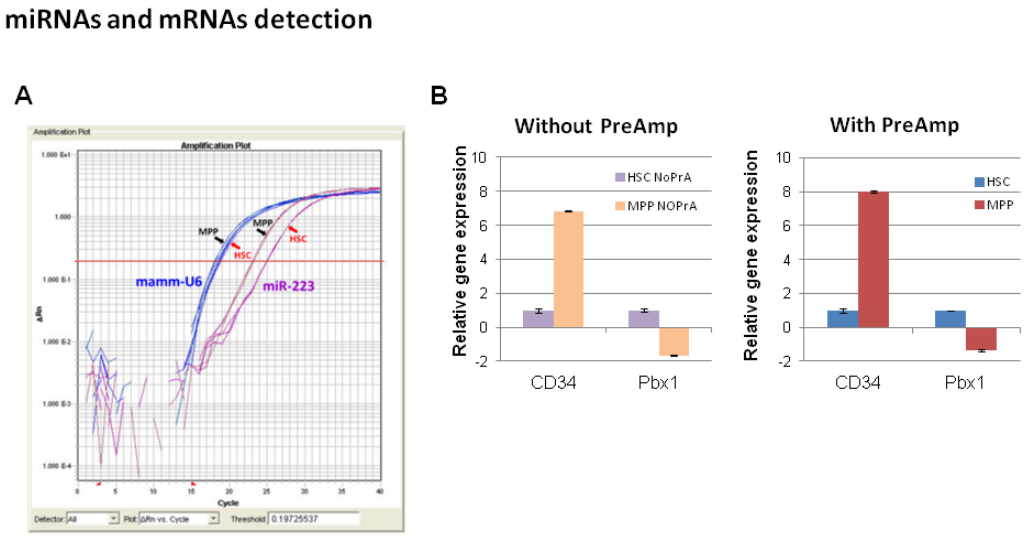


**Figure 3.2.6** miRNA and mRNA detection. (A) Representative amplification plot from a real-time PCR experiment showing expression of the ubiquitous small RNA mamm-U6 (in blue) and a representative miRNA (miRNA-223, in purple) in wt HSCs and Flk2-MPPs, after cDNA pre-amplification. (B) Expression level measured by real-time PCR of CD34 and Pbx1 in Flk2-MPPs relative to HSCs, in samples with or without cDNA pre-amplification (left and right, respectively). Data are normalized with β-Actin and refer to two independent experiments (each performed in triplicate with pooled RNA from two-three mice).

Higher expression of the CD34 marker and lower expression of Pbx1 in wt Flk2$^-$MPPs compared to HSCs is expected, and confirmed the good quality of the samples and the sorting procedure, even if sorting purity is routinely checked by FACS analysis (not shown).

We then confirmed some of the miRNA profiling data with independent real-time PCRs on these control samples (Figure 3.2.7) using individual TaqMan miRNA Assays.

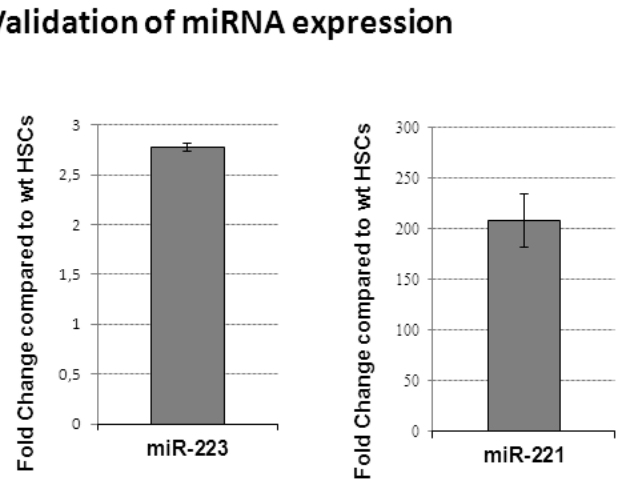


**Figure 3.2.7 Validation of miRNA expression**. Expression level measured by real-time PCR of miR-223 and miR-221 in wt Flk2$^-$MPPs relative to HSCs, in pre-amplificated samples. Data are normalized with mamm-U6 and refer to three independent experiments (each performed in triplicate with pooled RNA from two-three mice).

Interestingly, we found that the most up-regulated miRNA in the normal HSC-to-MPP transition is miR-221. This observation represents an important positive control of our analysis, since miR-221 has been previously predicted to be an important regulator of HSC maturation, thanks to its ability to repress cKit, based on data from human CD34$^+$ cells (Felli et al., 2005).

Validation of miRNA profiling data and mRNA analysis is more complicated with mutant mice, due to the severe phenotype leading to early death and to an extremely low number of HSCs. This forces us to pool cells from mutant Tie2Cre$^+$Pbx$^{-/f}$ mice. However, we pool the frozen samples only after confirming the Pbx1 deletion by PCR on genomic DNA extracted from blood or from colonies generated in CFC assays obtained from BM or spleen cells (Figure 3.2.8).

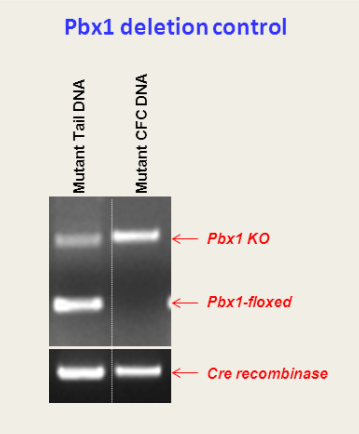


**Figure 3.2.8 PCR to check for deletion of Pbx1.** PCR on genomic DNA extracted from tail biopsies and from CFC colonies show correct Cre-mediated deletion of the floxed allele in mutant hematopoietic cells, where Cre is expressed.

Only by pooling three-four samples we are able to obtain enough HSCs ($LKS^+CD150^+CD48^-Flk2^-$) and $Flk2^-$MPPs ($LKS^+CD150^+CD48^+Flk2^-$) for further analysis (miRNA validation is ongoing).

## 3.2.6 Selection of candidate miRNAs

After correlation with mRNA profiling data, we are currently selecting few miRNA candidates with the future aim of studying the mechanism(s) through which they exert their function, and their potential regulation by Pbx1. The first selection of specific DE miRNAs in mutant *versus* wt HSCs is being made on the basis of the following criteria:

1. Relative abundance in HSCs (Ct levels in our miRNA profiling lower than 31 in at least one of the two groups);
2. Fold difference (we arbitrarily chose to consider FD higher than 2,8);
3. Presence of at least 10 anti-correlated predicted targets in the list of DE mRNAs.

According to these criteria, we have initially selected five miRNAs (mir-532-5p, miR-15a, miR-146a, miR 139-5p, miR-342-3p, Table 3.2.2), all up-regulated in the absence of Pbx1. Most of them are miRNAs that would also normally change in the HSC-to-MPP transition (Table 3.2.4), and have putative targets potentially interesting in HSC biology (Table 3.2.5).

On the other hand, in the list of miRNAs down-regulated in Pbx1-null HSCs, few miRNAs are potentially interesting even if condition 3 is not satisfied. They include miR-127 and miR-1 (Table 3.2.2), that are 92- and 12-fold decreased in the absence of

Pbx1, and that are also among the top down-regulated miRNAs in the normal HSC-to-Flk2$^-$MPP transition (Table 3.2.4).

We are currently planning luciferase assays on few putative targets of those miRNAs in order to validate the bioinformatics results. Targets have been short-listed on the basis of their function, their fold-change in Pbx1-null HSCs compared to controls, and on the co-targeting studies. Selected miRNAs and their targets are indicated in bold in the Table 3.2.2. Table 3.2.4 and Table 3.2.5.

# 4. DISCUSSION

In this study, we demonstrate that Pbx1 functions as a brake on cell differentiation in multi-potent and myeloid-restricted progenitors, to maintain progenitor reservoirs and lymphoid potential. Moreover, we show that in the absence of Pbx1 HSCs display an altered micro-RNA profile, which resembles the normal MPP profile, suggesting a role for miRNAs in maintaining HSC identity.

Understanding mechanisms of regulation of self-renewal *versus* differentiation of HSCs and downstream progenitors is a central issue in stem cell field since tiny alteration of these mechanisms may lead to hematopoietic failure and disease. If too few progenitors are produced, or if production of mature cells is unbalanced at the expense of one population respect to the others, the hematopoietic system will not be able to guarantee proper blood function, with different severity according to the cell population missing or more present (anemia, trombocytopenia, leucopenia, pancytopenia). Moreover, when HSC differentiation into committed progenitors is not accompanied by the typical loss of self-renewal capacity, or if downstream progenitors fail to fully differentiate into mature blood cells (Reya et al., 2001), leukemic transformation may occur (Weissman, 2005). Moreover, increasing evidences show that lineage-restricted progenitors might be targets for oncogenic transformations rather than HSCs. They may acquire stem properties normally lost during differentiation, like unlimited self-renewal capacity that, in addition to their intrinsic proliferative capacity, may confer them leukemia stem cell potential (Cano et al., 2008; Cleary, 2009; Krivtsov et al., 2006; Minami et al., 2008; Signer et al., 2010; Somervaille et al., 2009; Tremblay et al., 2010; Wojiski et al., 2009). In this perspective, the discovery of factors and pathways restraining progenitors or HSC differentiation is crucial for understanding leukemic stem cell biology and for future therapies.

Regulation of HSC differentiation into myeloid and lymphoid lineages has been intensively studied, and several transcription factors displaying lineage-instructive roles in specific progenitors have been identified (Orkin and Zon, 2008; Rothenberg, 2007) (reviewed in (Iwasaki and Akashi, 2007)). However factors that limit progenitor maturation and guarantee continuous presence of undifferentiated progenitor cells ready for transient expansion are poorly known, as well as factors important for maintaining the proper levels of specific peripheral lymphoid and myeloid mature cells, without improper skewing towards one lineage respect to the other. In addition, whether the

same factors regulating HSC self-renewal are also implicated in maintaining progenitor reservoirs is unknown.

Here, we show that Pbx1-null myeloid and multi-potent progenitors are characterized by a shorter cell cycle and a more rapid maturation rate toward the myeloid lineage at the expense of their expansion and of lymphoid lineage potential, making Pbx1 an essential regulator of progenitor lineage choice.

Previous developmental studies on Pbx1 deficiency have attributed the hypoplasia or aplasia of multiple organ systems to a progenitor proliferation defect (Schnabel et al., 2003a; Schnabel et al., 2003b; Selleri et al., 2001). In contrast, the gene expression profile of Pbx1-deficient CMPs, which reveals premature expression of downstream GMP genes, indicated that the reduction in myeloid-restricted progenitors is linked to an accelerated myeloid maturation rather than a proliferation defect. This was confirmed by our analysis of hematopoietic progenitors that shows increased short-term proliferation, rather than reduction, of MPPs and CMPs, followed by their premature exhaustion as they differentiate through myeloid fate. Accelerated maturation has also been observed in embryonic Pbx1-null chondrocytes, which undergo premature ossification (Selleri et al., 2001). Taken together, these data suggest that the primary myeloid defect caused by Pbx1 deficiency is accelerated maturation that shortens the temporal range of myeloid progenitor proliferative expansion, resulting in their final reduction.

In addition to functioning as a brake on myeloid differentiation, Pbx1 also maintains lymphoid potential in hematopoietic progenitors. A blastocyst complementation assay, in which Pbx1-deficient ES cells were used to generate chimeric Rag1-deficient mice, indicated a specific role for Pbx1 in lymphoid development (Sanyal et al., 2007). This experimental approach allows the evaluation of Pbx1 function in lymphocyte development overcoming the Pbx1-null embryonic lethality prior to formation of a lymphoid compartment. In this system lack of Pbx1 completely depletes CLPs and most of their lymphoid progenies (B and NK cells). T-cells are also decreased, but detectable. In our Pbx1 mutant model, progenitors having primed or restricted lymphoid differentiation capacity (LMPPs and CLPs, respectively) are reduced both in number and in function, with decreased lymphoid outputs in culture. The severe CLP reduction may be due either to a cell-intrinsic requirement for Pbx1 in CLPs or alternatively be the consequence of insufficient CLP generation due to an aberrant differentiation program initiated by Pbx1 null multipotent progenitors, as suggested by our B cell

differentiation assay from LMPPs. Moreover, a role for Pbx1 in maintaining proper lymphoid potential in HSCs has been hypothesized in previous studies showing compromised lymphoid gene expression in HSCs in the absence of Pbx1 (Ficara et al., 2008).

In the second part of this study, we investigated a possible role for miRNAs in modulating HSC self-renewal, by studying the transition from HSCs to Flk2$^-$MPPs, where loss of self-renewal occurs. Due to the profound self-renewal defect of Pbx1-null HSCs, Pbx1 conditional KO mice represent a useful tool to study whether the self-renewal defect induced by Pbx1 loss is mediated by miRNAs.

Cellular signals other than transcription factors that regulate the balance between self-renewal and differentiation in HSCs are poorly understood, including any role for miRNAs. Moreover, it has been demonstrated that miRNAs regulate almost each hematopoietic differentiation step but whether they function also at the top of the hematopoietic tree, regulating the first transition from self-renewing HSC to non-self-renewing multipotent cells, is still unclear. The interest in studying the role of miRNAs in HSC self-renewal is not unexpected, since it has been demonstrated that miRNAs have fundamental roles in hematopoietic development and they can be instructive determinants of cell fate, similarly to what transcription factors do (Graf and Enver, 2009). Moreover they have been extensively linked to differentiation and self-renewal, which are the main defective processes in Pbx1-null HSCs.

To elucidate the role of miRNAs in HSCs and/or progenitors, in this study we have generated a list of DE miRNAs in HSCs and Flk2$^-$MPPs in the absence of Pbx1 compared to wt. Moreover, combining miRNA data with the published transcriptional profile data of the same populations (Ficara et al., 2008) allowed searching for miRNA predicted targets whose change in expression inversely correlates with those of mRNAs. This analysis, coupled with extensive bioinformatics studies (such as promoter analysis, co-targeting and GSEA) allowed ultimate selection of very few candidate miRNAs to be further studied for their specific role in maintaining HSC self-renewal, and their possible regulation by Pbx1. In addition to a list of Pbx1-dependent miRNAs in HSCs and MPPs, this study analyzes for the first time miRNAs characteristic of the normal transition from HSCs to the first MPP stage, which represent an important finding for understanding physiological hematopoietic stem cell self-renewal and differentiation mechanisms. Indeed, in a few very recent studies a similar profiling has been performed on wt cells. However, additional studies are needed since either the complete list of

differentially regulated miRNAs has not been disclosed (Han et al., 2010; Ooi et al., 2010), or HSC and MPP populations were purified using markers that do not allow high level of enrichment (Petriv et al., 2010). In this context, our study represents an important step forward.

A substantial overlap (50%) in the lists of DE miRNAs in Pbx1-null HSCs and MPPs compared to their relative controls leads us to hypothesize a direct role of Pbx1 in their regulation. Although promoter analysis predicted the presence of Pbx1-Hox binding sites upstream of the coding region of few miRNAs, they are not relevant in our system according to our selection criteria. Nevertheless, chromatin immunoprecipitation sequencing (ChIP-seq) and ChIP-on-Chip experiments performed on tissues from wt and Prep hypomorphic E11.5 embryos demonstrate that Pbx1 directly binds some miRNA promoters (Penkov et al., 2013). Some of the miRNA genes, which showed a direct Pbx1-Meis binding are DE in mutant HSCv *versus* wt (mmu-let-7i, mmu-miR-148a and mmu-miR-99b), however with small fold change. Differences in the developmental stage and in tissues, and above all in the Pbx1 molecular partner chosen, may account for differences in the listed miRNAs.

Combinatorial miRNA:mRNA analysis reveals a tight connection between DE miRNAs and DE genes in Pbx1-null HSCs. Several genes are predicted targets of several miRNAs simultaneously and *vice versa*. Genes with multiple miRNA target sites could be subjected to a stronger regulation and therefore could be potential important regulators of the mutant phenotype. The most targeted genes are Usp24 and Msi2, targets of 15 DE miRNAs, and Hlf, target of 11 DE miRNAs (Figure 3.2.5 and Table 3.2.5). All of them are down-regulated targets of up regulated miRNAs. Musashi-2 (MSI2) is RNA binding-protein which increases proliferation of normal and malignant blood stem cells. Through inhibition of Numb transcription, Msi2 is a master switching regulator that is 'on' in normal HSCs and leukemic stem cells, and decreases in differentiating progenitors (Moore, 2010). This observation well correlates with the phenotype of Pbx1-null stem and progenitor cells, since in mutant HSCs, Msi2 is prematurely down-regulated. In human, higher expression of Msi2 correlates with poor prognosis in acute myeloid leukemia (Byers et al., 2011) and in adult B-cell acute lymphoblastic leukemia (Mu et al., 2013). Usp24 belongs to a large family of cysteine proteases that function as de-ubiquitinating enzymes and is involved in protein modifications and turnover (Zhang et al., 2012), while Hlf is a regulator of circadian rhythms, which influences HSCs (Mendez-Ferrer et al., 2009), and promotes resistance

to cell death (Waters et al., 2013). As Pbx1, Hlf is responsible for a subset of childhood B-lineage acute lymphoid leukemias characterized by the t(17;19) chromosomal translocation, which causes the formation of a fusion protein with the E2A gene (Hunger et al., 1996; Hunger et al., 1992; Waters et al., 2013).

Besides the aforementioned proteins, other putative multiple-miRNAs target are of particular interest (see Figure 3.2.5 and Table 3.2.5). Meis1, which is a well-known Pbx1 functional partner, is generally considered a typical HSC gene, due to its high expression in the most immature hematopoietic populations and its down-regulation upon differentiation (Argiropoulos and Humphries, 2007; Pineault et al., 2002). Meis1 regulation by Pbx1 is unexpected considering that it is a Pbx1 dimerization partner (Chang et al., 1997), although is consistent with a recent study showing compensatory increase in Pbx1 levels in response to loss of Meis1 (Unnisa et al., 2012). Moreover direct regulation of Pbx1 partners by Pbx1 itself has been reported in spleen progenitor cells during spleen ontogeny where Pbx1 directly regulates Hox11, and in turn, Hox11 regulates its own promoter in complex with Pbx1 (Brendolan et al., 2005). Direct or indirect regulation of Meis1 by Pbx1 has been hypothesized (Ficara et al., 2008). It will be interesting to study whether miRNAs paly a role in this regulation.

Another multiple-miRNA target is HoxA5, a transcription factor that plays important roles in embryogenesis, hematopoiesis, and tumorigenesis (Chen et al., 2005b). It is expressed during early myelopoiesis and simultaneously exerts inhibition of erythropoiesis and promotion of myelopoiesis, suggesting its role in lineage differentiation choice at the upstream multipotent progenitor stage (Fuller et al., 1999). Since HoxA5 could be a partner of Pbx1 and Pbx1 regulates different gene expression programs according to the different complexes it forms, modulation of the level of these proteins acting cooperatively with it, also maybe by miRNAs, could represent another mechanism through which Pbx1 acts. Moreover being HoxA5 implicated in lineage choice, it could be a possible downstream mediator of the defect in lineage choice showed in Pbx1-null progenitor cells.

Nuclear factor of activated T cells (NFAT) is involved in proper regulation of T cells development and differentiation, as well as in granulocyte and dendritic cell activation. NFAT also negatively regulates myeloid lineage development, likely acting at the progenitor stage, since hematopoietic ‘stem cell-like’ cell lines (derived from BM cells transduced with constructs encoding the Nucleoporin 98 (NUP)-HOXB4 fusion

protein), expressing an NFAT-inhibitory peptide, develop an enhanced myeloid compartment both *in vitro* and *in vivo* (Fric et al., 2012) .

Of note also Pbx1 is present among the putative targets of multiple miRNAs. If confirmed, this finding highlights a possible autocrine feed-back loop, as previously reported for other Pbx1 partners and for other miRNA-target pairs.

Following the selection criteria (see §3.2.6), we selected few miRNAs for future experiments. Among them, miR-146a is of particular interest due to its role in impairing differentiation of multipotent progenitor cells into common lymphoid progenitors (Starczynowski et al., 2011). Overexpression of miR-146a in hematopoietic stem and progenitor cells, followed by bone marrow transplantation, resulted in a transient myeloid expansion with a concomitant impaired lymphopoiesis. Moreover, impaired reconstitution of recipient mice and reduced survival of hematopoietic stem cells is observed upon enforced expression of miR-146a. miR-146a is mainly expressed in primitive hematopoietic stem and progenitor cells and T lymphocytes, however specific role for miR-146a in HSCs have not be investigated. According to our miRNA profile data, miR-146a is highly expressed in HSCs and Flk2$^-$MPPs and is down regulated (FD = 3,3) in the normal HSC-to-MPP transition, while it is upregulated in Pbx1-null HSCs compared to control. Thus we can speculate that normal miRNA-146a down regulation might allow MPPs to subsequently differentiate towards lymphoid lineage. This correlates with what observed in Pbx1-null HSCs where miR-146a is aberrantly upregulated.

So far, we have focused our analysis on miRNAs which have anti-correlated targets among the DE transcripts, however we do not exclude *a priori* other miRNAs with no predicted targets among the DE genes, especially those with an high level of fold difference, since mRNA-miRNA pairing may result in inhibition of translation rather that mRNA degradation.

Overall, this analysis set the basis for the discovery of miRNAs involved in the regulation of self-renewal *versus* differentiation.

# 5. Materials and Methods

## 5.1 Mice

$Tie2Cre^{+}.Pbx1^{-/f}$ and $Mx1Cre^{+}.Pbx1^{-/f}$ conditional knockout (KO) mouse models have been previously described (Ficara et al., 2008).

$Tie2Cre^{+}.Pbx1^{-/f}$ mice, also referred to as "mutant" mice in this thesis, are generated in two steps. First, Pbx1 heterozygous mice (Selleri et al., 2001), in which one Pbx1 allele is interrupted by the neomycine resistance gene (Neo) in exon 3, are crossed with $Tie2Cre^{+}$ mice, in which the Cre recombinase is under the control of the Tie2 promoter (Kisanuki et al., 2001), to obtain $Tie2Cre^{+}.Pbx1^{+/-}$ mice. The latter are then routinely mated with homozygous Floxed-Pbx1 ($Pbx1^{f/f}$) mice, in which *Pbx1* exon 3 is flanked by Lox-P sites (Koss et al., 2012), to generate $Tie2Cre^{+}.Pbx1^{-/f}$ mutant mice with a 25% frequency. The other littermates ($Tie2Cre^{+}.Pbx1^{+/f}$, $Tie2Cre^{-}.Pbx1^{-/f}$, $Tie2Cre^{-}.Pbx1^{-/f}$) do not differ in any of the described phenotypes hence were used indifferently as controls. All mice are in a C57BL/6 background. Mutant mice display a short life span and die between 2 and 4 weeks of age in our animal facility, slightly earlier than previously described.

Mice were genotyped by PCR on genomic DNA using a combination of three individual PCR reactions (one for the Cre recombinase, one for the presence of the Neo in one Pbx1 allele, and one for the Pbx1-floxed insertion). Genotyping is performed within week three of age. Genomic DNA was extracted from tail biopsies following standard Protein Kinase (Kanellopoulou et al.) digestion and chloroform-ethanol extraction protocol.

Primer sequences:

| | |
|---|---|
| Pbx1 Fw: | 5' TGA GTA TTC GGG GAG CCC AAG AA 3' |
| Pbx1 Rev: | 5' CAT GAT GCC CAG TCT GTA GGG GT 3' |
| Neo: | 5' CTA TCA GGA CAT AGC GTT GG 3' |
| | |
| Tie2Cre Fw: | 5' CCC TGT GCT CAG ACA GAA ATG AGA 3' |
| Tie2Cre Rev: | 5' CGC ATA ACC AGT GAA ACA GCA TTG C 3' |

Pbx1 Flox Fw: 5’ GAG TTT GTC AGA GGA TTT TGT AGA TCT C 3’

Pbx1 Flox Rev: 5’ CAC GTA CAA ATT GAG TTG ATA CAG TGG G 3’

All experiments were performed with the approval of and in accordance with the Istituto Clinico Humanitas Administrative Panel on Laboratory Animal Care.

$Mx1Cre^{+}.Pbx1^{-/f}$ mice were generated with a crossing scheme similar to the one described for $Tie2Cre^{+}.Pbx1^{-/f}$ mice by our collaborators at Stanford University.

# 5.2 Hematopoietic stem and progenitor cells isolation and flow cytometry

BM cell suspensions from control or mutant mice were obtained by crushing of multiple bones as previously described (Ficara et al., 2008). Briefly, after sacrifice, sternum, upper and lower limbs, shoulder blades, hips and vertebral column were dissected. After removal of connective tissues and spinal cord, bones were mechanically crushed with ceramic pestle and mortar, until BM cells were released from the bones cavity. The coarse suspension, made up of cell and bone debris, was then filtered through a 40μm filter, centrifuged at 1500 revolutions per minute (rpm), resuspended and counted. All bones and cell suspensions were constantly maintained on ice in cold PBS containing 2% fetal bovine serum (FBS) (Lonza) and 1mM EDTA. This buffer, referred to hereafter simply as staining buffer or PBS-FACS, was also used during staining for FACS analysis or sorting.

Hematopoietic progenitor cells were purified with magnetic enrichment systems based on the absence of lineage markers expression. We used a Lineage Cell Depletion kit (Mouse Hematopoietic Progenitor Cell Enrichment Kit, EasySep™, Stem Cell Technologies or Lineage Cell Depletion Kit, MACS, Miltenyi Biotec), and automated cell separators (RoboSep™, Stem Cell Technologies, or AutoMACS, Miltenyi Biotec).

The Lineage negative enriched fraction was then subjected to multicolor cell surface staining prior to cytofluorimetric analysis or cell sorting. Cell suspensions were incubated for 30 minute on ice (or 15 minute at room temperature) with the proper mix of antibodies (final volume/sample = 100μl), washed twice and resuspended at the concentration of $1x10^{7}$cells/ml (or a minimum of 150μl) prior to FACS analysis or cell sorting.

The following subpopulations were analyzed and/or sorted: HSCs ($Lin^-/cKit^{hi}/Sca^{hi}/CD34^-/Flk2^-$ or $Lin^-/cKit^{hi}/Sca^{hi}/CD150^+/CD48^-$); MPPs at different stages of maturation ($Lin^-/CD127^-/cKit^{hi}/Sca^{hi}/CD34^+/Flk2^-$ or $Flk2^{int}$ or $Flk2^{high}$); CLPs ($Lin^-/CD127^+/Flk2^{high}/cKit^{int}/Sca^{int}$); CMPs ($Lin^-/cKit^+/Sca^-/CD34^+/FcgRII/III^{int}$); GMPs ($Lin^-/cKit^+/Sca^-/CD34^+/FcgRII/III^{high}$); MEPs ($Lin^-/cKit^+/Sca^-/CD34^-/FcgRII/III^-$). CLPs were isolated without EDTA containing buffer, since it has been shown detrimental for cell survivial (Karsunky et al., 2008) .

Fluorochrome-conjugated monoclonal antibodies (mAbs) were purchased from BD Biosciences (BD), eBioscience or BioLegend. mAbs and relative concentrations used in this study are listed in Table 5.1.

| **mAbα** | **Fluorochrome** | **Clone** | **Dilution** | **Company** |
|---|---|---|---|---|
| CD34 | FITC | RAM34 | 1:25 | eBioscience |
| CD135 (Flk-2, Flt-3) | PE | A2F10 | 1:50 | eBioscience |
| Sca1 (Ly-6A/E) | FITC | D7 | 1:100 | eBioscience |
| | PE-Cy7 | D7 | 1:400 | eBioscience |
| | APC | D7 | 1:100 | eBioscience |
| c-Kit (CD117) | APC-eFluor780 | 2B8 | 1:100 | eBioscience |
| CD150 (Arboleda et al.) | APC | TC15-12F12.2 | 1:66 | Biolegend |
| CD48 (BCM1) | PE-Cy7 | HM48.1 | 1:200 | eBioscience |
| CD127 (IL7R) | APC | A7R34 | 1:100 | eBioscience |
| CD16/32 | PerCP-Cy5.5 | 93 | 1:100 | eBioscience |
| Mouse hematop. Lineage Cocktail* | eFluor450 | | 20μl/test | eBioscience |
| CD4 | eFluor450 | RM4-5 | 1:100 | Biolegend |
| CD8a | eFluor450 | 53-6.7 | 1:200 | eBioscience |
| CD41 | eFluor-450 | eBioMWReg30 | 1:50 | eBioscience |
| Mac1 (CD11b) | PE | M1/70 | 1:400 | eBioscience |
| CD11c | PE | HL3 | 1:200 | BD |
| CD19 | PE-Cy7 | eBio 1D3 | 1:300 | eBioscience |
| B220 (CD45R) | PerCP | RA3-6B2 | 1:100 | BD |
| Gr1 | APC | RB6-8C5 | 1:500 | eBioscience |
| NK1.1 | PE-Cy7 | PK136 | 1:100 | eBioscience |

**Table 5.1 Monoclonal antibodies and relative concentrations used in this study.** *The lineage cocktail is composed by the following eFluor450-conjugated mAbs: Mac1/CD11b (clone M1/70), Gr1 (Ly-G6) (clone RB6-8C5), B220 (clone RA3-6B2), TER-119 (clone TER-119), CD3 (clone 17A2).

Of note, since magnetic enrichment never reaches 100% purity, Lineage-depleted BM cells were further deprived of residual Lin positive cells by including in the combination of antibodies an additional PE-Cy7-conjugated Streptavidin (1:500; eBioscience) and

monoclonal antibodies (mAbs) to additional T cell and megakaryocyte markers not present in the lineage cocktail (CD4, 8, NK1.1 for T cells and in some instances CD41 for megakaryocytes (See Table 5.1).

Cytofluorimetric analyses were performed with FACS Canto I or II (BD Biosciences); Diva software (BD Biosciences) and FlowJo (Tree Star) were used for data acquisition and analysis, respectively.

Cell sorting was performed using a FACS Aria I, with a fluidic upgrade to the version III, (BD Biosciences) equipped with Diva software (BD Biosciences) and data were analyzed using FlowJo (Tree Star). Sorted cells were collected in FBS and centrifuged, and either resuspended in medium for culture, or frozen in RNA*later*® Solution (Ambion, Life Technologies) for subsequent RNA extraction.

# 5.3 Cell culture

## 5.3.1 Colony-forming unit (CFU) assay

Hematopoietic progenitors were sorted and seeded (200-500 cells/ml) into methylcellulose-containing medium (methoCult 3234; Stem Cell Technologies) supplemented with mSCF (20 ng/ml), hFlt3 ligand (20 ng/ml), mIL-6 (10 ng/ml), mIL-3 (10 ng/ml), mGM-CSF (10 ng/ml), mTPO (10 ng/ml) and hEpo (3 U/ml). All cytokines were purchased from PeproTech, except Epo (R&D Systems). CFU assays were performed in duplicate in 35mm dishes. Colonies composed of at least 50 cells were counted and type of colony scored after 9 days of culture by optical microscope. Colony counts were normalized to 1000 cells plated.

After counting, all colonies from each dish were harvested upon dilution of the methylcellulose-containing medium with warmed PBS (37°C). Cells were centrifuged at 1800 rpm for 10’ and residual methylcellulose was removed by vacuum aspiration. Cells were resuspended in PBS-FACS and counted or spotted for cytospyn preparation.

## 5.3.2 Myeloid differentiation assay

For *in vitro* myeloid differentiation freshly sorted MPPs and CMPs were plated in U-bottomed 96-well plates and cultured in IMDM medium (Lonza) supplemented with 10% FBS (Lonza) and SCF (20 ng/ml), IL-6, IL-3 (10 ng/ml each) for 3 or 6 days. At

each time point cells were harvested by gentle mechanical resuspension, stained with fluorochrome-conjugated monoclonal antibodies against Mac1/CD11b, Gr1, and/or with other antibodies listed in Table 5.1, and analyzed by FACS.

### 5.3.3 *in vitro* B cell differentiation assays

Freshly sorted LMPPs and CLPs were co-cultured with previously plated sub-confluent OP9 stromal cells in MEM-alpha medium supplemented with 10% heat-inactivated FBS (Lonza), 50 mM β-mercaptoethanol (Gibco, Life Technologies), and mSCF (20 ng/ml), hFlt3L (20 ng/ml) and mIL-7 (10 ng/ml) (Peprotech). Cells were then harvested by pipetting and analyzed by FACS 4 or 10–11 days later upon staining with fluorochrome-conjugated monoclonal antibodies to B220 and CD19 (see Table 5.1).
For limiting dilution assays, OP9 stromal cell layers were plated the day before in flat-bottomed 96-well plates and different amounts of prospectively isolated LMPPs and CLPs were seeded on each well (10, 30, 90 cells/well and 3, 10, 30 cells/well for mutant and control cells, respectively). Medium (see above) was half-replaced every third day. Wells with visible hematopoitic growth were scored by optical microscope observation at two time points (10 or 13 days) and cells were harvested from each positive well individually and analyzed by FACS to assess the presence of $B220^{+}CD19^{+}CD11b^{-}Gr1^{-}CD11c^{-}$ B cells.

### 5.3.4 Cytospin

Cells obtained from colonies were resuspended in 150μl of PBS-FACS and spotted on a glass slide according to standard cytospin protocol. Briefly a cytofunnel is attached to a glass slide and slide carrier. The entire apparatus is inserted into a cytocentrifuge and the cell suspension is added. 5’ at 800x*g* cytospin centrifugation is performed to spot the cells. Spotted cells were stained with standard May-Grunwald/Giemsa staining.

## 5.4 Statistical analysis

Significance of differences was determined by two-tailed Student’s t-test. Error bars in bar graphs indicate s.e.m.

# 5.5 microRNA profiling and Real-time quantitative PCR

MicroRNA profiling experiment was conducted in collaboration with Cleary's lab in Stanford University School of Medicine and with Dr. Yuley Wang in Applied Biosystem.

Briefly two-weeks-old $MxCre^{+}.Pbx1^{-/f}$ or $MxCre^{-}.Pbx1^{-/f}$ mice (5 mutants and 4 controls) were given seven poly(I:C) injections every other day and sacrificed 4 weeks after the last injection.

BM cells were obtained from multiple bones of individual mice and immunomagnetically selected, then stained with conjugated mAbs (to CD34, CD135, Sca-1, Lineage cocktail, and c-Kit) prior to sorting. Cells were maintained on ice when possible through all procedures.

RNA from sorted cell populations (1400–2000 HSCs, 2–6000 $Flk2^{-}$MPPs) was extracted with mirVana™ miRNA Isolation Kit (Applied Biosystems, Life Technologies), according to the manufacturer's protocol and then subjected to MegaPlex TaqMan® Assays system (Applied Biosystems, Life Technologies) for microRNA profiling. MegaPlex TaqMan® Assays system is a technology based on real-time PCR that enable analysis of small number of cells and allows simultaneous detection of more than 300 different miRNAs, including those expressed at low level. The system includes two main steps. The first step is a reverse transcription (RT) reaction, in which the miRNA is reversed transcribed into cDNA using a miRNA-target-specific stem looped RT primer (Chen et al., 2005a) (Figure 5.1).

In detail, the stem loop primer introduced a universal reverse primer sequence designed within a hairpin structure. The stem–loop RT primer displays two major advantages. First, it ensures specificity for only the mature form of miRNAs while miRNA precursors and other homologous sequences embedded in other transcripts will not be recognized. Second, it forms an RT primer/mature miRNA duplex that extends the 3' end of the miRNA, resulting in a longer RT product. This design overcomes a fundamental problem in miRNA quantitation: the short length of mature miRNAs (~22 nucleotides) which prohibits conventional design of a random-primed RT step (Chen et al., 2005a). With this strategy the longer cDNA template became suitable for the second step which is a standard real-time PCR using TaqMan® Assays, where another level of

specificity was provided during the real-time PCR process both by the miRNA specific forward primer and the TaqMan® probe.

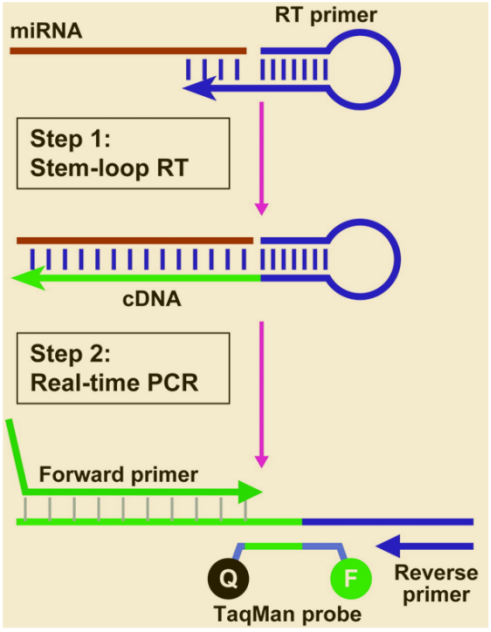


**Figure 5.1 Schematic description of TaqMan miRNA assays.** TaqMan-based real-time quantification of miRNAs includes two steps, stem–loop RT and realtime PCR. Stem–loop RT primers bind to at the 3' portion of miRNA molecules and are reverse transcribed with reverse transcriptase. Then, the RT product is quantified using conventional TaqMan PCR that includes miRNA-specific forward primer, reverse primer and a dye-labeled TaqMan probes (from (Chen et al., 2005a)).

miRNA RT was done with TaqMan® MicroRNA Reverse Transcription Kit (Applied Biosystems, Life Technologies), according to the manufacturer's protocol.

For profiling purpose the RT step was performed in Multiplex fashion, in which all the mature miRNAs are simultaneously reversed transcribed into cDNAs in one reaction using a specific pool of miRNA-stem looped RT primers designed to detect and quantitate up to 380 miRNAs (Megaplex™ RT Primers, Rodent Pool A, Applied Biosystems, Life Technologies). The same RT step was performed with individual RT primers for single analysis purposes with TaqMan miRNA Assays (see below).

An extra step of multiplexed pre-amplification was introduced between the RT and the Real time PCR to further enhance miRNA profiling sensitivity. With this pre-amplification step, multiplexed cDNA was simultaneously amplified before real time detection using another pool of sequence specific PCR primers (Megaplex™ PreAmp Primers, Rodent Pool A, Applied Biosystems, Life Technologies). TaqMan® PreAmp

Master Mix Kit (Applied Biosystems, Life Technologies) was used to perform pre amplification reaction. Twelve rounds of PCR amplification were performed, according to the manufacturer's protocol. Preamplified cDNAs were loaded in a 384 MW plate in which 376 TaqMan miRNA and 8 different control assays were preloaded.

For validation, individual real-time PCR reactions were performed to confirm some of the profiled miRNA on cDNA obtained with the above mentioned MegaPlex TaqMan® Assays system from freshly sorted HSCs and Flk2$^-$MPPs (pool of three/four wt mice). RNA was extracted with RNeasy Micro Kit (Qiagen), according to the manufacturer's protocol for recovery long and short RNA molecules. RNA was reverse transcribed in Multiplex fashion using TaqMan® MicroRNA Reverse Transcription Kit (Applied Biosystems, Life Technologies) with Megaplex™ RT Primers, Rodent Pool A (Applied Biosystems, Life Technologies), and preamplified using TaqMan® PreAmp Master Mix Kit (Applied Biosystems, Life Technologies).

The same Multiplexed analysis is applied to mRNA for validation purposes. RNA was reverse transcribed using High Capacity cDNA Reverse Transcription Kit (Applied Biosystems, Life Technologies) and cDNA pre amplified using the same TaqMan® PreAmp Master Mix Kit and a custom made pool of primers, according to the manufacturer's protocol. Up to one hundred transcripts can be preamplified simultaneously.

Multiplexed cDNA was then subjected to individual real-time PCR for miRNAs and mRNA using TaqMan® MicroRNA Assays and TaqMan® Gene Expression Assays respectively (all purchased from Applied Biosystems, Life technologies).

Since extracted RNA is under Nanodrop detection limit, a synthetic not mammalian miRNA-spike (cel-miR-39, from C. *elegans*) was added to the cell lysate prior to extraction as technical control. miRNA-spike follows all the extraction and preamplification procedures and is neither retrotrancribed nor preamplified with kits for mammalian miRNAs. It is separately detected with individual TaqMan® MicroRNA Assays. Every sample analyzed gave high reproducible results in term of cel-miR-39 Ct values, indicating a good quality of extraction procedure without loss of material.

TaqMan® Gene Expression Assays used in the present study were: mouse Cd34 assay (assay ID: Mm00519283_m1) and mouse Pbx1 assay (assay ID: Mm04207616_m1). Mouse bActin assay (assay ID: Mm00607939_s1) was used as endogenous housekeeping gene.

TaqMan® MicroRNA Assays used in the present study were: mmu-miR-223 assay (assay ID: 002295), mmu-miR-221 assay (assay ID: 000524), mmu-miR-99b assay (assay ID: 000436), mmu-miR-146a assay (assay ID: 000468) and mmu-let-7e assay (assay ID: 002406). U6 snRNA assay (assay ID: 001973) was used as endogenous control and cel-miR-39 assay (assay ID: 000200) was used as spike technical control.

## 5.6 Bioinformatics Analyses

All bioinformatics analyses were done by Dr. Paolo Uva in the Bioinformatics group of the Center for Advanced Studies, Research and Development in Sardinia (CRS4). See Result § 3.2 for specific analysis descriptions.

# APPENDIX A

## Raw data of Pbx1-null and control miRNA profile of HSCs and MPPs (quantile normalized)

| | Control HSCs | | | | Control Flk2-MPPs | | | | Mutant HSCs | | | | | Mutant Flk2-MPPs | | | | |
|---|---|---|---|---|---|---|---|---|---|---|---|---|---|---|---|---|---|---|
| "AssayID" | # 433 | # 434 | # 436 | # 437 | # 433 | # 434 | # 436 | # 437 | # 422 | # 423 | # 424 | # 425 | # 435 | # 422 | # 423 | # 424 | # 425 | # 435 |
| "mmu-let-7b" | 27,59 | 28,92 | 29,50 | 29,55 | 27,50 | 27,17 | 27,09 | 27,09 | 28,03 | 28,39 | 28,46 | 28,71 | 28,15 | 27,33 | 26,88 | 27,43 | 27,69 | 26,88 |
| "mmu-miR-7b" | 37,95 | 38,02 | 37,43 | 38,28 | 38,61 | 38,59 | 38,86 | 39,07 | 36,53 | 36,66 | 36,39 | 37,36 | 38,15 | 38,62 | 38,62 | 38,25 | 39,07 | 38,25 |
| "Mamm U6" | 20,92 | 20,92 | 22,05 | 21,28 | 20,92 | 20,92 | 21,28 | 20,51 | 20,51 | 20,51 | 20,51 | 20,51 | 20,32 | 20,51 | 20,51 | 20,51 | 20,32 | 20,44 |
| "Mamm U6" | 20,51 | 20,44 | 20,51 | 20,51 | 20,51 | 20,44 | 20,51 | 20,32 | 20,92 | 20,44 | 20,12 | 20,32 | 20,44 | 20,32 | 20,44 | 20,12 | 20,12 | 20,12 |
| "mmu-miR-9" | 34,84 | 38,02 | 37,43 | 38,28 | 38,61 | 35,50 | 38,86 | 39,07 | 32,08 | 38,62 | 37,36 | 35,30 | 32,53 | 37,36 | 38,96 | 39,98 | 39,71 | 37,60 |
| "mmu-miR-10a" | 27,17 | 27,17 | 27,17 | 27,00 | 27,25 | 27,09 | 27,43 | 27,33 | 26,20 | 27,69 | 28,03 | 28,15 | 26,71 | 26,35 | 26,35 | 26,57 | 26,57 | 26,79 |
| "mmu-miR-15a" | 32,43 | 33,45 | 37,43 | 35,50 | 31,76 | 31,07 | 33,35 | 31,50 | 31,29 | 31,07 | 32,08 | 31,29 | 34,35 | 30,79 | 31,07 | 30,69 | 31,07 | 30,79 |
| "mmu-miR-15b" | 26,20 | 26,46 | 25,49 | 26,20 | 25,73 | 25,49 | 25,73 | 25,90 | 25,73 | 25,95 | 25,60 | 25,95 | 26,02 | 25,49 | 26,28 | 25,90 | 25,90 | 25,82 |
| "mmu-miR-16" | 22,95 | 23,14 | 22,95 | 23,14 | 23,14 | 22,95 | 23,14 | 23,37 | 23,51 | 22,71 | 22,71 | 22,71 | 23,14 | 23,37 | 23,37 | 23,51 | 23,37 | 23,37 |
| "rno-miR-17-3p" | 37,95 | 38,02 | 37,43 | 38,28 | 35,50 | 36,08 | 38,86 | 38,25 | 38,96 | 38,62 | 37,20 | 39,07 | 38,15 | 39,14 | 38,59 | 38,40 | 37,89 | 36,95 |
| "mmu-let-7c" | 25,28 | 25,82 | 26,02 | 25,49 | 25,49 | 24,93 | 25,49 | 25,60 | 25,82 | 26,12 | 25,90 | 26,46 | 25,60 | 25,82 | 25,15 | 25,60 | 26,12 | 25,60 |
| "mmu-miR-18a" | 32,25 | 32,19 | 29,55 | 29,78 | 27,78 | 28,77 | 27,69 | 27,78 | 28,77 | 29,50 | 29,38 | 30,27 | 31,76 | 28,15 | 28,24 | 27,87 | 28,15 | 27,95 |
| "mmu-miR-19a" | 25,60 | 26,02 | 25,28 | 25,60 | 24,67 | 24,67 | 24,67 | 24,67 | 26,02 | 26,46 | 26,12 | 26,88 | 25,90 | 25,28 | 25,49 | 25,49 | 25,28 | 24,93 |
| "mmu-miR-19b" | 20,44 | 20,51 | 20,32 | 20,44 | 20,44 | 20,51 | 20,12 | 21,28 | 21,28 | 22,60 | 21,28 | 22,41 | 21,28 | 21,28 | 21,28 | 21,28 | 21,28 | 20,92 |
| "mmu-miR-20a" | 22,05 | 22,41 | 20,92 | 22,41 | 22,05 | 22,05 | 22,05 | 22,05 | 22,05 | 22,95 | 22,60 | 23,14 | 22,60 | 22,05 | 22,05 | 22,05 | 22,05 | 22,05 |
| "mmu-let-7d" | 27,87 | 27,50 | 27,78 | 27,50 | 27,17 | 27,33 | 27,25 | 27,25 | 27,69 | 27,87 | 27,69 | 27,33 | 27,78 | 27,59 | 27,50 | 27,59 | 27,87 | 27,50 |
| "mmu-let-7e" | 27,43 | 28,15 | 28,54 | 27,78 | 26,79 | 26,35 | 26,20 | 26,12 | 26,94 | 26,02 | 25,95 | 26,12 | 27,59 | 26,46 | 26,57 | 26,12 | 26,46 | 26,02 |
| "mmu-let-7g" | 29,38 | 30,27 | 29,27 | 29,73 | 28,97 | 28,65 | 28,60 | 28,54 | 28,71 | 28,46 | 28,39 | 27,95 | 29,33 | 28,46 | 28,39 | 28,39 | 28,54 | 28,39 |
| "mmu-let-7i" | 28,15 | 28,97 | 28,87 | 27,87 | 26,57 | 26,88 | 26,57 | 26,71 | 26,88 | 27,00 | 26,35 | 26,71 | 28,24 | 26,71 | 27,09 | 26,71 | 26,71 | 26,71 |
| "mmu-miR-1" | 31,50 | 30,37 | 30,59 | 29,89 | 34,95 | 31,58 | 32,91 | 34,25 | 37,36 | 36,39 | 38,79 | 28,60 | 30,27 | 37,74 | 37,20 | 37,50 | 38,65 | 35,64 |
| "rno-miR-1" | 28,97 | 29,55 | 30,27 | 28,92 | 31,83 | 31,40 | 32,00 | 33,01 | 34,95 | 37,20 | 36,20 | 27,50 | 29,10 | 36,30 | 32,74 | 35,41 | 38,62 | 32,53 |
| "mmu-miR-7a" | 34,11 | 34,25 | 33,25 | 34,04 | 34,63 | 36,80 | 35,98 | 38,18 | 38,96 | 32,84 | 32,00 | 34,04 | 38,15 | 34,04 | 34,84 | 36,39 | 36,53 | 33,77 |
| "mmu-miR-20b" | 26,71 | 26,57 | 26,57 | 26,79 | 25,28 | 25,73 | 25,15 | 25,15 | 26,57 | 26,88 | 26,88 | 27,59 | 26,28 | 25,90 | 25,60 | 25,28 | 25,49 | 25,49 |
| "mmu-miR-27b" | 29,18 | 31,40 | 28,15 | 28,71 | 28,24 | 28,39 | 28,24 | 28,24 | 29,89 | 29,60 | 29,66 | 29,78 | 29,23 | 28,31 | 28,60 | 28,24 | 28,31 | 28,24 |
| "Mamm U6" | 21,28 | 21,28 | 21,28 | 20,92 | 21,28 | 21,28 | 20,92 | 20,92 | 20,44 | 20,32 | 20,32 | 20,12 | 20,51 | 20,44 | 20,12 | 20,44 | 20,51 | 20,51 |
| "Mamm U6" | 20,32 | 20,32 | 20,44 | 20,32 | 20,32 | 20,32 | 20,32 | 20,12 | 20,12 | 20,12 | 24,50 | 20,92 | 20,12 | 20,12 | 20,32 | 20,32 | 20,44 | 20,32 |
| "mmu-miR-28" | 29,73 | 31,50 | 30,11 | 31,40 | 30,90 | 30,47 | 30,47 | 30,69 | 30,37 | 29,89 | 29,50 | 29,50 | 30,07 | 30,59 | 30,90 | 31,17 | 30,79 | 31,07 |
| "mmu-miR-29b" | 32,08 | 38,02 | 30,37 | 32,08 | 32,43 | 33,25 | 32,19 | 34,11 | 32,34 | 31,17 | 32,74 | 32,08 | 38,15 | 32,84 | 33,35 | 33,60 | 32,43 | 32,43 |
| "mmu-miR-29c" | 31,69 | 31,83 | 31,50 | 32,19 | 32,34 | 31,83 | 31,92 | 32,08 | 30,69 | 30,07 | 30,79 | 29,89 | 31,40 | 30,90 | 31,29 | 31,29 | 30,90 | 31,58 |
| "mmu-miR-30b" | 23,70 | 24,15 | 23,70 | 24,15 | 23,85 | 23,70 | 24,15 | 24,15 | 23,85 | 23,85 | 23,70 | 23,37 | 24,50 | 24,15 | 23,85 | 23,85 | 24,15 | 23,85 |
| "mmu-miR-30c" | 23,37 | 22,95 | 23,37 | 23,37 | 23,37 | 23,37 | 23,51 | 23,70 | 23,70 | 23,51 | 23,37 | 22,95 | 23,51 | 23,51 | 23,70 | 23,37 | 23,51 | 23,51 |
| "mmu-miR-30d" | 28,31 | 27,87 | 28,39 | 28,39 | 28,46 | 27,87 | 28,31 | 28,31 | 28,46 | 27,95 | 27,33 | 27,87 | 28,65 | 28,24 | 28,31 | 28,46 | 28,46 | 28,60 |
| "mmu-miR-32" | 37,95 | 38,02 | 37,43 | 33,77 | 38,61 | 36,53 | 36,66 | 37,06 | 38,96 | 36,08 | 38,79 | 38,12 | 38,15 | 37,06 | 36,80 | 36,80 | 37,06 | 34,74 |
| "mmu-miR-34a" | 37,95 | 38,02 | 37,43 | 38,28 | 38,61 | 38,59 | 36,53 | 36,20 | 34,04 | 34,11 | 35,07 | 34,52 | 38,15 | 30,97 | 32,34 | 30,90 | 30,97 | 34,04 |
| "mmu-miR-93" | 26,46 | 26,79 | 26,12 | 26,71 | 25,40 | 25,60 | 25,40 | 24,93 | 27,00 | 27,09 | 26,94 | 27,17 | 27,25 | 26,20 | 25,82 | 25,73 | 25,95 | 25,73 |
| "mmu-miR-21" | 26,35 | 26,71 | 26,20 | 26,46 | 26,28 | 26,71 | 26,46 | 26,57 | 25,60 | 26,28 | 26,46 | 26,35 | 26,88 | 26,02 | 25,95 | 26,28 | 26,20 | 26,35 |
| "mmu-miR-23b" | 37,95 | 38,02 | 30,79 | 35,74 | 32,19 | 34,04 | 31,58 | 31,58 | 34,74 | 36,53 | 37,50 | 34,25 | 30,20 | 31,69 | 32,25 | 32,25 | 31,83 | 31,76 |
| "mmu-miR-24" | 23,85 | 23,85 | 24,15 | 23,85 | 23,70 | 23,85 | 23,85 | 23,85 | 24,67 | 24,50 | 24,15 | 24,67 | 24,15 | 23,70 | 23,51 | 23,70 | 23,85 | 23,70 |
| "mmu-miR-25" | 27,78 | 28,03 | 26,79 | 27,69 | 27,59 | 27,50 | 27,33 | 27,50 | 28,65 | 29,10 | 28,60 | 28,97 | 28,54 | 27,50 | 28,03 | 27,50 | 27,59 | 27,09 |
| "mmu-miR-26a" | 25,95 | 25,60 | 25,82 | 25,82 | 25,90 | 25,95 | 25,90 | 25,95 | 25,95 | 25,82 | 25,73 | 25,73 | 25,49 | 25,95 | 26,12 | 26,35 | 26,28 | 26,20 |
| "mmu-miR-26b" | 26,12 | 26,20 | 26,88 | 26,28 | 27,00 | 26,94 | 27,17 | 27,00 | 26,28 | 25,73 | 26,02 | 25,82 | 26,12 | 26,88 | 27,17 | 27,25 | 27,17 | 27,00 |
| "mmu-miR-27a" | 28,60 | 28,54 | 28,60 | 29,01 | 28,60 | 28,97 | 28,87 | 28,77 | 29,73 | 29,66 | 29,27 | 30,20 | 31,58 | 28,92 | 29,23 | 29,10 | 28,92 | 28,77 |
| "mmu-miR-99a" | 29,23 | 29,73 | 32,84 | 30,37 | 29,99 | 29,45 | 30,20 | 28,92 | 28,39 | 32,19 | 32,19 | 29,66 | 31,29 | 29,18 | 29,66 | 29,38 | 29,33 | 29,55 |
| "mmu-miR-125a-3p" | 37,95 | 38,02 | 37,43 | 38,28 | 38,61 | 38,59 | 38,86 | 39,07 | 37,60 | 38,62 | 38,79 | 37,60 | 32,84 | 38,96 | 39,66 | 39,71 | 38,32 | 37,74 |
| "mmu-miR-125a-5p" | 28,92 | 29,10 | 32,62 | 30,69 | 29,60 | 30,20 | 30,11 | 30,27 | 30,07 | 30,20 | 29,73 | 30,11 | 29,38 | 30,11 | 29,60 | 29,78 | 29,60 | 29,78 |
| "mmu-miR-125b-5p" | 28,87 | 28,39 | 29,78 | 26,88 | 29,33 | 28,87 | 29,33 | 29,23 | 29,33 | 30,37 | 29,99 | 30,47 | 29,18 | 28,77 | 28,97 | 28,97 | 28,97 | 29,18 |
| "mmu-miR-126-3p" | 26,02 | 25,28 | 25,60 | 25,40 | 26,02 | 25,28 | 24,93 | 25,49 | 24,93 | 25,28 | 25,40 | 25,40 | 24,67 | 23,85 | 24,15 | 24,15 | 23,70 | 24,50 |
| "mmu-miR-126-5p" | 30,69 | 29,33 | 29,60 | 29,10 | 30,37 | 29,60 | 29,18 | 29,33 | 28,24 | 28,87 | 28,92 | 28,87 | 27,50 | 27,95 | 27,78 | 28,31 | 27,33 | 28,03 |
| "mmu-miR-127" | 31,92 | 29,27 | 30,69 | 33,35 | 38,61 | 34,63 | 37,74 | 36,80 | 38,96 | 38,62 | 38,79 | 34,63 | 38,15 | 39,25 | 38,79 | 39,98 | 39,25 | 38,12 |
| "mmu-miR-128a" | 32,62 | 38,02 | 32,34 | 30,07 | 35,64 | 38,59 | 32,62 | 32,19 | 30,47 | 31,40 | 30,97 | 31,50 | 34,95 | 33,25 | 35,41 | 34,04 | 33,35 | 34,11 |
| "mmu-miR-130a" | 30,11 | 30,20 | 30,47 | 30,27 | 29,55 | 29,38 | 29,99 | 29,66 | 29,66 | 30,59 | 31,17 | 31,69 | 29,66 | 29,23 | 29,55 | 29,23 | 29,27 | 29,50 |
| "mmu-miR-130b" | 29,55 | 28,46 | 37,43 | 29,66 | 29,10 | 28,60 | 28,54 | 28,71 | 29,78 | 29,23 | 29,60 | 29,10 | 29,45 | 28,87 | 28,77 | 28,65 | 28,87 | 28,65 |
| "mmu-miR-99b" | 29,33 | 28,31 | 29,66 | 29,45 | 30,59 | 30,11 | 30,79 | 29,78 | 29,55 | 30,79 | 31,50 | 30,97 | 29,89 | 30,20 | 30,47 | 30,47 | 30,37 | 30,20 |

| | | | | | | | | | | | | | | | | | | | |
|---|---|---|---|---|---|---|---|---|---|---|---|---|---|---|---|---|---|---|---|
| "mmu-miR-133a" | 25,73 | 27,33 | 27,87 | 27,59 | 29,78 | 29,10 | 28,77 | 31,69 | 28,92 | 34,35 | 33,13 | 23,51 | 26,57 | 34,35 | 32,62 | 31,76 | 35,83 | 30,69 |
| "mmu-miR-135a" | 37,95 | 38,02 | 37,43 | 38,28 | 38,61 | 38,59 | 37,06 | 37,20 | 38,96 | 38,62 | 38,79 | 39,07 | 32,91 | 38,47 | 38,86 | 38,62 | 38,40 | 37,20 |
| "mmu-miR-100" | 29,66 | 31,58 | 32,25 | 31,76 | 30,20 | 29,33 | 30,37 | 28,87 | 27,95 | 31,83 | 31,76 | 28,92 | 31,50 | 29,45 | 29,73 | 29,73 | 29,45 | 29,66 |
| "mmu-miR-101a" | 28,71 | 28,24 | 27,95 | 28,87 | 28,92 | 28,92 | 29,01 | 29,27 | 29,45 | 29,33 | 29,18 | 29,38 | 28,71 | 29,50 | 29,27 | 29,45 | 29,23 | 28,97 |
| "mmu-miR-103" | 31,58 | 33,13 | 34,04 | 32,91 | 31,50 | 31,29 | 32,08 | 30,79 | 31,58 | 33,91 | 34,35 | 39,07 | 33,77 | 31,07 | 32,00 | 31,40 | 31,76 | 31,40 |
| "mmu-miR-107" | 37,95 | 38,02 | 37,43 | 38,28 | 32,91 | 36,66 | 32,74 | 34,74 | 36,39 | 38,62 | 36,08 | 38,02 | 32,43 | 33,77 | 35,20 | 33,91 | 34,63 | 33,91 |
| "mmu-miR-124" | 37,95 | 32,43 | 37,43 | 38,28 | 36,08 | 34,84 | 35,07 | 38,40 | 35,30 | 33,01 | 33,35 | 34,84 | 34,11 | 37,50 | 34,11 | 37,20 | 36,80 | 36,66 |
| "mmu-miR-142-5p" | 32,00 | 32,74 | 37,43 | 31,50 | 31,69 | 31,50 | 31,29 | 32,00 | 32,00 | 32,25 | 31,69 | 31,76 | 31,17 | 32,00 | 32,53 | 32,43 | 32,53 | 31,69 |
| "snoRNA135" | 24,93 | 25,15 | 24,93 | 25,15 | 24,93 | 24,50 | 25,28 | 25,28 | 25,15 | 25,49 | 25,15 | 25,49 | 25,73 | 24,93 | 24,50 | 24,67 | 24,93 | 25,28 |
| "mmu-miR-145" | 30,79 | 31,76 | 31,07 | 31,92 | 34,11 | 32,53 | 32,34 | 36,08 | 32,84 | 38,62 | 35,41 | 30,07 | 30,79 | 35,74 | 31,40 | 34,25 | 34,84 | 36,20 |
| "mmu-miR-146a" | 23,14 | 23,70 | 24,50 | 22,71 | 26,88 | 26,12 | 26,79 | 26,28 | 22,60 | 21,28 | 20,92 | 21,28 | 22,95 | 26,28 | 26,02 | 26,02 | 25,73 | 25,90 |
| "mmu-miR-146b" | 25,82 | 25,73 | 26,28 | 25,90 | 26,12 | 26,02 | 26,28 | 26,20 | 25,49 | 25,60 | 25,82 | 25,90 | 24,93 | 25,40 | 25,28 | 25,40 | 25,15 | 25,15 |
| "mmu-miR-148a" | 26,88 | 26,88 | 27,43 | 26,12 | 29,18 | 29,50 | 28,97 | 29,73 | 25,90 | 25,15 | 25,28 | 24,15 | 26,79 | 29,55 | 29,38 | 29,50 | 29,89 | 29,27 |
| "mmu-miR-148b" | 31,29 | 33,01 | 37,43 | 38,28 | 34,84 | 35,07 | 32,53 | 32,25 | 32,62 | 33,13 | 32,84 | 33,13 | 38,15 | 33,45 | 34,25 | 34,35 | 34,11 | 32,91 |
| "mmu-miR-150" | 24,67 | 24,50 | 23,85 | 23,70 | 25,82 | 25,40 | 25,95 | 25,40 | 23,14 | 22,41 | 22,41 | 22,60 | 23,85 | 24,67 | 25,40 | 24,93 | 24,67 | 25,40 |
| "mmu-miR-152" | 28,24 | 27,95 | 28,46 | 28,03 | 28,87 | 29,99 | 29,78 | 30,59 | 28,31 | 27,25 | 27,43 | 26,02 | 28,31 | 29,78 | 30,11 | 29,99 | 29,99 | 29,99 |
| "mmu-miR-181a" | 29,78 | 30,59 | 28,24 | 28,77 | 28,77 | 28,54 | 28,46 | 28,03 | 29,23 | 28,65 | 28,54 | 28,46 | 29,55 | 28,71 | 29,18 | 28,87 | 29,38 | 29,10 |
| "mmu-miR-181c" | 34,74 | 32,53 | 33,60 | 34,95 | 32,00 | 32,34 | 33,01 | 32,34 | 32,91 | 33,77 | 34,11 | 34,95 | 32,34 | 33,01 | 34,52 | 33,35 | 33,45 | 32,62 |
| "mmu-miR-138" | 37,95 | 31,17 | 30,97 | 30,79 | 31,29 | 31,92 | 31,76 | 31,29 | 32,19 | 31,76 | 30,90 | 33,60 | 31,69 | 31,83 | 32,43 | 32,62 | 32,34 | 31,50 |
| "mmu-miR-139-5p" | 30,07 | 28,60 | 31,58 | 28,60 | 29,50 | 29,89 | 29,23 | 28,60 | 27,25 | 27,50 | 27,59 | 28,03 | 29,78 | 28,54 | 27,95 | 28,71 | 28,65 | 29,33 |
| "mmu-miR-140" | 26,57 | 26,35 | 26,35 | 26,57 | 26,94 | 27,00 | 26,88 | 26,88 | 27,50 | 26,94 | 27,25 | 26,57 | 26,94 | 27,00 | 27,25 | 27,09 | 26,94 | 27,17 |
| "mmu-miR-142-3p" | 24,50 | 24,93 | 23,51 | 24,50 | 24,50 | 24,15 | 24,50 | 24,50 | 24,50 | 24,93 | 24,93 | 23,85 | 25,15 | 24,50 | 24,93 | 24,50 | 24,50 | 24,67 |
| "mmu-miR-182" | 37,95 | 38,02 | 37,43 | 33,45 | 38,61 | 38,59 | 34,84 | 35,64 | 33,45 | 31,92 | 32,25 | 32,74 | 34,04 | 39,96 | 38,32 | 39,29 | 40,00 | 38,86 |
| "mmu-miR-193b" | 27,69 | 27,43 | 27,00 | 27,09 | 27,95 | 27,95 | 27,95 | 29,10 | 26,46 | 26,20 | 27,17 | 28,39 | 25,95 | 28,03 | 27,59 | 27,95 | 27,95 | 27,33 |
| "mmu-miR-194" | 31,40 | 32,91 | 32,74 | 32,43 | 33,13 | 32,43 | 31,40 | 32,74 | 31,07 | 32,34 | 30,07 | 30,59 | 30,97 | 32,53 | 31,69 | 33,25 | 32,74 | 32,25 |
| "mmu-miR-195" | 29,27 | 29,66 | 29,10 | 29,38 | 29,89 | 29,27 | 29,55 | 29,50 | 29,18 | 28,92 | 29,01 | 28,77 | 29,01 | 29,99 | 29,78 | 30,11 | 30,11 | 29,60 |
| "mmu-miR-196b" | 29,01 | 28,87 | 28,97 | 29,33 | 27,87 | 27,69 | 28,15 | 28,39 | 29,10 | 29,38 | 29,89 | 30,79 | 28,60 | 27,87 | 27,87 | 28,03 | 28,03 | 28,15 |
| "rno-miR-196c" | 27,00 | 27,09 | 27,59 | 26,94 | 26,35 | 26,28 | 26,35 | 26,35 | 27,17 | 28,31 | 28,24 | 29,18 | 26,46 | 26,57 | 25,90 | 26,46 | 26,35 | 26,46 |
| "mmu-miR-197" | 29,10 | 29,45 | 29,73 | 28,54 | 33,45 | 31,69 | 31,83 | 31,17 | 30,20 | 29,73 | 30,20 | 31,40 | 29,27 | 31,58 | 31,17 | 32,34 | 32,25 | 33,01 |
| "mmu-miR-199a-3p" | 37,95 | 38,02 | 34,25 | 38,28 | 38,61 | 38,59 | 37,36 | 39,07 | 37,74 | 38,62 | 38,79 | 39,07 | 38,15 | 38,86 | 37,74 | 38,52 | 38,86 | 38,79 |
| "mmu-miR-200c" | 37,95 | 38,02 | 37,43 | 38,28 | 38,61 | 38,59 | 37,60 | 38,02 | 35,98 | 28,03 | 35,83 | 33,01 | 38,15 | 35,50 | 36,20 | 35,83 | 36,08 | 36,30 |
| "mmu-miR-203" | 25,15 | 24,67 | 25,15 | 25,73 | 26,46 | 26,57 | 26,94 | 27,17 | 26,35 | 27,33 | 27,78 | 27,69 | 25,28 | 26,94 | 27,33 | 27,00 | 27,00 | 27,25 |
| "mmu-miR-184" | 30,90 | 29,89 | 37,43 | 31,69 | 34,52 | 38,59 | 38,86 | 39,07 | 32,53 | 37,36 | 34,63 | 39,07 | 32,19 | 38,65 | 36,66 | 39,14 | 39,29 | 34,95 |
| "mmu-miR-185" | 37,95 | 35,07 | 37,43 | 38,28 | 37,20 | 36,39 | 36,08 | 37,74 | 38,96 | 34,84 | 38,79 | 34,11 | 38,15 | 36,66 | 38,52 | 35,98 | 35,20 | 38,59 |
| "mmu-miR-186" | 28,46 | 29,18 | 28,92 | 28,65 | 28,71 | 28,46 | 28,65 | 28,97 | 29,60 | 28,54 | 28,87 | 28,31 | 28,39 | 29,73 | 28,92 | 29,01 | 28,77 | 28,71 |
| "mmu-miR-191" | 22,41 | 22,05 | 22,41 | 22,05 | 22,71 | 22,71 | 22,71 | 22,71 | 22,41 | 22,05 | 22,05 | 22,05 | 22,41 | 22,95 | 22,71 | 22,95 | 22,71 | 22,71 |
| "mmu-miR-192" | 30,47 | 30,69 | 31,83 | 30,97 | 30,97 | 32,08 | 31,50 | 31,83 | 31,17 | 30,69 | 30,27 | 29,99 | 29,99 | 32,74 | 32,08 | 32,00 | 31,40 | 31,29 |
| "snoRNA202" | 20,12 | 20,12 | 20,12 | 20,12 | 20,12 | 20,12 | 20,44 | 20,44 | 20,32 | 20,92 | 20,44 | 20,44 | 20,92 | 20,92 | 20,92 | 20,92 | 20,92 | 21,28 |
| "mmu-miR-218" | 31,07 | 34,35 | 31,29 | 33,13 | 35,20 | 33,45 | 33,13 | 32,62 | 33,13 | 32,53 | 35,74 | 32,91 | 30,59 | 34,74 | 33,91 | 35,20 | 34,25 | 33,35 |
| "mmu-miR-221" | 37,95 | 38,02 | 37,43 | 38,28 | 29,01 | 30,27 | 27,87 | 27,69 | 31,83 | 34,74 | 37,74 | 36,30 | 38,15 | 27,17 | 28,15 | 26,94 | 27,09 | 27,69 |
| "mmu-miR-222" | 24,15 | 23,37 | 24,67 | 24,67 | 23,51 | 23,51 | 23,37 | 23,51 | 24,15 | 24,67 | 24,67 | 25,60 | 23,70 | 23,14 | 23,14 | 23,14 | 23,14 | 23,14 |
| "mmu-miR-223" | 25,90 | 25,95 | 26,94 | 27,17 | 24,15 | 25,15 | 23,70 | 23,14 | 27,33 | 28,15 | 28,31 | 28,54 | 26,20 | 25,15 | 24,67 | 25,15 | 25,82 | 24,15 |
| "mmu-miR-224" | 33,77 | 34,11 | 37,43 | 38,28 | 32,74 | 32,84 | 35,30 | 31,07 | 31,50 | 34,63 | 32,91 | 33,77 | 30,90 | 31,92 | 31,92 | 32,19 | 31,92 | 31,83 |
| "rno-miR-207" | 31,76 | 32,62 | 37,43 | 32,62 | 30,11 | 30,37 | 30,59 | 29,99 | 31,76 | 29,99 | 32,53 | 31,83 | 33,60 | 30,07 | 29,10 | 30,20 | 29,78 | 30,07 |
| "mmu-miR-210" | 37,95 | 38,02 | 37,43 | 38,28 | 38,61 | 38,59 | 38,86 | 39,07 | 38,96 | 38,62 | 38,79 | 39,07 | 38,15 | 38,32 | 39,66 | 38,32 | 38,79 | 39,45 |
| "mmu-miR-301a" | 28,39 | 29,78 | 28,03 | 29,50 | 28,31 | 28,24 | 28,92 | 28,65 | 28,87 | 29,27 | 29,33 | 29,60 | 28,97 | 28,60 | 28,71 | 28,60 | 28,71 | 28,46 |
| "mmu-miR-301b" | 30,59 | 28,65 | 28,71 | 29,27 | 28,15 | 28,31 | 28,39 | 28,46 | 29,01 | 29,55 | 29,55 | 29,55 | 29,73 | 28,65 | 29,01 | 28,77 | 28,60 | 28,92 |
| "mmu-miR-320" | 28,03 | 27,78 | 28,31 | 28,24 | 28,39 | 28,03 | 28,71 | 28,15 | 28,15 | 27,17 | 26,57 | 27,25 | 28,46 | 28,97 | 28,46 | 28,92 | 29,18 | 29,01 |
| "mmu-miR-324-5p" | 32,19 | 30,11 | 33,91 | 30,20 | 30,27 | 30,79 | 30,69 | 29,89 | 31,40 | 30,27 | 30,11 | 31,07 | 31,92 | 30,47 | 30,69 | 30,27 | 30,47 | 30,59 |
| "rno-miR-327" | 37,95 | 38,02 | 37,43 | 34,52 | 38,61 | 37,20 | 38,18 | 35,98 | 38,18 | 35,20 | 33,01 | 35,74 | 38,15 | 37,89 | 37,06 | 38,59 | 37,36 | 38,96 |
| "mmu-miR-328" | 27,09 | 26,94 | 26,71 | 27,33 | 27,09 | 27,43 | 27,00 | 26,79 | 26,71 | 26,79 | 26,79 | 27,00 | 27,33 | 27,09 | 27,43 | 27,17 | 27,43 | 27,59 |
| "mmu-miR-331-3p" | 29,50 | 29,60 | 29,89 | 29,99 | 29,38 | 29,23 | 29,60 | 29,60 | 29,38 | 28,97 | 28,97 | 28,65 | 28,87 | 29,60 | 29,50 | 29,66 | 29,55 | 29,73 |
| "mmu-miR-331-5p" | 37,95 | 38,02 | 32,53 | 33,91 | 33,60 | 32,62 | 37,50 | 34,84 | 37,20 | 32,91 | 34,84 | 33,25 | 38,15 | 35,64 | 34,35 | 35,07 | 34,52 | 36,39 |
| "mmu-miR-294" | 37,95 | 34,52 | 37,43 | 34,74 | 38,61 | 35,64 | 38,86 | 38,12 | 38,96 | 38,62 | 35,64 | 38,25 | 34,84 | 39,07 | 38,12 | 38,12 | 38,18 | 39,45 |
| "mmu-miR-296-5p" | 32,74 | 32,25 | 29,99 | 33,01 | 32,25 | 32,19 | 30,97 | 31,92 | 32,43 | 31,58 | 30,59 | 32,34 | 35,64 | 32,25 | 31,76 | 31,07 | 32,08 | 34,52 |
| "mmu-miR-339-5p" | 37,95 | 38,02 | 37,43 | 38,28 | 35,98 | 37,06 | 33,91 | 34,52 | 37,50 | 38,62 | 36,30 | 39,07 | 38,15 | 32,91 | 34,63 | 31,92 | 32,62 | 35,41 |
| "U87" | 27,33 | 27,69 | 27,33 | 27,95 | 27,33 | 27,59 | 27,59 | 27,59 | 27,43 | 27,43 | 27,09 | 27,78 | 28,03 | 27,25 | 26,79 | 26,79 | 26,88 | 27,78 |
| "mmu-miR-340-3p" | 33,01 | 30,79 | 30,20 | 32,34 | 29,23 | 28,71 | 29,45 | 29,55 | 30,27 | 31,50 | 31,83 | 32,00 | 30,47 | 29,89 | 29,45 | 30,07 | 30,20 | 29,45 |
| "mmu-miR-340-5p" | 29,60 | 30,47 | 29,33 | 31,07 | 29,45 | 29,18 | 29,27 | 29,38 | 30,59 | 30,90 | 30,47 | 31,17 | 29,50 | 29,66 | 29,89 | 29,89 | 29,73 | 29,38 |
| "mmu-miR-342-3p" | 28,65 | 29,23 | 28,65 | 28,31 | 31,07 | 30,90 | 30,07 | 30,37 | 27,09 | 26,71 | 27,00 | 27,43 | 27,95 | 31,17 | 30,59 | 30,97 | 30,59 | 30,97 |
| "rno-miR-345-3p" | 37,95 | 38,02 | 32,08 | 35,83 | 34,35 | 36,95 | 36,20 | 35,30 | 38,96 | 38,62 | 38,79 | 37,89 | 33,35 | 36,53 | 35,98 | 36,95 | 36,20 | 35,98 |
| "mmu-miR-345-5p" | 37,95 | 38,02 | 37,43 | 38,28 | 38,61 | 38,59 | 38,02 | 39,07 | 36,95 | 38,62 | 38,79 | 37,74 | 38,15 | 36,39 | 37,89 | 36,30 | 36,66 | 39,45 |

| | | | | | | | | | | | | | | | | | | | |
|---|---|---|---|---|---|---|---|---|---|---|---|---|---|---|---|---|---|---|---|
| "mmu-miR-337-5p" | 37,95 | 35,30 | 32,00 | 32,53 | 36,53 | 36,20 | 34,25 | 36,66 | 38,96 | 35,30 | 34,25 | 36,66 | 34,63 | 38,40 | 38,65 | 38,18 | 38,59 | 38,18 |
| "mmu-miR-375" | 34,52 | 31,07 | 29,01 | 29,60 | 31,58 | 31,76 | 32,43 | 32,84 | 30,97 | 29,45 | 28,65 | 29,73 | 31,83 | 35,98 | 31,83 | 34,63 | 35,07 | 39,45 |
| "mmu-miR-376b" | 26,28 | 25,90 | 26,46 | 24,93 | 25,15 | 25,82 | 26,02 | 25,82 | 27,59 | 25,90 | 26,71 | 26,79 | 27,00 | 27,69 | 26,71 | 27,69 | 27,50 | 26,57 |
| "mmu-miR-379" | 37,95 | 38,02 | 37,43 | 38,28 | 38,61 | 38,59 | 38,86 | 39,07 | 38,32 | 35,50 | 32,43 | 36,39 | 38,15 | 39,29 | 37,50 | 39,25 | 39,96 | 39,45 |
| "mmu-miR-383" | 34,04 | 35,20 | 37,43 | 33,25 | 35,83 | 35,20 | 35,74 | 39,07 | 35,41 | 35,98 | 33,45 | 35,50 | 35,30 | 38,52 | 38,40 | 39,07 | 38,25 | 38,65 |
| "mmu-miR-350" | 34,25 | 38,02 | 33,45 | 38,28 | 35,30 | 35,41 | 35,50 | 34,35 | 36,20 | 36,20 | 36,80 | 35,07 | 35,07 | 39,96 | 37,36 | 37,60 | 35,74 | 35,50 |
| "rno-miR-351" | 33,60 | 33,35 | 37,43 | 34,35 | 31,92 | 32,74 | 32,25 | 32,43 | 34,11 | 33,45 | 33,91 | 36,80 | 38,15 | 34,63 | 33,01 | 32,74 | 32,91 | 32,34 |
| "mmu-miR-361" | 37,95 | 38,02 | 37,43 | 35,07 | 35,74 | 38,59 | 36,80 | 33,13 | 36,66 | 38,62 | 37,06 | 35,20 | 32,25 | 34,25 | 36,08 | 33,77 | 34,35 | 32,19 |
| "mmu-miR-362-3p" | 37,95 | 31,69 | 37,43 | 31,83 | 32,84 | 34,25 | 35,20 | 37,60 | 34,52 | 34,25 | 38,79 | 36,53 | 38,15 | 34,84 | 35,83 | 34,52 | 34,74 | 34,63 |
| "mmu-miR-365" | 28,77 | 29,38 | 29,23 | 29,18 | 30,47 | 30,59 | 30,27 | 30,47 | 28,60 | 28,24 | 27,95 | 27,09 | 28,77 | 30,69 | 30,79 | 30,59 | 30,69 | 29,89 |
| "Y1" | 30,97 | 29,50 | 29,45 | 30,47 | 29,66 | 29,73 | 29,73 | 30,11 | 29,99 | 29,78 | 29,78 | 30,69 | 30,69 | 30,37 | 30,07 | 29,60 | 30,07 | 30,11 |
| "mmu-miR-434-3p" | 32,84 | 31,92 | 30,90 | 31,17 | 36,95 | 34,35 | 33,77 | 35,41 | 36,30 | 34,52 | 33,77 | 32,43 | 32,74 | 37,60 | 38,02 | 37,74 | 38,47 | 37,89 |
| "mmu-miR-450a-5p" | 37,95 | 32,84 | 37,43 | 38,28 | 33,77 | 33,01 | 34,35 | 32,91 | 33,35 | 35,83 | 37,60 | 39,07 | 33,91 | 32,43 | 32,91 | 33,01 | 33,13 | 32,00 |
| "mmu-miR-451" | 30,37 | 38,02 | 31,69 | 35,98 | 34,74 | 38,59 | 34,52 | 39,07 | 35,64 | 35,41 | 34,95 | 39,07 | 38,15 | 39,96 | 38,25 | 38,02 | 36,95 | 36,53 |
| "mmu-miR-409-3p" | 32,53 | 31,29 | 31,76 | 32,00 | 33,25 | 33,77 | 33,25 | 34,04 | 32,25 | 30,47 | 28,71 | 31,58 | 33,25 | 34,95 | 33,13 | 34,84 | 36,39 | 35,07 |
| "mmu-miR-411" | 31,83 | 33,91 | 37,43 | 32,84 | 37,06 | 38,59 | 38,86 | 39,07 | 38,96 | 38,62 | 34,52 | 38,32 | 38,15 | 38,12 | 39,66 | 38,86 | 39,14 | 39,45 |
| "mmu-miR-423-5p" | 37,95 | 38,02 | 37,43 | 38,28 | 38,61 | 38,59 | 38,86 | 35,50 | 38,96 | 38,62 | 36,95 | 38,18 | 38,15 | 39,61 | 39,66 | 38,96 | 39,61 | 37,06 |
| "mmu-miR-425" | 34,63 | 38,02 | 33,35 | 38,28 | 36,66 | 36,30 | 34,95 | 34,95 | 35,20 | 35,74 | 34,04 | 36,08 | 38,15 | 32,62 | 34,74 | 32,08 | 32,00 | 32,84 |
| "mmu-miR-484" | 25,49 | 25,40 | 25,40 | 25,28 | 25,60 | 25,90 | 25,60 | 25,73 | 25,28 | 24,15 | 23,85 | 24,50 | 25,40 | 25,60 | 25,73 | 25,82 | 25,40 | 25,95 |
| "mmu-miR-491" | 35,07 | 34,74 | 37,43 | 38,28 | 38,61 | 34,95 | 38,86 | 36,53 | 37,06 | 35,64 | 34,74 | 33,91 | 38,15 | 36,20 | 35,74 | 36,66 | 37,20 | 38,02 |
| "mmu-miR-494" | 37,95 | 38,02 | 33,13 | 38,28 | 34,04 | 34,11 | 37,20 | 39,07 | 36,80 | 34,95 | 35,98 | 36,20 | 38,15 | 34,52 | 32,19 | 35,50 | 34,04 | 37,50 |
| "mmu-miR-503" | 37,95 | 38,02 | 37,43 | 38,28 | 38,61 | 38,59 | 38,86 | 39,07 | 38,96 | 38,62 | 38,79 | 39,07 | 38,15 | 36,80 | 39,07 | 37,06 | 34,95 | 38,40 |
| "mmu-miR-467a" | 37,95 | 34,84 | 37,43 | 34,84 | 33,01 | 33,13 | 31,69 | 33,45 | 35,74 | 35,07 | 35,30 | 35,98 | 33,45 | 33,60 | 34,95 | 32,84 | 32,84 | 33,45 |
| "mmu-miR-467c" | 37,95 | 38,02 | 34,11 | 35,41 | 34,25 | 34,74 | 36,30 | 35,83 | 34,63 | 36,95 | 35,50 | 38,47 | 35,20 | 35,30 | 36,95 | 34,74 | 36,30 | 35,74 |
| "mmu-miR-542-3p" | 37,95 | 38,02 | 37,43 | 33,60 | 35,41 | 35,98 | 34,63 | 33,77 | 34,84 | 34,04 | 36,53 | 35,64 | 38,15 | 35,07 | 35,07 | 35,64 | 35,41 | 35,30 |
| "mmu-miR-544" | 37,95 | 38,02 | 37,43 | 38,28 | 38,61 | 38,59 | 35,64 | 33,91 | 35,50 | 37,50 | 38,79 | 35,83 | 32,00 | 38,59 | 39,66 | 39,61 | 38,02 | 38,52 |
| "mmu-miR-574-3p" | 30,20 | 30,90 | 37,43 | 30,90 | 29,73 | 29,78 | 29,66 | 29,45 | 30,79 | 29,18 | 29,23 | 29,33 | 30,37 | 30,27 | 29,99 | 30,37 | 30,27 | 30,27 |
| "mmu-miR-532-3p" | 29,45 | 28,71 | 29,38 | 29,23 | 28,65 | 29,55 | 29,50 | 29,18 | 28,97 | 29,01 | 29,45 | 29,01 | 29,60 | 29,01 | 29,33 | 29,18 | 29,10 | 29,23 |
| "mmu-miR-532-5p" | 37,95 | 34,95 | 37,43 | 34,11 | 33,35 | 33,60 | 33,45 | 31,40 | 30,90 | 30,97 | 31,92 | 30,37 | 35,50 | 29,38 | 30,20 | 29,33 | 29,50 | 30,37 |
| "rno-miR-532-5p" | 37,95 | 38,02 | 37,43 | 38,28 | 38,61 | 38,59 | 38,86 | 38,47 | 38,02 | 38,62 | 38,79 | 38,40 | 38,15 | 35,83 | 38,18 | 36,53 | 35,98 | 38,47 |
| "mmu-miR-674" | 37,95 | 38,02 | 37,43 | 38,28 | 38,61 | 38,59 | 38,86 | 39,07 | 38,25 | 38,62 | 38,79 | 39,07 | 38,15 | 37,20 | 36,30 | 37,36 | 37,74 | 38,32 |
| "mmu-miR-744" | 29,99 | 29,01 | 29,18 | 28,46 | 28,03 | 28,15 | 28,03 | 27,95 | 29,27 | 28,77 | 28,77 | 29,27 | 30,11 | 28,39 | 28,65 | 28,15 | 28,24 | 28,31 |
| "mmu-miR-669a" | 37,95 | 38,02 | 37,43 | 38,28 | 38,61 | 38,59 | 38,86 | 37,36 | 38,96 | 38,62 | 38,79 | 39,07 | 38,15 | 38,02 | 38,47 | 38,79 | 38,52 | 39,45 |
| "mmu-miR-671-3p" | 34,35 | 33,60 | 33,77 | 32,74 | 30,69 | 30,69 | 30,90 | 30,97 | 31,92 | 33,35 | 31,07 | 32,53 | 33,01 | 31,76 | 31,50 | 31,50 | 31,50 | 30,90 |
| "mmu-miR-872" | 32,34 | 32,08 | 30,07 | 32,25 | 30,79 | 30,97 | 31,07 | 31,76 | 33,01 | 33,60 | 32,34 | 34,35 | 38,15 | 32,19 | 31,58 | 32,91 | 32,19 | 31,92 |
| "rno-miR-224" | 33,25 | 34,63 | 31,92 | 34,25 | 32,62 | 33,35 | 38,86 | 33,35 | 32,74 | 36,80 | 36,66 | 35,41 | 33,13 | 33,13 | 35,30 | 33,45 | 33,01 | 33,13 |
| "mmu-miR-324-3p" | 34,95 | 38,02 | 37,43 | 38,28 | 35,07 | 34,52 | 34,74 | 33,25 | 34,25 | 33,25 | 35,20 | 31,92 | 35,41 | 32,08 | 33,77 | 32,53 | 33,77 | 35,83 |
| "mmu-miR-351" | 37,95 | 38,02 | 37,43 | 38,28 | 36,80 | 38,59 | 36,39 | 36,95 | 38,96 | 38,62 | 38,79 | 39,07 | 38,15 | 36,08 | 37,60 | 35,74 | 35,64 | 37,36 |
| "rno-miR-381" | 32,91 | 32,00 | 31,40 | 30,59 | 32,53 | 32,91 | 33,60 | 35,20 | 33,25 | 32,62 | 32,62 | 33,35 | 32,08 | 35,41 | 36,39 | 36,20 | 37,60 | 36,08 |
| "rno-miR-450a" | 37,95 | 38,02 | 37,43 | 35,30 | 38,61 | 38,59 | 38,86 | 39,07 | 38,96 | 38,62 | 38,79 | 39,07 | 38,15 | 38,25 | 39,66 | 38,65 | 38,96 | 39,45 |
| "mmu-miR-652" | 33,13 | 33,25 | 32,19 | 35,20 | 31,17 | 31,17 | 31,17 | 30,90 | 31,69 | 31,69 | 31,58 | 32,19 | 34,74 | 29,33 | 30,27 | 29,55 | 29,66 | 30,47 |
| "mmu-miR-667" | 31,17 | 29,99 | 31,17 | 31,29 | 32,08 | 32,25 | 32,84 | 33,60 | 33,77 | 32,08 | 31,29 | 32,62 | 31,07 | 33,35 | 33,25 | 34,95 | 33,60 | 33,25 |
| "mmu-miR-676" | 37,95 | 38,02 | 37,43 | 38,28 | 37,36 | 35,83 | 36,95 | 36,39 | 35,83 | 38,62 | 37,89 | 37,20 | 38,15 | 33,91 | 35,50 | 33,13 | 33,25 | 35,20 |
| "mmu-miR-680" | 35,20 | 32,34 | 37,43 | 36,08 | 36,30 | 35,30 | 34,11 | 35,07 | 33,91 | 31,29 | 30,37 | 32,25 | 34,25 | 35,20 | 32,84 | 35,30 | 35,50 | 33,60 |
| "mmu-miR-682" | 33,35 | 34,04 | 32,91 | 35,64 | 36,39 | 38,59 | 37,89 | 34,63 | 34,35 | 36,30 | 38,79 | 37,50 | 38,15 | 36,95 | 35,64 | 36,08 | 35,30 | 36,80 |
| "mmu-miR-467b" | 37,95 | 38,02 | 37,43 | 38,28 | 38,61 | 38,59 | 38,86 | 37,89 | 38,12 | 38,62 | 38,79 | 39,07 | 38,15 | 38,79 | 39,14 | 37,89 | 37,50 | 38,62 |
| "mmu-miR-29a" | 25,40 | 25,49 | 25,73 | 25,95 | 26,20 | 26,46 | 26,12 | 26,46 | 25,40 | 25,40 | 25,49 | 25,28 | 25,82 | 26,12 | 26,20 | 26,20 | 25,60 | 26,28 |
| "mmu-miR-30a" | 26,94 | 26,12 | 25,95 | 26,35 | 26,71 | 26,79 | 26,71 | 26,94 | 26,79 | 26,35 | 26,20 | 26,28 | 27,09 | 26,79 | 26,94 | 26,88 | 26,79 | 26,94 |
| "mmu-miR-30e" | 27,50 | 27,59 | 27,25 | 27,43 | 27,69 | 27,78 | 27,78 | 27,87 | 27,78 | 27,59 | 27,50 | 26,94 | 27,17 | 27,78 | 27,69 | 27,78 | 27,78 | 27,87 |
| "mmu-miR-31" | 28,54 | 28,77 | 27,69 | 28,97 | 30,07 | 30,07 | 29,89 | 30,07 | 28,54 | 28,71 | 29,10 | 29,45 | 27,69 | 29,27 | 28,54 | 28,54 | 28,39 | 28,54 |
| "mmu-miR-34b-3p" | 30,27 | 30,97 | 28,77 | 30,11 | 31,40 | 32,00 | 34,04 | 32,53 | 33,60 | 32,00 | 31,40 | 33,45 | 32,62 | 38,18 | 36,53 | 38,47 | 38,12 | 34,25 |
| "mmu-miR-92a" | 23,51 | 23,51 | 23,14 | 23,51 | 22,95 | 23,14 | 22,95 | 22,95 | 23,37 | 23,70 | 23,51 | 25,15 | 23,37 | 22,71 | 22,95 | 22,41 | 22,95 | 22,95 |
| "mmu-miR-685" | 33,45 | 38,02 | 37,43 | 38,28 | 36,20 | 35,74 | 35,41 | 38,32 | 36,08 | 32,43 | 33,25 | 32,84 | 38,15 | 34,11 | 34,04 | 34,11 | 33,91 | 34,35 |
| "mmu-miR-106a" | 22,60 | 22,60 | 22,71 | 22,60 | 22,60 | 22,60 | 22,41 | 22,41 | 22,95 | 23,37 | 23,14 | 23,70 | 22,05 | 22,41 | 22,41 | 22,71 | 22,41 | 22,60 |
| "mmu-miR-188-5p" | 27,95 | 27,25 | 27,09 | 27,25 | 29,27 | 29,66 | 29,38 | 30,20 | 30,11 | 28,60 | 28,15 | 29,23 | 27,87 | 31,40 | 30,37 | 31,58 | 31,58 | 31,17 |
| "mmu-miR-322" | 29,89 | 30,07 | 32,43 | 31,58 | 28,54 | 29,01 | 29,10 | 29,01 | 29,50 | 30,11 | 30,69 | 30,90 | 28,92 | 29,10 | 28,87 | 29,27 | 29,01 | 28,87 |
| "mmu-miR-687" | 33,91 | 33,77 | 33,01 | 34,63 | 33,91 | 33,91 | 35,83 | 36,30 | 35,07 | 32,74 | 33,60 | 34,74 | 34,52 | 32,34 | 30,97 | 31,83 | 31,29 | 32,08 |
| "mmu-let-7a" | 37,95 | 38,02 | 37,43 | 38,28 | 38,61 | 38,59 | 38,86 | 37,50 | 38,96 | 38,62 | 38,79 | 37,06 | 38,15 | 31,29 | 33,45 | 30,79 | 31,17 | 34,84 |
| "mmu-let-7f" | 37,95 | 38,02 | 37,43 | 38,28 | 38,61 | 38,59 | 38,12 | 35,74 | 37,89 | 37,06 | 38,02 | 36,95 | 38,15 | 31,50 | 33,60 | 31,69 | 31,69 | 32,74 |
| "mmu-miR-106b" | 26,79 | 26,28 | 25,90 | 26,02 | 25,95 | 26,20 | 25,82 | 26,02 | 26,12 | 26,57 | 26,28 | 26,20 | 26,35 | 25,73 | 26,46 | 25,95 | 26,02 | 26,12 |
| "mmu-miR-155" | 27,25 | 27,00 | 27,50 | 28,15 | 27,43 | 27,25 | 27,50 | 27,43 | 27,87 | 27,78 | 27,87 | 28,24 | 27,43 | 27,43 | 27,00 | 27,33 | 27,25 | 27,43 |
| "mmu-miR-17" | 22,71 | 22,71 | 22,60 | 22,95 | 22,41 | 22,41 | 22,60 | 22,60 | 22,71 | 23,14 | 22,95 | 24,93 | 22,71 | 22,60 | 22,60 | 22,60 | 22,60 | 22,41 |

# 6. BIBLIOGRAPHY


Abu-Shaar, M., Ryoo, H.D., and Mann, R.S. (1999). Control of the nuclear localization of Extradenticle by competing nuclear import and export signals. Genes Dev *13*, 935-945.

Adams, B., Dorfler, P., Aguzzi, A., Kozmik, Z., Urbanek, P., Maurer-Fogy, I., and Busslinger, M. (1992). Pax-5 encodes the transcription factor BSAP and is expressed in B lymphocytes, the developing CNS, and adult testis. Genes Dev *6*, 1589-1607.

Adolfsson, J., Borge, O.J., Bryder, D., Theilgaard-Monch, K., Astrand-Grundstrom, I., Sitnicka, E., Sasaki, Y., and Jacobsen, S.E. (2001). Upregulation of Flt3 expression within the bone marrow Lin(-)Sca1(+)c-kit(+) stem cell compartment is accompanied by loss of self-renewal capacity. Immunity *15*, 659-669.

Adolfsson, J., Mansson, R., Buza-Vidas, N., Hultquist, A., Liuba, K., Jensen, C.T., Bryder, D., Yang, L., Borge, O.J., Thoren, L.A., *et al.* (2005). Identification of Flt3+ lympho-myeloid stem cells lacking erythro-megakaryocytic potential a revised road map for adult blood lineage commitment. Cell *121*, 295-306.

Akashi, K., Traver, D., Miyamoto, T., and Weissman, I.L. (2000). A clonogenic common myeloid progenitor that gives rise to all myeloid lineages. Nature *404*, 193-197.

Ambros, V. (2004). The functions of animal microRNAs. Nature *431*, 350-355.

Ambros, V., Bartel, B., Bartel, D.P., Burge, C.B., Carrington, J.C., Chen, X., Dreyfuss, G., Eddy, S.R., Griffiths-Jones, S., Marshall, M., *et al.* (2003). A uniform system for microRNA annotation. Rna *9*, 277-279.

Antonchuk, J., Sauvageau, G., and Humphries, R.K. (2002). HOXB4-induced expansion of adult hematopoietic stem cells ex vivo. Cell *109*, 39-45.

Arai, F., Hirao, A., Ohmura, M., Sato, H., Matsuoka, S., Takubo, K., Ito, K., Koh, G.Y., and Suda, T. (2004). Tie2/angiopoietin-1 signaling regulates hematopoietic stem cell quiescence in the bone marrow niche. Cell *118*, 149-161.

Arai, F., Ohneda, O., Miyamoto, T., Zhang, X.Q., and Suda, T. (2002). Mesenchymal stem cells in perichondrium express activated leukocyte cell adhesion molecule and participate in bone marrow formation. J Exp Med *195*, 1549-1563.

Arboleda, M.J., Lyons, J.F., Kabbinavar, F.F., Bray, M.R., Snow, B.E., Ayala, R., Danino, M., Karlan, B.Y., and Slamon, D.J. (2003). Overexpression of AKT2/protein kinase Bbeta leads to up-regulation of beta1 integrins, increased invasion, and metastasis of human breast and ovarian cancer cells. Cancer Res *63*, 196-206.

Argiropoulos, B., and Humphries, R.K. (2007). Hox genes in hematopoiesis and leukemogenesis. Oncogene *26*, 6766-6776.

Arinobu, Y., Mizuno, S., Chong, Y., Shigematsu, H., Iino, T., Iwasaki, H., Graf, T., Mayfield, R., Chan, S., Kastner, P., *et al.* (2007). Reciprocal activation of GATA-1 and PU.1 marks initial specification of hematopoietic stem cells into myeloerythroid and myelolymphoid lineages. Cell Stem Cell *1*, 416-427.

Asahara, H., Dutta, S., Kao, H.Y., Evans, R.M., and Montminy, M. (1999). Pbx-Hox heterodimers recruit coactivator-corepressor complexes in an isoform-specific manner. Mol Cell Biol *19*, 8219-8225.

Avecilla, S.T., Hattori, K., Heissig, B., Tejada, R., Liao, F., Shido, K., Jin, D.K., Dias, S., Zhang, F., Hartman, T.E., *et al.* (2004). Chemokine-mediated interaction of hematopoietic progenitors with the bone marrow vascular niche is required for thrombopoiesis. Nat Med *10*, 64-71.

Baek, D., Villen, J., Shin, C., Camargo, F.D., Gygi, S.P., and Bartel, D.P. (2008). The impact of microRNAs on protein output. Nature *455*, 64-71.

Bailey, T.L., and Gribskov, M. (1998). Combining evidence using p-values: application to sequence homology searches. Bioinformatics *14*, 48-54.

Bartel, D.P. (2004). MicroRNAs: genomics, biogenesis, mechanism, and function. Cell *116*, 281-297.

Bartel, D.P. (2009). MicroRNAs: target recognition and regulatory functions. Cell *136*, 215-233.

Becker, A.J., Mc, C.E., and Till, J.E. (1963). Cytological demonstration of the clonal nature of spleen colonies derived from transplanted mouse marrow cells. Nature *197*, 452-454.

Berezikov, E., Chung, W.J., Willis, J., Cuppen, E., and Lai, E.C. (2007). Mammalian mirtron genes. Mol Cell *28*, 328-336.

Berezikov, E., Guryev, V., van de Belt, J., Wienholds, E., Plasterk, R.H., and Cuppen, E. (2005). Phylogenetic shadowing and computational identification of human microRNA genes. Cell *120*, 21-24.

Berkes, C.A., Bergstrom, D.A., Penn, B.H., Seaver, K.J., Knoepfler, P.S., and Tapscott, S.J. (2004). Pbx marks genes for activation by MyoD indicating a role for a homeodomain protein in establishing myogenic potential. Mol Cell *14*, 465-477.

Bernstein, E., Kim, S.Y., Carmell, M.A., Murchison, E.P., Alcorn, H., Li, M.Z., Mills, A.A., Elledge, S.J., Anderson, K.V., and Hannon, G.J. (2003). Dicer is essential for mouse development. Nat Genet *35*, 215-217.

Berthelsen, J., Kilstrup-Nielsen, C., Blasi, F., Mavilio, F., and Zappavigna, V. (1999). The subcellular localization of PBX1 and EXD proteins depends on nuclear import and export signals and is modulated by association with PREP1 and HTH. Genes Dev *13*, 946-953.

Berthelsen, J., Zappavigna, V., Ferretti, E., Mavilio, F., and Blasi, F. (1998). The novel homeoprotein Prep1 modulates Pbx-Hox protein cooperativity. The EMBO journal *17*, 1434-1445.

Bertrand, J.Y., Jalil, A., Klaine, M., Jung, S., Cumano, A., and Godin, I. (2005). Three pathways to mature macrophages in the early mouse yolk sac. Blood *106*, 3004-3011.

Betschinger, J., and Knoblich, J.A. (2004). Dare to be different: asymmetric cell division in Drosophila, C. elegans and vertebrates. Curr Biol *14*, R674-685.

Bhardwaj, G., Murdoch, B., Wu, D., Baker, D.P., Williams, K.P., Chadwick, K., Ling, L.E., Karanu, F.N., and Bhatia, M. (2001). Sonic hedgehog induces the proliferation of primitive human hematopoietic cells via BMP regulation. Nat Immunol *2*, 172-180.

Billingham, R.E., Brent, L., and Medawar, P.B. (1953). Actively acquired tolerance of foreign cells. Nature *172*, 603-606.

Bissels, U., Bosio, A., and Wagner, W. (2011a). MicroRNAs are shaping the hematopoietic landscape. Haematologica *97*, 160-167.

Bissels, U., Wild, S., Tomiuk, S., Hafner, M., Scheel, H., Mihailovic, A., Choi, Y.H., Tuschl, T., and Bosio, A. (2011b). Combined characterization of microRNA and mRNA profiles delineates early differentiation pathways of CD133+ and CD34+ hematopoietic stem and progenitor cells. Stem Cells *29*, 847-857.

Blow, M.J., Grocock, R.J., van Dongen, S., Enright, A.J., Dicks, E., Futreal, P.A., Wooster, R., and Stratton, M.R. (2006). RNA editing of human microRNAs. Genome Biol *7*, R27.

Bohnsack, M.T., Czaplinski, K., and Gorlich, D. (2004). Exportin 5 is a RanGTP-dependent dsRNA-binding protein that mediates nuclear export of pre-miRNAs. Rna *10*, 185-191.

Borchert, G.M., Lanier, W., and Davidson, B.L. (2006). RNA polymerase III transcribes human microRNAs. Nat Struct Mol Biol *13*, 1097-1101.

Brendolan, A., Ferretti, E., Salsi, V., Moses, K., Quaggin, S., Blasi, F., Cleary, M.L., and Selleri, L. (2005). A Pbx1-dependent genetic and transcriptional network regulates spleen ontogeny. Development *132*, 3113-3126.

Brennecke, J., Hipfner, D.R., Stark, A., Russell, R.B., and Cohen, S.M. (2003). bantam encodes a developmentally regulated microRNA that controls cell proliferation and regulates the proapoptotic gene hid in Drosophila. Cell *113*, 25-36.

Brodersen, P., Sakvarelidze-Achard, L., Bruun-Rasmussen, M., Dunoyer, P., Yamamoto, Y.Y., Sieburth, L., and Voinnet, O. (2008). Widespread translational inhibition by plant miRNAs and siRNAs. Science *320*, 1185-1190.

Burglin, T.R. (1997). Analysis of TALE superclass homeobox genes (MEIS, PBC, KNOX, Iroquois, TGIF) reveals a novel domain conserved between plants and animals. Nucleic Acids Res *25*, 4173-4180.

Burglin, T.R. (1998). The PBC domain contains a MEINOX domain: coevolution of Hox and TALE homeobox genes? Dev Genes Evol *208*, 113-116.

Busslinger, M., Nutt, S.L., and Rolink, A.G. (2000). Lineage commitment in lymphopoiesis. Curr Opin Immunol *12*, 151-158.

Byers, R.J., Currie, T., Tholouli, E., Rodig, S.J., and Kutok, J.L. (2011). MSI2 protein expression predicts unfavorable outcome in acute myeloid leukemia. Blood *118*, 2857-2867.

Cai, X., Hagedorn, C.H., and Cullen, B.R. (2004). Human microRNAs are processed from capped, polyadenylated transcripts that can also function as mRNAs. Rna *10*, 1957-1966.

Calin, G.A., and Croce, C.M. (2006). MicroRNA signatures in human cancers. Nat Rev Cancer *6*, 857-866.

Calvi, L.M., Adams, G.B., Weibrecht, K.W., Weber, J.M., Olson, D.P., Knight, M.C., Martin, R.P., Schipani, E., Divieti, P., Bringhurst, F.R., *et al.* (2003). Osteoblastic cells regulate the haematopoietic stem cell niche. Nature *425*, 841-846.

Calvo, K.R., Knoepfler, P., McGrath, S., and Kamps, M.P. (1999). An inhibitory switch derepressed by pbx, hox, and Meis/Prep1 partners regulates DNA-binding by pbx1 and E2a-pbx1 and is dispensable for myeloid immortalization by E2a-pbx1. Oncogene *18*, 8033-8043.

Cano, F., Drynan, L.F., Pannell, R., and Rabbitts, T.H. (2008). Leukaemia lineage specification caused by cell-specific Mll-Enl translocations. Oncogene *27*, 1945-1950.

Carr, A., and Biggin, M.D. (1999). A comparison of in vivo and in vitro DNA-binding specificities suggests a new model for homeoprotein DNA binding in Drosophila embryos. The EMBO journal *18*, 1598-1608.

Ceredig, R., and Rolink, A.G. (2012). The key role of IL-7 in lymphopoiesis. Semin Immunol *24*, 159-164.

Chan, S.K., Ryoo, H.D., Gould, A., Krumlauf, R., and Mann, R.S. (1997). Switching the in vivo specificity of a minimal Hox-responsive element. Development *124*, 2007-2014.

Chang, C.P., Brocchieri, L., Shen, W.F., Largman, C., and Cleary, M.L. (1996). Pbx modulation of Hox homeodomain amino-terminal arms establishes different DNA-binding specificities across the Hox locus. Mol Cell Biol *16*, 1734-1745.

Chang, C.P., Jacobs, Y., Nakamura, T., Jenkins, N.A., Copeland, N.G., and Cleary, M.L. (1997). Meis proteins are major in vivo DNA binding partners for wild-type but not chimeric Pbx proteins. Mol Cell Biol *17*, 5679-5687.

Chang, C.P., Neilson, J.R., Bayle, J.H., Gestwicki, J.E., Kuo, A., Stankunas, K., Graef, I.A., and Crabtree, G.R. (2004). A field of myocardial-endocardial NFAT signaling underlies heart valve morphogenesis. Cell *118*, 649-663.

Chatterjee, S., Fasler, M., Bussing, I., and Grosshans, H. (2011). Target-mediated protection of endogenous microRNAs in C. elegans. Developmental cell *20*, 388-396.

Chatterjee, S., and Grosshans, H. (2009). Active turnover modulates mature microRNA activity in Caenorhabditis elegans. Nature *461*, 546-549.

Chekulaeva, M., and Filipowicz, W. (2009). Mechanisms of miRNA-mediated post-transcriptional regulation in animal cells. Curr Opin Cell Biol *21*, 452-460.

Chen, C., Ridzon, D.A., Broomer, A.J., Zhou, Z., Lee, D.H., Nguyen, J.T., Barbisin, M., Xu, N.L., Mahuvakar, V.R., Andersen, M.R., *et al.* (2005a). Real-time quantification of microRNAs by stem-loop RT-PCR. Nucleic Acids Res *33*, e179.

Chen, C.Z., Li, L., Lodish, H.F., and Bartel, D.P. (2004). MicroRNAs modulate hematopoietic lineage differentiation. Science *303*, 83-86.

Chen, F., and Capecchi, M.R. (1997). Targeted mutations in hoxa-9 and hoxb-9 reveal synergistic interactions. Dev Biol *181*, 186-196.

Chen, H., Rubin, E., Zhang, H., Chung, S., Jie, C.C., Garrett, E., Biswal, S., and Sukumar, S. (2005b). Identification of transcriptional targets of HOXA5. The Journal of biological chemistry *280*, 19373-19380.

Chen, J., Singh, K., Mukherjee, B.B., and Sodek, J. (1993). Developmental expression of osteopontin (OPN) mRNA in rat tissues: evidence for a role for OPN in bone formation and resorption. Matrix *13*, 113-123.

Chen, K., and Rajewsky, N. (2007). The evolution of gene regulation by transcription factors and microRNAs. Nat Rev Genet *8*, 93-103.

Christensen, J.L., and Weissman, I.L. (2001). Flk-2 is a marker in hematopoietic stem cell differentiation: a simple method to isolate long-term stem cells. Proc Natl Acad Sci U S A *98*, 14541-14546.

Cleary, M.L. (2009). Regulating the leukaemia stem cell. Best Pract Res Clin Haematol *22*, 483-487.

Cobb, B.S., Nesterova, T.B., Thompson, E., Hertweck, A., O'Connor, E., Godwin, J., Wilson, C.B., Brockdorff, N., Fisher, A.G., Smale, S.T., *et al.* (2005). T cell lineage choice and differentiation in the absence of the RNase III enzyme Dicer. J Exp Med *201*, 1367-1373.

Constien, R., Forde, A., Liliensiek, B., Grone, H.J., Nawroth, P., Hammerling, G., and Arnold, B. (2001). Characterization of a novel EGFP reporter mouse to monitor Cre recombination as demonstrated by a Tie2 Cre mouse line. Genesis *30*, 36-44.

Coulombel, L. (2004). Identification of hematopoietic stem/progenitor cells: strength and drawbacks of functional assays. Oncogene *23*, 7210-7222.

Cuellar, T.L., and McManus, M.T. (2005). MicroRNAs and endocrine biology. J Endocrinol *187*, 327-332.

Cumano, A., Dieterlen-Lievre, F., and Godin, I. (1996). Lymphoid potential, probed before circulation in mouse, is restricted to caudal intraembryonic splanchnopleura. Cell *86*, 907-916.

Czechowicz, A., Kraft, D., Weissman, I.L., and Bhattacharya, D. (2007). Efficient transplantation via antibody-based clearance of hematopoietic stem cell niches. Science *318*, 1296-1299.

Dar, A., Kollet, O., and Lapidot, T. (2006). Mutual, reciprocal SDF-1/CXCR4 interactions between hematopoietic and bone marrow stromal cells regulate human stem cell migration and development in NOD/SCID chimeric mice. Experimental hematology *34*, 967-975.

Davis-Dusenbery, B.N., and Hata, A. (2010). Mechanisms of control of microRNA biogenesis. J Biochem *148*, 381-392.

Davis, B.N., Hilyard, A.C., Lagna, G., and Hata, A. (2008). SMAD proteins control DROSHA-mediated microRNA maturation. Nature *454*, 56-61.

Davis, S., Aldrich, T.H., Jones, P.F., Acheson, A., Compton, D.L., Jain, V., Ryan, T.E., Bruno, J., Radziejewski, C., Maisonpierre, P.C., *et al.* (1996). Isolation of angiopoietin-1, a ligand for the TIE2 receptor, by secretion-trap expression cloning. Cell *87*, 1161-1169.

de Bruijn, M.F., Speck, N.A., Peeters, M.C., and Dzierzak, E. (2000). Definitive hematopoietic stem cells first develop within the major arterial regions of the mouse embryo. The EMBO journal *19*, 2465-2474.

DeKoter, R.P., and Singh, H. (2000). Regulation of B lymphocyte and macrophage development by graded expression of PU.1. Science *288*, 1439-1441.

Denli, A.M., Tops, B.B., Plasterk, R.H., Ketting, R.F., and Hannon, G.J. (2004). Processing of primary microRNAs by the Microprocessor complex. Nature *432*, 231-235.

Deo, A., Carlsson, J., and Lindlof, A. (2011). How to choose a normalization strategy for miRNA quantitative real-time (qPCR) arrays. J Bioinform Comput Biol *9*, 795-812.

DiMartino, J.F., Selleri, L., Traver, D., Firpo, M.T., Rhee, J., Warnke, R., O'Gorman, S., Weissman, I.L., and Cleary, M.L. (2001). The Hox cofactor and proto-oncogene Pbx1 is required for maintenance of definitive hematopoiesis in the fetal liver. Blood *98*, 618-626.

Doe, C.Q., and Bowerman, B. (2001). Asymmetric cell division: fly neuroblast meets worm zygote. Curr Opin Cell Biol *13*, 68-75.

Driessen, R.L., Johnston, H.M., and Nilsson, S.K. (2003). Membrane-bound stem cell factor is a key regulator in the initial lodgment of stem cells within the endosteal marrow region. Experimental hematology *31*, 1284-1291.

Duboule, D. (2000). Developmental genetics. A Hox by any other name. Nature *403*, 607, 609-610.

Easow, G., Teleman, A.A., and Cohen, S.M. (2007). Isolation of microRNA targets by miRNP immunopurification. Rna *13*, 1198-1204.

Ebner, A., Cabernard, C., Affolter, M., and Merabet, S. (2005). Recognition of distinct target sites by a unique Labial/Extradenticle/Homothorax complex. Development *132*, 1591-1600.

Esquela-Kerscher, A., and Slack, F.J. (2006). Oncomirs - microRNAs with a role in cancer. Nat Rev Cancer *6*, 259-269.

Essers, M.A., Offner, S., Blanco-Bose, W.E., Waibler, Z., Kalinke, U., Duchosal, M.A., and Trumpp, A. (2009). IFNalpha activates dormant haematopoietic stem cells in vivo. Nature *458*, 904-908.

Fahlgren, N., Jogdeo, S., Kasschau, K.D., Sullivan, C.M., Chapman, E.J., Laubinger, S., Smith, L.M., Dasenko, M., Givan, S.A., Weigel, D., *et al.* (2010). MicroRNA gene evolution in Arabidopsis lyrata and Arabidopsis thaliana. Plant Cell *22*, 1074-1089.

Felli, N., Fontana, L., Pelosi, E., Botta, R., Bonci, D., Facchiano, F., Liuzzi, F., Lulli, V., Morsilli, O., Santoro, S., *et al.* (2005). MicroRNAs 221 and 222 inhibit normal erythropoiesis and erythroleukemic cell growth via kit receptor down-modulation. Proc Natl Acad Sci U S A *102*, 18081-18086.

Ferretti, E., Marshall, H., Popperl, H., Maconochie, M., Krumlauf, R., and Blasi, F. (2000). Segmental expression of Hoxb2 in r4 requires two separate sites that integrate cooperative interactions between Prep1, Pbx and Hox proteins. Development *127*, 155-166.

Ferretti, E., Schulz, H., Talarico, D., Blasi, F., and Berthelsen, J. (1999). The PBX-regulating protein PREP1 is present in different PBX-complexed forms in mouse. Mech Dev *83*, 53-64.

Ficara, F., Crisafulli, L., Lin, C., Iwasaki, M., Smith, K.S., Zammataro, L., and Cleary, M.L. (2013). Pbx1 restrains myeloid maturation while preserving lymphoid potential in hematopoietic progenitors. J Cell Sci *126*, 3181-3191.

Ficara, F., Murphy, M.J., Lin, M., and Cleary, M.L. (2008). Pbx1 regulates self-renewal of long-term hematopoietic stem cells by maintaining their quiescence. Cell Stem Cell *2*, 484-496.

Filipowicz, W., Bhattacharyya, S.N., and Sonenberg, N. (2008). Mechanisms of post-transcriptional regulation by microRNAs: are the answers in sight? Nat Rev Genet *9*, 102-114.

Fleming, H.E., Janzen, V., Lo Celso, C., Guo, J., Leahy, K.M., Kronenberg, H.M., and Scadden, D.T. (2008). Wnt signaling in the niche enforces hematopoietic stem cell quiescence and is necessary to preserve self-renewal in vivo. Cell Stem Cell *2*, 274-283.

Forsberg, E.C., Prohaska, S.S., Katzman, S., Heffner, G.C., Stuart, J.M., and Weissman, I.L. (2005). Differential expression of novel potential regulators in hematopoietic stem cells. PLoS Genet *1*, e28.

Forsberg, E.C., Serwold, T., Kogan, S., Weissman, I.L., and Passegue, E. (2006). New evidence supporting megakaryocyte-erythrocyte potential of flk2/flt3+ multipotent hematopoietic progenitors. Cell *126*, 415-426.

Foudi, A., Hochedlinger, K., Van Buren, D., Schindler, J.W., Jaenisch, R., Carey, V., and Hock, H. (2009). Analysis of histone 2B-GFP retention reveals slowly cycling hematopoietic stem cells. Nat Biotechnol *27*, 84-90.

Fric, J., Lim, C.X., Koh, E.G., Hofmann, B., Chen, J., Tay, H.S., Mohammad Isa, S.A., Mortellaro, A., Ruedl, C., and Ricciardi-Castagnoli, P. (2012). Calcineurin/NFAT signalling inhibits myeloid haematopoiesis. EMBO Mol Med *4*, 269-282.

Friedman, R.C., Farh, K.K., Burge, C.B., and Bartel, D.P. (2009). Most mammalian mRNAs are conserved targets of microRNAs. Genome Res *19*, 92-105.

Fuchs, E., Tumbar, T., and Guasch, G. (2004). Socializing with the neighbors: stem cells and their niche. Cell *116*, 769-778.

Fuller, J.F., McAdara, J., Yaron, Y., Sakaguchi, M., Fraser, J.K., and Gasson, J.C. (1999). Characterization of HOX gene expression during myelopoiesis: role of HOX A5 in lineage commitment and maturation. Blood *93*, 3391-3400.

Galan-Caridad, J.M., Harel, S., Arenzana, T.L., Hou, Z.E., Doetsch, F.K., Mirny, L.A., and Reizis, B. (2007). Zfx controls the self-renewal of embryonic and hematopoietic stem cells. Cell *129*, 345-357.

Galant, R., Walsh, C.M., and Carroll, S.B. (2002). Hox repression of a target gene: extradenticle-independent, additive action through multiple monomer binding sites. Development *129*, 3115-3126.

Galloway, J.L., Wingert, R.A., Thisse, C., Thisse, B., and Zon, L.I. (2005). Loss of gata1 but not gata2 converts erythropoiesis to myelopoiesis in zebrafish embryos. Developmental cell *8*, 109-116.

Gangaraju, V.K., and Lin, H. (2009). MicroRNAs: key regulators of stem cells. Nat Rev Mol Cell Biol *10*, 116-125.

Gekas, C., Dieterlen-Lievre, F., Orkin, S.H., and Mikkola, H.K. (2005). The placenta is a niche for hematopoietic stem cells. Developmental cell *8*, 365-375.

Gentner, B., Schira, G., Giustacchini, A., Amendola, M., Brown, B.D., Ponzoni, M., and Naldini, L. (2009). Stable knockdown of microRNA in vivo by lentiviral vectors. Nat Methods *6*, 63-66.

Gentner, B., Visigalli, I., Hiramatsu, H., Lechman, E., Ungari, S., Giustacchini, A., Schira, G., Amendola, M., Quattrini, A., Martino, S., *et al.* (2010). Identification of hematopoietic stem cell-specific miRNAs enables gene therapy of globoid cell leukodystrophy. Sci Transl Med *2*, 3001522.

Georgantas, R.W., 3rd, Hildreth, R., Morisot, S., Alder, J., Liu, C.G., Heimfeld, S., Calin, G.A., Croce, C.M., and Civin, C.I. (2007). CD34+ hematopoietic stem-progenitor cell microRNA expression and function: a circuit diagram of differentiation control. Proc Natl Acad Sci U S A *104*, 2750-2755.

Gerber, H.P., Malik, A.K., Solar, G.P., Sherman, D., Liang, X.H., Meng, G., Hong, K., Marsters, J.C., and Ferrara, N. (2002). VEGF regulates haematopoietic stem cell survival by an internal autocrine loop mechanism. Nature *417*, 954-958.

Ginhoux, F., Greter, M., Leboeuf, M., Nandi, S., See, P., Gokhan, S., Mehler, M.F., Conway, S.J., Ng, L.G., Stanley, E.R., *et al.* Fate mapping analysis reveals that adult microglia derive from primitive macrophages. Science *330*, 841-845.

Goldschneider, I., Gordon, L.K., and Morris, R.J. (1978). Demonstration of Thy-1 antigen on pluripotent hemopoietic stem cells in the rat. J Exp Med *148*, 1351-1366.

Gonzalez-Crespo, S., Abu-Shaar, M., Torres, M., Martinez, A.C., Mann, R.S., and Morata, G. (1998). Antagonism between extradenticle function and Hedgehog signalling in the developing limb. Nature *394*, 196-200.

Goodell, M.A., Brose, K., Paradis, G., Conner, A.S., and Mulligan, R.C. (1996). Isolation and functional properties of murine hematopoietic stem cells that are replicating in vivo. J Exp Med *183*, 1797-1806.

Goyama, S., Yamamoto, G., Shimabe, M., Sato, T., Ichikawa, M., Ogawa, S., Chiba, S., and Kurokawa, M. (2008). Evi-1 is a critical regulator for hematopoietic stem cells and transformed leukemic cells. Cell Stem Cell 2008 Aug 7;3(2):207-20 doi: 101016/jstem200806002.

Graf, T., and Enver, T. (2009). Forcing cells to change lineages. Nature *462*, 587-594.

Greer, J.M., Puetz, J., Thomas, K.R., and Capecchi, M.R. (2000). Maintenance of functional equivalence during paralogous Hox gene evolution. Nature *403*, 661-665.

Gregory, R.I., Chendrimada, T.P., and Shiekhattar, R. (2006). MicroRNA biogenesis: isolation and characterization of the microprocessor complex. Methods Mol Biol *342*, 33-47.

Griffiths-Jones, S., Grocock, R.J., van Dongen, S., Bateman, A., and Enright, A.J. (2006). miRBase: microRNA sequences, targets and gene nomenclature. Nucleic Acids Res *34*, D140-144.

Griffiths-Jones, S., Moxon, S., Marshall, M., Khanna, A., Eddy, S.R., and Bateman, A. (2005). Rfam: annotating non-coding RNAs in complete genomes. Nucleic Acids Res *33*, D121-124.

Guo, S., Lu, J., Schlanger, R., Zhang, H., Wang, J.Y., Fox, M.C., Purton, L.E., Fleming, H.H., Cobb, B., Merkenschlager, M., *et al.* (2010). MicroRNA miR-125a controls hematopoietic stem cell number. Proc Natl Acad Sci U S A *107*, 14229-14234.

Hagan, J.P., Piskounova, E., and Gregory, R.I. (2009). Lin28 recruits the TUTase Zcchc11 to inhibit let-7 maturation in mouse embryonic stem cells. Nat Struct Mol Biol *16*, 1021-1025.

Han, Y.C., Park, C.Y., Bhagat, G., Zhang, J., Wang, Y., Fan, J.B., Liu, M., Zou, Y., Weissman, I.L., and Gu, H. (2010). microRNA-29a induces aberrant self-renewal capacity in hematopoietic progenitors, biased myeloid development, and acute myeloid leukemia. J Exp Med *207*, 475-489.

Harfe, B.D., McManus, M.T., Mansfield, J.H., Hornstein, E., and Tabin, C.J. (2005). The RNaseIII enzyme Dicer is required for morphogenesis but not patterning of the vertebrate limb. Proc Natl Acad Sci U S A *102*, 10898-10903.

Harrison, D.E. (1980). Competitive repopulation: a new assay for long-term stem cell functional capacity. Blood *55*, 77-81.

Harrison, D.E., Jordan, C.T., Zhong, R.K., and Astle, C.M. (1993). Primitive hemopoietic stem cells: direct assay of most productive populations by competitive repopulation with simple binomial, correlation and covariance calculations. Experimental hematology *21*, 206-219.

Harvey Lodish, A.B., Chris A. Kaiser and Monty Krieger (2012). Molecular Cell Biology, 7th edn (W.H.Freeman & Co Ltd).

Havelange, V., and Garzon, R. (2010). MicroRNAs: emerging key regulators of hematopoiesis. Am J Hematol *85*, 935-942.

He, L., and Hannon, G.J. (2004). MicroRNAs: small RNAs with a big role in gene regulation. Nat Rev Genet *5*, 522-531.

Heissig, B., Hattori, K., Dias, S., Friedrich, M., Ferris, B., Hackett, N.R., Crystal, R.G., Besmer, P., Lyden, D., Moore, M.A., *et al.* (2002). Recruitment of stem and progenitor cells from the bone marrow niche requires MMP-9 mediated release of kit-ligand. Cell *109*, 625-637.

Heo, I., Joo, C., Cho, J., Ha, M., Han, J., and Kim, V.N. (2008). Lin28 mediates the terminal uridylation of let-7 precursor MicroRNA. Mol Cell *32*, 276-284.

Heo, I., Joo, C., Kim, Y.K., Ha, M., Yoon, M.J., Cho, J., Yeom, K.H., Han, J., and Kim, V.N. (2009). TUT4 in concert with Lin28 suppresses microRNA biogenesis through pre-microRNA uridylation. Cell *138*, 696-708.

Herbomel, P., Thisse, B., and Thisse, C. (1999). Ontogeny and behaviour of early macrophages in the zebrafish embryo. Development *126*, 3735-3745.

Herrera-Merchan, A., Cerrato, C., Luengo, G., Dominguez, O., Piris, M.A., Serrano, M., and Gonzalez, S. (2010). miR-33-mediated downregulation of p53 controls hematopoietic stem cell self-renewal. Cell Cycle *9*, 3277-3285.

Houbaviy, H.B., Murray, M.F., and Sharp, P.A. (2003). Embryonic stem cell-specific MicroRNAs. Developmental cell *5*, 351-358.

Huang, H., Paliouras, M., Rambaldi, I., Lasko, P., and Featherstone, M. (2003). Nonmuscle myosin promotes cytoplasmic localization of PBX. Mol Cell Biol *23*, 3636-3645.

Hunger, S.P., Li, S., Fall, M.Z., Naumovski, L., and Cleary, M.L. (1996). The proto-oncogene HLF and the related basic leucine zipper protein TEF display highly similar DNA-binding and transcriptional regulatory properties. Blood *87*, 4607-4617.

Hunger, S.P., Ohyashiki, K., Toyama, K., and Cleary, M.L. (1992). Hlf, a novel hepatic bZIP protein, shows altered DNA-binding properties following fusion to E2A in t(17;19) acute lymphoblastic leukemia. Genes Dev *6*, 1608-1620.

Ihle, J.N. (1992). Interleukin-3 and hematopoiesis. Chem Immunol *51*, 65-106.

Ikuta, K., and Weissman, I.L. (1992). Evidence that hematopoietic stem cells express mouse c-kit but do not depend on steel factor for their generation. Proc Natl Acad Sci U S A *89*, 1502-1506.

Inman, K.E., and Downs, K.M. (2007). The murine allantois: emerging paradigms in development of the mammalian umbilical cord and its relation to the fetus. Genesis *45*, 237-258.

Iwasaki, H., and Akashi, K. (2007). Myeloid lineage commitment from the hematopoietic stem cell. Immunity *26*, 726-740.

Jacobs, Y., Schnabel, C.A., and Cleary, M.L. (1999). Trimeric association of Hox and TALE homeodomain proteins mediates Hoxb2 hindbrain enhancer activity. Mol Cell Biol *19*, 5134-5142.

Jaw, T.J., You, L.R., Knoepfler, P.S., Yao, L.C., Pai, C.Y., Tang, C.Y., Chang, L.P., Berthelsen, J., Blasi, F., Kamps, M.P., *et al.* (2000). Direct interaction of two homeoproteins, homothorax and extradenticle, is essential for EXD nuclear localization and function. Mech Dev *91*, 279-291.

Ji, X. (2008). The mechanism of RNase III action: how dicer dices. Curr Top Microbiol Immunol *320*, 99-116.

Jin, P., Wang, E., Ren, J., Childs, R., Shin, J.W., Khuu, H., Marincola, F.M., and Stroncek, D.F. (2008). Differentiation of two types of mobilized peripheral blood stem cells by microRNA and cDNA expression analysis. J Transl Med *6*, 39.

Johnson, S.M., Grosshans, H., Shingara, J., Byrom, M., Jarvis, R., Cheng, A., Labourier, E., Reinert, K.L., Brown, D., and Slack, F.J. (2005). RAS is regulated by the let-7 microRNA family. Cell *120*, 635-647.

Joseph, C., Quach, J.M., Walkley, C.R., Lane, S.W., Lo Celso, C., and Purton, L.E. (2013). Deciphering hematopoietic stem cells in their niches: a critical appraisal of genetic models, lineage tracing, and imaging strategies. Cell Stem Cell *13*, 520-533.

Kamps, M.P., Murre, C., Sun, X.H., and Baltimore, D. (1990). A new homeobox gene contributes the DNA binding domain of the t(1;19) translocation protein in pre-B ALL. Cell *60*, 547-555.

Kanellopoulou, C., Muljo, S.A., Kung, A.L., Ganesan, S., Drapkin, R., Jenuwein, T., Livingston, D.M., and Rajewsky, K. (2005). Dicer-deficient mouse embryonic stem cells are defective in differentiation and centromeric silencing. Genes Dev *19*, 489-501.

Karsunky, H., Inlay, M.A., Serwold, T., Bhattacharya, D., and Weissman, I.L. (2008). Flk2+ common lymphoid progenitors possess equivalent differentiation potential for the B and T lineages. Blood *111*, 5562-5570.

Kawahara, Y., Megraw, M., Kreider, E., Iizasa, H., Valente, L., Hatzigeorgiou, A.G., and Nishikura, K. (2008). Frequency and fate of microRNA editing in human brain. Nucleic Acids Res *36*, 5270-5280.

Kawamoto, H., and Katsura, Y. (2009). A new paradigm for hematopoietic cell lineages: revision of the classical concept of the myeloid-lymphoid dichotomy. Trends Immunol *30*, 193-200.

Kiel, M.J., Yilmaz, O.H., Iwashita, T., Yilmaz, O.H., Terhorst, C., and Morrison, S.J. (2005). SLAM family receptors distinguish hematopoietic stem and progenitor cells and reveal endothelial niches for stem cells. Cell *121*, 1109-1121.

Kim, I., Kim, J.H., Moon, S.O., Kwak, H.J., Kim, N.G., and Koh, G.Y. (2000). Angiopoietin-2 at high concentration can enhance endothelial cell survival through the phosphatidylinositol 3'-kinase/Akt signal transduction pathway. Oncogene *19*, 4549-4552.

Kim, S.K., Selleri, L., Lee, J.S., Zhang, A.Y., Gu, X., Jacobs, Y., and Cleary, M.L. (2002). Pbx1 inactivation disrupts pancreas development and in Ipf1-deficient mice promotes diabetes mellitus. Nat Genet *30*, 430-435.

Kim, Y.K., and Kim, V.N. (2007). Processing of intronic microRNAs. The EMBO journal *26*, 775-783.

Kisanuki, Y.Y., Hammer, R.E., Miyazaki, J., Williams, S.C., Richardson, J.A., and Yanagisawa, M. (2001). Tie2-Cre transgenic mice: a new model for endothelial cell-lineage analysis in vivo. Dev Biol *230*, 230-242.

Knoepfler, P.S., Calvo, K.R., Chen, H., Antonarakis, S.E., and Kamps, M.P. (1997). Meis1 and pKnox1 bind DNA cooperatively with Pbx1 utilizing an interaction surface disrupted in oncoprotein E2a-Pbx1. Proc Natl Acad Sci U S A *94*, 14553-14558.

Kondo, M., Weissman, I.L., and Akashi, K. (1997). Identification of clonogenic common lymphoid progenitors in mouse bone marrow. Cell *91*, 661-672.

Koralov, S.B., Muljo, S.A., Galler, G.R., Krek, A., Chakraborty, T., Kanellopoulou, C., Jensen, K., Cobb, B.S., Merkenschlager, M., Rajewsky, N., *et al.* (2008). Dicer ablation affects antibody diversity and cell survival in the B lymphocyte lineage. Cell *132*, 860-874.

Koss, M., Bolze, A., Brendolan, A., Saggese, M., Capellini, T.D., Bojilova, E., Boisson, B., Prall, O.W., Elliott, D.A., Solloway, M., *et al.* (2012). Congenital asplenia in mice and humans with mutations in a Pbx/Nkx2-5/p15 module. Developmental cell *22*, 913-926.

Krivtsov, A.V., Twomey, D., Feng, Z., Stubbs, M.C., Wang, Y., Faber, J., Levine, J.E., Wang, J., Hahn, W.C., Gilliland, D.G., *et al.* (2006). Transformation from committed progenitor to leukaemia stem cell initiated by MLL-AF9. Nature *442*, 818-822.

Krol, J., Loedige, I., and Filipowicz, W. (2010). The widespread regulation of microRNA biogenesis, function and decay. Nat Rev Genet *11*, 597-610.

Kuhn, R., Schwenk, F., Aguet, M., and Rajewsky, K. (1995). Inducible gene targeting in mice. Science *269*, 1427-1429.

Kulessa, H., Frampton, J., and Graf, T. (1995). GATA-1 reprograms avian myelomonocytic cell lines into eosinophils, thromboblasts, and erythroblasts. Genes Dev *9*, 1250-1262.

Lagos-Quintana, M., Rauhut, R., Yalcin, A., Meyer, J., Lendeckel, W., and Tuschl, T. (2002). Identification of tissue-specific microRNAs from mouse. Curr Biol *12*, 735-739.

Lai, E.C. (2002). Micro RNAs are complementary to 3' UTR sequence motifs that mediate negative post-transcriptional regulation. Nat Genet *30*, 363-364.

Laine, S.K., Hentunen, T., and Laitala-Leinonen, T. (2012). Do microRNAs regulate bone marrow stem cell niche physiology? Gene *497*, 1-9.

Lal, A., Navarro, F., Maher, C.A., Maliszewski, L.E., Yan, N., O'Day, E., Chowdhury, D., Dykxhoorn, D.M., Tsai, P., Hofmann, O., *et al.* (2009). miR-24 Inhibits cell proliferation by targeting E2F2, MYC, and other cell-cycle genes via binding to "seedless" 3'UTR microRNA recognition elements. Mol Cell *35*, 610-625.

Lau, N.C., Lim, L.P., Weinstein, E.G., and Bartel, D.P. (2001). An abundant class of tiny RNAs with probable regulatory roles in Caenorhabditis elegans. Science *294*, 858-862.

Laurent, A., Bihan, R., Omilli, F., Deschamps, S., and Pellerin, I. (2008). PBX proteins: much more than Hox cofactors. Int J Dev Biol *52*, 9-20.

Lechman, E.R., Gentner, B., van Galen, P., Giustacchini, A., Saini, M., Boccalatte, F.E., Hiramatsu, H., Restuccia, U., Bachi, A., Voisin, V., *et al.* (2012). Attenuation of miR-126 activity expands HSC in vivo without exhaustion. Cell Stem Cell *11*, 799-811.

Lee, R.C., Feinbaum, R.L., and Ambros, V. (1993). The C. elegans heterochronic gene lin-4 encodes small RNAs with antisense complementarity to lin-14. Cell *75*, 843-854.

Lee, Y., Ahn, C., Han, J., Choi, H., Kim, J., Yim, J., Lee, J., Provost, P., Radmark, O., Kim, S., *et al.* (2003). The nuclear RNase III Drosha initiates microRNA processing. Nature *425*, 415-419.

Lee, Y., Kim, M., Han, J., Yeom, K.H., Lee, S., Baek, S.H., and Kim, V.N. (2004). MicroRNA genes are transcribed by RNA polymerase II. The EMBO journal *23*, 4051-4060.

Lelandais-Briere, C., Sorin, C., Declerck, M., Benslimane, A., Crespi, M., and Hartmann, C. (2010). Small RNA diversity in plants and its impact in development. Curr Genomics *11*, 14-23.

Lemischka, I.R., Raulet, D.H., and Mulligan, R.C. (1986). Developmental potential and dynamic behavior of hematopoietic stem cells. Cell *45*, 917-927.

Lewis, B.P., Burge, C.B., and Bartel, D.P. (2005). Conserved seed pairing, often flanked by adenosines, indicates that thousands of human genes are microRNA targets. Cell *120*, 15-20.

Li, C.L., and Johnson, G.R. (1992). Rhodamine123 reveals heterogeneity within murine Lin-, Sca-1+ hemopoietic stem cells. J Exp Med *175*, 1443-1447.

Liao, R., Sun, J., Zhang, L., Lou, G., Chen, M., Zhou, D., Chen, Z., and Zhang, S. (2008). MicroRNAs play a role in the development of human hematopoietic stem cells. J Cell Biochem *104*, 805-817.

Lim, L.P., Lau, N.C., Garrett-Engele, P., Grimson, A., Schelter, J.M., Castle, J., Bartel, D.P., Linsley, P.S., and Johnson, J.M. (2005). Microarray analysis shows that some microRNAs downregulate large numbers of target mRNAs. Nature *433*, 769-773.

Lin, K.K., and Goodell, M.A. (2006). Purification of hematopoietic stem cells using the side population. Methods Enzymol *420*, 255-264.

Liu, Y., Elf, S.E., Asai, T., Miyata, Y., Liu, Y., Sashida, G., Huang, G., Di Giandomenico, S., Koff, A., and Nimer, S.D. (2009). The p53 tumor suppressor protein is a critical regulator of hematopoietic stem cell behavior. Cell Cycle *8*, 3120-3124.

Longobardi, E., and Blasi, F. (2003). Overexpression of PREP-1 in F9 teratocarcinoma cells leads to a functionally relevant increase of PBX-2 by preventing its degradation. The Journal of biological chemistry *278*, 39235-39241.

Luc, S., Buza-Vidas, N., and Jacobsen, S.E. (2008). Delineating the cellular pathways of hematopoietic lineage commitment. Semin Immunol *20*, 213-220.

Luciano, D.J., Mirsky, H., Vendetti, N.J., and Maas, S. (2004). RNA editing of a miRNA precursor. Rna *10*, 1174-1177.

Maisonpierre, P.C., Suri, C., Jones, P.F., Bartunkova, S., Wiegand, S.J., Radziejewski, C., Compton, D., McClain, J., Aldrich, T.H., Papadopoulos, N., *et al.* (1997). Angiopoietin-2, a natural antagonist for Tie2 that disrupts in vivo angiogenesis. Science *277*, 55-60.

Manley, N.R., Selleri, L., Brendolan, A., Gordon, J., and Cleary, M.L. (2004). Abnormalities of caudal pharyngeal pouch development in Pbx1 knockout mice mimic loss of Hox3 paralogs. Dev Biol *276*, 301-312.

Mann, R.S., and Affolter, M. (1998). Hox proteins meet more partners. Curr Opin Genet Dev *8*, 423-429.

Mansson, R., Hultquist, A., Luc, S., Yang, L., Anderson, K., Kharazi, S., Al-Hashmi, S., Liuba, K., Thoren, L., Adolfsson, J., *et al.* (2007). Molecular evidence for hierarchical transcriptional lineage priming in fetal and adult stem cells and multipotent progenitors. Immunity *26*, 407-419.

Mathieu, J., and Ruohola-Baker, H. (2013). Regulation of stem cell populations by microRNAs. Adv Exp Med Biol *786*, 329-351.

Matsuoka, S., Ebihara, Y., Xu, M., Ishii, T., Sugiyama, D., Yoshino, H., Ueda, T., Manabe, A., Tanaka, R., Ikeda, Y., *et al.* (2001). CD34 expression on long-term repopulating hematopoietic stem cells changes during developmental stages. Blood *97*, 419-425.

Matsuzaki, Y., Kinjo, K., Mulligan, R.C., and Okano, H. (2004). Unexpectedly efficient homing capacity of purified murine hematopoietic stem cells. Immunity *20*, 87-93.

McAlister, I., Wolf, N.S., Pietrzyk, M.E., Rabinovitch, P.S., Priestley, G., and Jaeger, B. (1990). Transplantation of hematopoietic stem cells obtained by a combined dye method fractionation of murine bone marrow. Blood *75*, 1240-1246.

McDevitt, M.A., Shivdasani, R.A., Fujiwara, Y., Yang, H., and Orkin, S.H. (1997). A "knockdown" mutation created by cis-element gene targeting reveals the dependence of erythroid cell maturation on the level of transcription factor GATA-1. Proc Natl Acad Sci U S A *94*, 6781-6785.

Medvinsky, A., and Dzierzak, E. (1996). Definitive hematopoiesis is autonomously initiated by the AGM region. Cell *86*, 897-906.

Mendez-Ferrer, S., Chow, A., Merad, M., and Frenette, P.S. (2009). Circadian rhythms influence hematopoietic stem cells. Curr Opin Hematol *16*, 235-242.

Mercader, N., Leonardo, E., Azpiazu, N., Serrano, A., Morata, G., Martinez, C., and Torres, M. (1999). Conserved regulation of proximodistal limb axis development by Meis1/Hth. Nature *402*, 425-429.

Merkerova, M., Vasikova, A., Bruchova, H., Libalova, H., Topinka, J., Balascak, I., Sram, R.J., and Brdicka, R. (2009). Differential gene expression in umbilical cord blood and maternal peripheral blood. Eur J Haematol *83*, 183-190.

Metcalf, D., Dakic, A., Mifsud, S., Di Rago, L., Wu, L., and Nutt, S. (2006). Inactivation of PU.1 in adult mice leads to the development of myeloid leukemia. Proc Natl Acad Sci U S A *103*, 1486-1491.

Milech, N., Kees, U.R., and Watt, P.M. (2001). Novel alternative PBX3 isoforms in leukemia cells with distinct interaction specificities. Genes Chromosomes Cancer *32*, 275-280.

Min, I.M., Pietramaggiori, G., Kim, F.S., Passegue, E., Stevenson, K.E., and Wagers, A.J. (2008). The transcription factor EGR1 controls both the proliferation and localization of hematopoietic stem cells. Cell Stem Cell *2*, 380-391.

Minami, Y., Stuart, S.A., Ikawa, T., Jiang, Y., Banno, A., Hunton, I.C., Young, D.J., Naoe, T., Murre, C., Jamieson, C.H., *et al.* (2008). BCR-ABL-transformed GMP as myeloid leukemic stem cells. Proc Natl Acad Sci U S A *105*, 17967-17972.

Moens, C.B., and Selleri, L. (2006). Hox cofactors in vertebrate development. Dev Biol *291*, 193-206.

Monica, K., Galili, N., Nourse, J., Saltman, D., and Cleary, M.L. (1991). PBX2 and PBX3, new homeobox genes with extensive homology to the human proto-oncogene PBX1. Mol Cell Biol *11*, 6149-6157.

Moore, M.A. (2010). A cancer fate in the hands of a samurai (Nat Med. 2010 Sep;16(9):963-5. doi: 10.1038/nm0910-963.).

Mootha, V.K., Lindgren, C.M., Eriksson, K.F., Subramanian, A., Sihag, S., Lehar, J., Puigserver, P., Carlsson, E., Ridderstrale, M., Laurila, E., *et al.* (2003). PGC-1alpha-responsive genes involved in oxidative phosphorylation are coordinately downregulated in human diabetes. Nat Genet *34*, 267-273.

Morlando, M., Ballarino, M., Gromak, N., Pagano, F., Bozzoni, I., and Proudfoot, N.J. (2008). Primary microRNA transcripts are processed co-transcriptionally. Nat Struct Mol Biol *15*, 902-909.

Morrison, S.J., and Kimble, J. (2006). Asymmetric and symmetric stem-cell divisions in development and cancer. Nature *441*, 1068-1074.

Morrison, S.J., and Weissman, I.L. (1994). The long-term repopulating subset of hematopoietic stem cells is deterministic and isolatable by phenotype. Immunity *1*, 661-673.

Moskow, J.J., Bullrich, F., Huebner, K., Daar, I.O., and Buchberg, A.M. (1995). Meis1, a PBX1-related homeobox gene involved in myeloid leukemia in BXH-2 mice. Mol Cell Biol *15*, 5434-5443.

Mu, Q., Wang, Y., Chen, B., Qian, W., Meng, H., Tong, H., Chen, F., Ma, Q., Ni, W., Chen, S., *et al.* (2013). High expression of Musashi-2 indicates poor prognosis in adult B-cell acute lymphoblastic leukemia. Leuk Res *37*, 922-927.

Muljo, S.A., Ansel, K.M., Kanellopoulou, C., Livingston, D.M., Rao, A., and Rajewsky, K. (2005). Aberrant T cell differentiation in the absence of Dicer. J Exp Med *202*, 261-269.

Muller, A.M., Medvinsky, A., Strouboulis, J., Grosveld, F., and Dzierzak, E. (1994). Development of hematopoietic stem cell activity in the mouse embryo. Immunity *1*, 291-301.

Nagasawa, T., Hirota, S., Tachibana, K., Takakura, N., Nishikawa, S., Kitamura, Y., Yoshida, N., Kikutani, H., and Kishimoto, T. (1996). Defects of B-cell lymphopoiesis and bone-marrow myelopoiesis in mice lacking the CXC chemokine PBSF/SDF-1. Nature *382*, 635-638.

Nakorn, T.N., Miyamoto, T., and Weissman, I.L. (2003). Characterization of mouse clonogenic megakaryocyte progenitors. Proc Natl Acad Sci U S A *100*, 205-210.

Navarro, F., and Lieberman, J. (2010). Small RNAs guide hematopoietic cell differentiation and function. J Immunol *184*, 5939-5947.

Neuteboom, S.T., and Murre, C. (1997). Pbx raises the DNA binding specificity but not the selectivity of antennapedia Hox proteins. Mol Cell Biol *17*, 4696-4706.

Nimmo, R., Ciau-Uitz, A., Ruiz-Herguido, C., Soneji, S., Bigas, A., Patient, R., and Enver, T. (2013). MiR-142-3p controls the specification of definitive hemangioblasts during ontogeny. Developmental cell *26*, 237-249.

Nourse, J., Mellentin, J.D., Galili, N., Wilkinson, J., Stanbridge, E., Smith, S.D., and Cleary, M.L. (1990). Chromosomal translocation t(1;19) results in synthesis of a homeobox fusion mRNA that codes for a potential chimeric transcription factor. Cell *60*, 535-545.

Nutt, S.L., Heavey, B., Rolink, A.G., and Busslinger, M. (1999). Commitment to the B-lymphoid lineage depends on the transcription factor Pax5. Nature *401*, 556-562.

Nutt, S.L., and Kee, B.L. (2007). The transcriptional regulation of B cell lineage commitment. Immunity *26*, 715-725.

O'Carroll, D., Mecklenbrauker, I., Das, P.P., Santana, A., Koenig, U., Enright, A.J., Miska, E.A., and Tarakhovsky, A. (2007). A Slicer-independent role for Argonaute 2 in hematopoiesis and the microRNA pathway. Genes Dev *21*, 1999-2004.

Ogawa, M. (1993). Differentiation and proliferation of hematopoietic stem cells. Blood *81*, 2844-2853.

Ogawa, M., Matsuzaki, Y., Nishikawa, S., Hayashi, S., Kunisada, T., Sudo, T., Kina, T., Nakauchi, H., and Nishikawa, S. (1991). Expression and function of c-kit in hemopoietic progenitor cells. J Exp Med *174*, 63-71.

Okada, S., Nakauchi, H., Nagayoshi, K., Nishikawa, S., Miura, Y., and Suda, T. (1992). In vivo and in vitro stem cell function of c-kit- and Sca-1-positive murine hematopoietic cells. Blood *80*, 3044-3050.

Ooi, A.G., Sahoo, D., Adorno, M., Wang, Y., Weissman, I.L., and Park, C.Y. (2010). MicroRNA-125b expands hematopoietic stem cells and enriches for the lymphoid-balanced and lymphoid-biased subsets. Proc Natl Acad Sci U S A *107*, 21505-21510.

Orford, K.W., and Scadden, D.T. (2008). Deconstructing stem cell self-renewal: genetic insights into cell-cycle regulation. Nat Rev Genet *9*, 115-128.

Orkin, S.H. (2000). Diversification of haematopoietic stem cells to specific lineages. Nat Rev Genet *1*, 57-64.

Orkin, S.H., and Zon, L.I. (2008). Hematopoiesis: an evolving paradigm for stem cell biology. Cell *132*, 631-644.

Osawa, M., Hanada, K., Hamada, H., and Nakauchi, H. (1996). Long-term lymphohematopoietic reconstitution by a single CD34-low/negative hematopoietic stem cell. Science *273*, 242-245.

Ottersbach, K., and Dzierzak, E. (2005). The murine placenta contains hematopoietic stem cells within the vascular labyrinth region. Developmental cell *8*, 377-387.

Palis, J., Robertson, S., Kennedy, M., Wall, C., and Keller, G. (1999). Development of erythroid and myeloid progenitors in the yolk sac and embryo proper of the mouse. Development *126*, 5073-5084.

Peers, B., Sharma, S., Johnson, T., Kamps, M., and Montminy, M. (1995). The pancreatic islet factor STF-1 binds cooperatively with Pbx to a regulatory element in the somatostatin promoter: importance of the FPWMK motif and of the homeodomain. Mol Cell Biol *15*, 7091-7097.

Peled, A., Petit, I., Kollet, O., Magid, M., Ponomaryov, T., Byk, T., Nagler, A., Ben-Hur, H., Many, A., Shultz, L., *et al.* (1999). Dependence of human stem cell engraftment and repopulation of NOD/SCID mice on CXCR4. Science *283*, 845-848.

Penkov, D., Mateos San Martin, D., Fernandez-Diaz, L.C., Rossello, C.A., Torroja, C., Sanchez-Cabo, F., Warnatz, H.J., Sultan, M., Yaspo, M.L., Gabrieli, A., *et al.* (2013). Analysis of the DNA-binding profile and function of TALE homeoproteins reveals their specialization and specific interactions with Hox genes/proteins. Cell Rep *3*, 1321-1333.

Petriv, O.I., Kuchenbauer, F., Delaney, A.D., Lecault, V., White, A., Kent, D., Marmolejo, L., Heuser, M., Berg, T., Copley, M., *et al.* (2010). Comprehensive microRNA expression profiling of the hematopoietic hierarchy. Proc Natl Acad Sci U S A *107*, 15443-15448.

Phillips, R.L., Reinhart, A.J., and Van Zant, G. (1992). Genetic control of murine hematopoietic stem cell pool sizes and cycling kinetics. Proc Natl Acad Sci U S A *89*, 11607-11611.

Pillai, M.M., Yang, X., Balakrishnan, I., Bemis, L., and Torok-Storb, B. (2010). MiR-886-3p down regulates CXCL12 (SDF1) expression in human marrow stromal cells. PLoS One *5*, e14304.

Pineault, N., Helgason, C.D., Lawrence, H.J., and Humphries, R.K. (2002). Differential expression of Hox, Meis1, and Pbx1 genes in primitive cells throughout murine hematopoietic ontogeny. Experimental hematology *30*, 49-57.

Piper, D.E., Batchelor, A.H., Chang, C.P., Cleary, M.L., and Wolberger, C. (1999). Structure of a HoxB1-Pbx1 heterodimer bound to DNA: role of the hexapeptide and a fourth homeodomain helix in complex formation. Cell *96*, 587-597.

Popperl, H., Rikhof, H., Chang, H., Haffter, P., Kimmel, C.B., and Moens, C.B. (2000). lazarus is a novel pbx gene that globally mediates hox gene function in zebrafish. Mol Cell *6*, 255-267.

Poy, M.N., Eliasson, L., Krutzfeldt, J., Kuwajima, S., Ma, X., Macdonald, P.E., Pfeffer, S., Tuschl, T., Rajewsky, N., Rorsman, P., *et al.* (2004). A pancreatic islet-specific microRNA regulates insulin secretion. Nature *432*, 226-230.

Pronk, C.J., Rossi, D.J., Mansson, R., Attema, J.L., Norddahl, G.L., Chan, C.K., Sigvardsson, M., Weissman, I.L., and Bryder, D. (2007). Elucidation of the phenotypic, functional, and molecular topography of a myeloerythroid progenitor cell hierarchy. Cell Stem Cell *1*, 428-442.

Puri, M.C., and Bernstein, A. (2003). Requirement for the TIE family of receptor tyrosine kinases in adult but not fetal hematopoiesis. Proc Natl Acad Sci U S A *100*, 12753-12758.

Purton, L.E., Dworkin, S., Olsen, G.H., Walkley, C.R., Fabb, S.A., Collins, S.J., and Chambon, P. (2006). RARgamma is critical for maintaining a balance between hematopoietic stem cell self-renewal and differentiation. J Exp Med *203*, 1283-1293.

Purton, L.E., and Scadden, D.T. (2007). Limiting factors in murine hematopoietic stem cell assays. Cell Stem Cell *1*, 263-270.

Rafii, S., Lyden, D., Benezra, R., Hattori, K., and Heissig, B. (2002). Vascular and haematopoietic stem cells: novel targets for anti-angiogenesis therapy? Nat Rev Cancer *2*, 826-835.

Ramachandran, V., and Chen, X. (2008). Degradation of microRNAs by a family of exoribonucleases in Arabidopsis. Science *321*, 1490-1492.

Ramkissoon, S.H., Mainwaring, L.A., Ogasawara, Y., Keyvanfar, K., McCoy, J.P., Jr., Sloand, E.M., Kajigaya, S., and Young, N.S. (2006). Hematopoietic-specific microRNA expression in human cells. Leuk Res *30*, 643-647.

Rana, T.M. (2007). Illuminating the silence: understanding the structure and function of small RNAs. Nat Rev Mol Cell Biol *8*, 23-36.

Randall, T.D., and Weissman, I.L. (1997). Phenotypic and functional changes induced at the clonal level in hematopoietic stem cells after 5-fluorouracil treatment. Blood *89*, 3596-3606.

Rauskolb, C., Peifer, M., and Wieschaus, E. (1993). extradenticle, a regulator of homeotic gene activity, is a homolog of the homeobox-containing human proto-oncogene pbx1. Cell *74*, 1101-1112.

Reinhart, B.J., Slack, F.J., Basson, M., Pasquinelli, A.E., Bettinger, J.C., Rougvie, A.E., Horvitz, H.R., and Ruvkun, G. (2000). The 21-nucleotide let-7 RNA regulates developmental timing in Caenorhabditis elegans. Nature *403*, 901-906.

Reya, T., Duncan, A.W., Ailles, L., Domen, J., Scherer, D.C., Willert, K., Hintz, L., Nusse, R., and Weissman, I.L. (2003). A role for Wnt signalling in self-renewal of haematopoietic stem cells. Nature *423*, 409-414.

Reya, T., Morrison, S.J., Clarke, M.F., and Weissman, I.L. (2001). Stem cells, cancer, and cancer stem cells. Nature *414*, 105-111.

Rhee, J.W., Arata, A., Selleri, L., Jacobs, Y., Arata, S., Onimaru, H., and Cleary, M.L. (2004). Pbx3 deficiency results in central hypoventilation. Am J Pathol *165*, 1343-1350.

Rhodes, J., Hagen, A., Hsu, K., Deng, M., Liu, T.X., Look, A.T., and Kanki, J.P. (2005). Interplay of pu.1 and gata1 determines myelo-erythroid progenitor cell fate in zebrafish. Developmental cell *8*, 97-108.

Rieckhof, G.E., Casares, F., Ryoo, H.D., Abu-Shaar, M., and Mann, R.S. (1997). Nuclear translocation of extradenticle requires homothorax, which encodes an extradenticle-related homeodomain protein. Cell *91*, 171-183.

Rigoutsos, I. (2009). New tricks for animal microRNAS: targeting of amino acid coding regions at conserved and nonconserved sites. Cancer Res *69*, 3245-3248.

Rodriguez, A., Griffiths-Jones, S., Ashurst, J.L., and Bradley, A. (2004). Identification of mammalian microRNA host genes and transcription units. Genome Res *14*, 1902-1910.

Rodriguez, A., Vigorito, E., Clare, S., Warren, M.V., Couttet, P., Soond, D.R., van Dongen, S., Grocock, R.J., Das, P.P., Miska, E.A., *et al.* (2007). Requirement of bic/microRNA-155 for normal immune function. Science *316*, 608-611.

Rosa, A., Ballarino, M., Sorrentino, A., Sthandier, O., De Angelis, F.G., Marchioni, M., Masella, B., Guarini, A., Fatica, A., Peschle, C., *et al.* (2007). The interplay between the master transcription factor PU.1 and miR-424 regulates human monocyte/macrophage differentiation. Proc Natl Acad Sci U S A *104*, 19849-19854.

Rosendaal, M., Hodgson, G.S., and Bradley, T.R. (1979). Organization of haemopoietic stem cells: the generation-age hypothesis. Cell Tissue Kinet *12*, 17-29.

Rossi, D.J., Seita, J., Czechowicz, A., Bhattacharya, D., Bryder, D., and Weissman, I.L. (2007). Hematopoietic stem cell quiescence attenuates DNA damage response and permits DNA damage accumulation during aging. Cell Cycle *6*, 2371-2376.

Rothenberg, E.V. (2007). Negotiation of the T lineage fate decision by transcription-factor interplay and microenvironmental signals. Immunity *26*, 690-702.

Ruby, J.G., Jan, C.H., and Bartel, D.P. (2007). Intronic microRNA precursors that bypass Drosha processing. Nature *448*, 83-86.

Ryoo, H.D., Marty, T., Casares, F., Affolter, M., and Mann, R.S. (1999). Regulation of Hox target genes by a DNA bound Homothorax/Hox/Extradenticle complex. Development *126*, 5137-5148.

Saleh, M., Rambaldi, I., Yang, X.J., and Featherstone, M.S. (2000). Cell signaling switches HOX-PBX complexes from repressors to activators of transcription mediated by histone deacetylases and histone acetyltransferases. Mol Cell Biol *20*, 8623-8633.

Santaguida, M., Schepers, K., King, B., Sabnis, A.J., Forsberg, E.C., Attema, J.L., Braun, B.S., and Passegue, E. (2009). JunB protects against myeloid malignancies by limiting hematopoietic stem cell proliferation and differentiation without affecting self-renewal. Cancer Cell *15*, 341-352.

Sanyal, M., Tung, J.W., Karsunky, H., Zeng, H., Selleri, L., Weissman, I.L., Herzenberg, L.A., and Cleary, M.L. (2007). B-cell development fails in the absence of the Pbx1 proto-oncogene. Blood *109*, 4191-4199.

Schmitt, T.M., and Zuniga-Pflucker, J.C. (2002). Induction of T cell development from hematopoietic progenitor cells by delta-like-1 in vitro. Immunity *17*, 749-756.

Schnabel, C.A., Godin, R.E., and Cleary, M.L. (2003a). Pbx1 regulates nephrogenesis and ureteric branching in the developing kidney. Dev Biol *254*, 262-276.

Schnabel, C.A., Selleri, L., and Cleary, M.L. (2003b). Pbx1 is essential for adrenal development and urogenital differentiation. Genesis *37*, 123-130.

Schnabel, C.A., Selleri, L., Jacobs, Y., Warnke, R., and Cleary, M.L. (2001). Expression of Pbx1b during mammalian organogenesis. Mech Dev *100*, 131-135.

Schnurch, H., and Risau, W. (1993). Expression of tie-2, a member of a novel family of receptor tyrosine kinases, in the endothelial cell lineage. Development *119*, 957-968.

Schofield, R. (1978). The relationship between the spleen colony-forming cell and the haemopoietic stem cell. Blood Cells *4*, 7-25.

Schwarz, D.S., Hutvagner, G., Du, T., Xu, Z., Aronin, N., and Zamore, P.D. (2003). Asymmetry in the assembly of the RNAi enzyme complex. Cell *115*, 199-208.

Schwarz, D.S., and Zamore, P.D. (2002). Why do miRNAs live in the miRNP? Genes Dev *16*, 1025-1031.

Seita, J., and Weissman, I.L. (2010). Hematopoietic stem cell: self-renewal versus differentiation. Wiley Interdiscip Rev Syst Biol Med *2*, 640-653.

Selbach, M., Schwanhausser, B., Thierfelder, N., Fang, Z., Khanin, R., and Rajewsky, N. (2008). Widespread changes in protein synthesis induced by microRNAs. Nature *455*, 58-63.

Selleri, L., Depew, M.J., Jacobs, Y., Chanda, S.K., Tsang, K.Y., Cheah, K.S., Rubenstein, J.L., O'Gorman, S., and Cleary, M.L. (2001). Requirement for Pbx1 in skeletal patterning and programming chondrocyte proliferation and differentiation. Development *128*, 3543-3557.

Selleri, L., DiMartino, J., van Deursen, J., Brendolan, A., Sanyal, M., Boon, E., Capellini, T., Smith, K.S., Rhee, J., Popperl, H., *et al.* (2004). The TALE homeodomain protein Pbx2 is not essential for development and long-term survival. Mol Cell Biol *24*, 5324-5331.

Serwold, T., Ehrlich, L.I., and Weissman, I.L. (2009). Reductive isolation from bone marrow and blood implicates common lymphoid progenitors as the major source of thymopoiesis. Blood *113*, 807-815.

Shanmugam, K., Green, N.C., Rambaldi, I., Saragovi, H.U., and Featherstone, M.S. (1999). PBX and MEIS as non-DNA-binding partners in trimeric complexes with HOX proteins. Mol Cell Biol *19*, 7577-7588.

Shen, W.F., Rozenfeld, S., Kwong, A., Kom ves, L.G., Lawrence, H.J., and Largman, C. (1999). HOXA9 forms triple complexes with PBX2 and MEIS1 in myeloid cells. Mol Cell Biol *19*, 3051-3061.

Shiojima, I., and Walsh, K. (2002). Role of Akt signaling in vascular homeostasis and angiogenesis. Circ Res *90*, 1243-1250.

Shivdasani, R.A. (2006). MicroRNAs: regulators of gene expression and cell differentiation. Blood *108*, 3646-3653.

Signer, R.A., Montecino-Rodriguez, E., Witte, O.N., and Dorshkind, K. (2010). Immature B-cell progenitors survive oncogenic stress and efficiently initiate Ph+ B-acute lymphoblastic leukemia. Blood *116*, 2522-2530.

Siminovitch, L., McCulloch, E.A., and Till, J.E. (1963). The Distribution of Colony-Forming Cells among Spleen Colonies. J Cell Physiol *62*, 327-336.

Somervaille, T.C., Matheny, C.J., Spencer, G.J., Iwasaki, M., Rinn, J.L., Witten, D.M., Chang, H.Y., Shurtleff, S.A., Downing, J.R., and Cleary, M.L. (2009). Hierarchical maintenance of MLL myeloid leukemia stem cells employs a transcriptional program shared with embryonic rather than adult stem cells. Cell Stem Cell *4*, 129-140.

Spangrude, G.J., and Brooks, D.M. (1992). Phenotypic analysis of mouse hematopoietic stem cells shows a Thy-1-negative subset. Blood *80*, 1957-1964.

Spangrude, G.J., Heimfeld, S., and Weissman, I.L. (1988). Purification and characterization of mouse hematopoietic stem cells. Science *241*, 58-62.

Stadler, B.M., and Ruohola-Baker, H. (2008). Small RNAs: keeping stem cells in line. Cell *132*, 563-566.

Starczynowski, D.T., Kuchenbauer, F., Wegrzyn, J., Rouhi, A., Petriv, O., Hansen, C.L., Humphries, R.K., and Karsan, A. (2011). MicroRNA-146a disrupts hematopoietic differentiation and survival. Experimental hematology *39*, 167-178.

Subramanian, A., Tamayo, P., Mootha, V.K., Mukherjee, S., Ebert, B.L., Gillette, M.A., Paulovich, A., Pomeroy, S.L., Golub, T.R., Lander, E.S., *et al.* (2005). Gene set enrichment analysis: a knowledge-based approach for interpreting genome-wide expression profiles. Proc Natl Acad Sci U S A *102*, 15545-15550.

Suda, T., Arai, F., and Hirao, A. (2005). Hematopoietic stem cells and their niche. Trends Immunol *26*, 426-433.

Suzuki, H.I., Yamagata, K., Sugimoto, K., Iwamoto, T., Kato, S., and Miyazono, K. (2009). Modulation of microRNA processing by p53. Nature *460*, 529-533.

Szilvassy, S.J., Humphries, R.K., Lansdorp, P.M., Eaves, A.C., and Eaves, C.J. (1990). Quantitative assay for totipotent reconstituting hematopoietic stem cells by a competitive repopulation strategy. Proc Natl Acad Sci U S A *87*, 8736-8740.

Szilvassy, S.J., Lansdorp, P.M., Humphries, R.K., Eaves, A.C., and Eaves, C.J. (1989). Isolation in a single step of a highly enriched murine hematopoietic stem cell population with competitive long-term repopulating ability. Blood *74*, 930-939.

Takakura, N., Huang, X.L., Naruse, T., Hamaguchi, I., Dumont, D.J., Yancopoulos, G.D., and Suda, T. (1998). Critical role of the TIE2 endothelial cell receptor in the development of definitive hematopoiesis. Immunity *9*, 677-686.

Tang, Y., Harrington, A., Yang, X., Friesel, R.E., and Liaw, L. (2010). The contribution of the Tie2+ lineage to primitive and definitive hematopoietic cells. Genesis *48*, 563-567.

Taswell, C. (1981). Limiting dilution assays for the determination of immunocompetent cell frequencies. I. Data analysis. J Immunol *126*, 1614-1619.

Tay, Y., Zhang, J., Thomson, A.M., Lim, B., and Rigoutsos, I. (2008). MicroRNAs to Nanog, Oct4 and Sox2 coding regions modulate embryonic stem cell differentiation. Nature *455*, 1124-1128.

Thai, T.H., Calado, D.P., Casola, S., Ansel, K.M., Xiao, C., Xue, Y., Murphy, A., Frendewey, D., Valenzuela, D., Kutok, J.L., *et al.* (2007). Regulation of the germinal center response by microRNA-155. Science *316*, 604-608.

Thomson, J.M., Newman, M., Parker, J.S., Morin-Kensicki, E.M., Wright, T., and Hammond, S.M. (2006). Extensive post-transcriptional regulation of microRNAs and its implications for cancer. Genes Dev *20*, 2202-2207.

Thoren, L.A., Liuba, K., Bryder, D., Nygren, J.M., Jensen, C.T., Qian, H., Antonchuk, J., and Jacobsen, S.E. (2008). Kit regulates maintenance of quiescent hematopoietic stem cells. J Immunol *180*, 2045-2053.

Till, J.E., and Mc, C.E. (1961). A direct measurement of the radiation sensitivity of normal mouse bone marrow cells. Radiat Res *14*, 213-222.

Tokoyoda, K., Egawa, T., Sugiyama, T., Choi, B.I., and Nagasawa, T. (2004). Cellular niches controlling B lymphocyte behavior within bone marrow during development. Immunity *20*, 707-718.

Tothova, Z., Kollipara, R., Huntly, B.J., Lee, B.H., Castrillon, D.H., Cullen, D.E., McDowell, E.P., Lazo-Kallanian, S., Williams, I.R., Sears, C., *et al.* (2007). FoxOs are critical mediators of hematopoietic stem cell resistance to physiologic oxidative stress. Cell *128*, 325-339.

Trang, P., Weidhaas, J.B., and Slack, F.J. (2008). MicroRNAs as potential cancer therapeutics. Oncogene *27 Suppl 2*, S52-57.

Tremblay, M., Tremblay, C.S., Herblot, S., Aplan, P.D., Hebert, J., Perreault, C., and Hoang, T. (2010). Modeling T-cell acute lymphoblastic leukemia induced by the SCL and LMO1 oncogenes. Genes Dev *24*, 1093-1105.

Tristram G. Parslow, D.P.S., Abba I. Terr, John B. Imboden (2001). Medical Immunology (Lange Medical Books/McGraw-Hill Medical Publishing Division).

Tsuchida, A., Ohno, S., Wu, W., Borjigin, N., Fujita, K., Aoki, T., Ueda, S., Takanashi, M., and Kuroda, M. (2011). miR-92 is a key oncogenic component of the miR-17-92 cluster in colon cancer. Cancer Sci *102*, 2264-2271.

Tusher, V.G., Tibshirani, R., and Chu, G. (2001). Significance analysis of microarrays applied to the ionizing radiation response. Proc Natl Acad Sci U S A *98*, 5116-5121.

Uchida, N., and Weissman, I.L. (1992). Searching for hematopoietic stem cells: evidence that Thy-1.1lo Lin- Sca-1+ cells are the only stem cells in C57BL/Ka-Thy-1.1 bone marrow. J Exp Med *175*, 175-184.

Unnisa, Z., Clark, J.P., Roychoudhury, J., Thomas, E., Tessarollo, L., Copeland, N.G., Jenkins, N.A., Grimes, H.L., and Kumar, A.R. (2012). Meis1 preserves hematopoietic stem cells in mice by limiting oxidative stress. Blood *120*, 4973-4981.

Urbanek, P., Wang, Z.Q., Fetka, I., Wagner, E.F., and Busslinger, M. (1994). Complete block of early B cell differentiation and altered patterning of the posterior midbrain in mice lacking Pax5/BSAP. Cell *79*, 901-912.

van der Wath, R.C., Wilson, A., Laurenti, E., Trumpp, A., and Lio, P. (2009). Estimating dormant and active hematopoietic stem cell kinetics through extensive modeling of bromodeoxyuridine label-retaining cell dynamics. PLoS One *4*, e6972.

Varnum-Finney, B., Wu, L., Yu, M., Brashem-Stein, C., Staats, S., Flowers, D., Griffin, J.D., and Bernstein, I.D. (2000). Immobilization of Notch ligand, Delta-1, is required for induction of notch signaling. J Cell Sci *113 Pt 23*, 4313-4318.

Vasudevan, S., Tong, Y., and Steitz, J.A. (2007). Switching from repression to activation: microRNAs can up-regulate translation. Science *318*, 1931-1934.

Venezia, T.A., Merchant, A.A., Ramos, C.A., Whitehouse, N.L., Young, A.S., Shaw, C.A., and Goodell, M.A. (2004). Molecular signatures of proliferation and quiescence in hematopoietic stem cells. PLoS Biol *2*, e301.

Verfaillie, C.M. (1994). Can human hematopoietic stem cells be cultured ex vivo? Stem Cells *12*, 466-476.

Viatour, P., Somervaille, T.C., Venkatasubrahmanyam, S., Kogan, S., McLaughlin, M.E., Weissman, I.L., Butte, A.J., Passegue, E., and Sage, J. (2008). Hematopoietic

stem cell quiescence is maintained by compound contributions of the retinoblastoma gene family. Cell Stem Cell *3*, 416-428.

Visser, J.W., and Bol, S.J. (1982). A two-step procedure for obtaining 80-fold enriched suspensions of murine pluripotent hemopoietic stem cells. Stem Cells *1*, 240-249.

Visser, J.W., Bol, S.J., and van den Engh, G. (1981). Characterization and enrichment of murine hemopoietic stem cells by fluorescence activated cell sorting. Experimental hematology *9*, 644-655.

Waghmare, S.K., Bansal, R., Lee, J., Zhang, Y.V., McDermitt, D.J., and Tumbar, T. (2008). Quantitative proliferation dynamics and random chromosome segregation of hair follicle stem cells. The EMBO journal *27*, 1309-1320.

Wagner, K., Mincheva, A., Korn, B., Lichter, P., and Popperl, H. (2001). Pbx4, a new Pbx family member on mouse chromosome 8, is expressed during spermatogenesis. Mech Dev *103*, 127-131.

Walter, J., Dever, C.A., and Biggin, M.D. (1994). Two homeo domain proteins bind with similar specificity to a wide range of DNA sites in Drosophila embryos. Genes Dev *8*, 1678-1692.

Wang, Y., Baskerville, S., Shenoy, A., Babiarz, J.E., Baehner, L., and Blelloch, R. (2008). Embryonic stem cell-specific microRNAs regulate the G1-S transition and promote rapid proliferation. Nat Genet *40*, 1478-1483.

Wang, Y., Medvid, R., Melton, C., Jaenisch, R., and Blelloch, R. (2007). DGCR8 is essential for microRNA biogenesis and silencing of embryonic stem cell self-renewal. Nat Genet *39*, 380-385.

Waskiewicz, A.J., Rikhof, H.A., Hernandez, R.E., and Moens, C.B. (2001). Zebrafish Meis functions to stabilize Pbx proteins and regulate hindbrain patterning. Development *128*, 4139-4151.

Waskiewicz, A.J., Rikhof, H.A., and Moens, C.B. (2002). Eliminating zebrafish pbx proteins reveals a hindbrain ground state. Developmental cell *3*, 723-733.

Waters, K.M., Sontag, R.L., and Weber, T.J. (2013). Hepatic leukemia factor promotes resistance to cell death: implications for therapeutics and chronotherapy. Toxicol Appl Pharmacol *268*, 141-148.

Weber, M.J. (2005). New human and mouse microRNA genes found by homology search. Febs J *272*, 59-73.

Weinmann, L., Hock, J., Ivacevic, T., Ohrt, T., Mutze, J., Schwille, P., Kremmer, E., Benes, V., Urlaub, H., and Meister, G. (2009). Importin 8 is a gene silencing factor that targets argonaute proteins to distinct mRNAs. Cell *136*, 496-507.

Weissman, I. (2005). Stem cell research: paths to cancer therapies and regenerative medicine. Jama *294*, 1359-1366.

Weissman, I.L., and Shizuru, J.A. (2008). The origins of the identification and isolation of hematopoietic stem cells, and their capability to induce donor-specific transplantation tolerance and treat autoimmune diseases. Blood *112*, 3543-3553.

Weksberg, D.C., Chambers, S.M., Boles, N.C., and Goodell, M.A. (2008). CD150- side population cells represent a functionally distinct population of long-term hematopoietic stem cells. Blood *111*, 2444-2451.

Whetton, A.D., and Graham, G.J. (1999). Homing and mobilization in the stem cell niche. Trends Cell Biol *9*, 233-238.

Whitlock, C.A., and Witte, O.N. (1982). Long-term culture of B lymphocytes and their precursors from murine bone marrow. Proc Natl Acad Sci U S A *79*, 3608-3612.

Wiesen, J.L., and Tomasi, T.B. (2009). Dicer is regulated by cellular stresses and interferons. Mol Immunol *46*, 1222-1228.

Wilfred, B.R., Wang, W.X., and Nelson, P.T. (2007). Energizing miRNA research: a review of the role of miRNAs in lipid metabolism, with a prediction that miR-103/107 regulates human metabolic pathways. Mol Genet Metab *91*, 209-217.

Williams, T.M., Williams, M.E., and Innis, J.W. (2005). Range of HOX/TALE superclass associations and protein domain requirements for HOXA13:MEIS interaction. Dev Biol *277*, 457-471.

Wilson, A., Laurenti, E., Oser, G., van der Wath, R.C., Blanco-Bose, W., Jaworski, M., Offner, S., Dunant, C.F., Eshkind, L., Bockamp, E., *et al.* (2008). Hematopoietic stem cells reversibly switch from dormancy to self-renewal during homeostasis and repair. Cell *135*, 1118-1129.

Wilson, A., Laurenti, E., and Trumpp, A. (2009). Balancing dormant and self-renewing hematopoietic stem cells. Curr Opin Genet Dev *19*, 461-468.

Wilson, A., and Trumpp, A. (2006). Bone-marrow haematopoietic-stem-cell niches. Nat Rev Immunol *6*, 93-106.

Woehrer, S., Miller, C.L., and Eaves, C.J. (2010). Long-term culture-initiating cell assay for mouse cells. Methods Mol Biol *946*, 257-266.

Wojiski, S., Guibal, F.C., Kindler, T., Lee, B.H., Jesneck, J.L., Fabian, A., Tenen, D.G., and Gilliland, D.G. (2009). PML-RARalpha initiates leukemia by conferring properties of self-renewal to committed promyelocytic progenitors. Leukemia *23*, 1462-1471.

Wolf, N.S., Kone, A., Priestley, G.V., and Bartelmez, S.H. (1993). In vivo and in vitro characterization of long-term repopulating primitive hematopoietic cells isolated by sequential Hoechst 33342-rhodamine 123 FACS selection. Experimental hematology *21*, 614-622.

Wu, A.M., Till, J.E., Siminovitch, L., and McCulloch, E.A. (1968). Cytological evidence for a relationship between normal hemotopoietic colony-forming cells and cells of the lymphoid system. J Exp Med *127*, 455-464.

Xiao, C., Calado, D.P., Galler, G., Thai, T.H., Patterson, H.C., Wang, J., Rajewsky, N., Bender, T.P., and Rajewsky, K. (2007). MiR-150 controls B cell differentiation by targeting the transcription factor c-Myb. Cell *131*, 146-159.

Yamashita, Y.M., and Fuller, M.T. (2005). Asymmetric stem cell division and function of the niche in the Drosophila male germ line. Int J Hematol *82*, 377-380.

Yamazaki, S., Iwama, A., Takayanagi, S., Eto, K., Ema, H., and Nakauchi, H. (2009). TGF-beta as a candidate bone marrow niche signal to induce hematopoietic stem cell hibernation. Blood *113*, 1250-1256.

Yang, L., Bryder, D., Adolfsson, J., Nygren, J., Mansson, R., Sigvardsson, M., and Jacobsen, S.E. (2005). Identification of Lin(-)Sca1(+)kit(+)CD34(+)Flt3- short-term hematopoietic stem cells capable of rapidly reconstituting and rescuing myeloablated transplant recipients. Blood *105*, 2717-2723.

Yi, R., and Fuchs, E. (2011). MicroRNAs and their roles in mammalian stem cells. J Cell Sci *124*, 1775-1783.

Yilmaz, O.H., Kiel, M.J., and Morrison, S.J. (2006a). SLAM family markers are conserved among hematopoietic stem cells from old and reconstituted mice and markedly increase their purity. Blood *107*, 924-930.

Yilmaz, O.H., Valdez, R., Theisen, B.K., Guo, W., Ferguson, D.O., Wu, H., and Morrison, S.J. (2006b). Pten dependence distinguishes haematopoietic stem cells from leukaemia-initiating cells. Nature *441*, 475-482.

Yoshida, T., Hazan, I., Zhang, J., Ng, S.Y., Naito, T., Snippert, H.J., Heller, E.J., Qi, X., Lawton, L.N., Williams, C.J., *et al.* (2008). The role of the chromatin remodeler Mi-2beta in hematopoietic stem cell self-renewal and multilineage differentiation. Genes Dev *22*, 1174-1189.

Yoshihara, H., Arai, F., Hosokawa, K., Hagiwara, T., Takubo, K., Nakamura, Y., Gomei, Y., Iwasaki, H., Matsuoka, S., Miyamoto, K., *et al.* (2007). Thrombopoietin/MPL signaling regulates hematopoietic stem cell quiescence and interaction with the osteoblastic niche. Cell Stem Cell *1*, 685-697.

Yuan, R., Astle, C.M., Chen, J., and Harrison, D.E. (2005). Genetic regulation of hematopoietic stem cell exhaustion during development and growth. Experimental hematology *33*, 243-250.

Zhang, J., Niu, C., Ye, L., Huang, H., He, X., Tong, W.G., Ross, J., Haug, J., Johnson, T., Feng, J.Q., *et al.* (2003). Identification of the haematopoietic stem cell niche and control of the niche size. Nature *425*, 836-841.

Zhang, L., Lubin, A., Chen, H., Sun, Z., and Gong, F. (2012). The deubiquitinating protein USP24 interacts with DDB2 and regulates DDB2 stability. Cell Cycle *11*, 4378-4384.

Zhao, Y., and Potter, S.S. (2001). Functional specificity of the Hoxa13 homeobox. Development *128*, 3197-3207.